Alma Mater Studiorum - Università di Bologna

DOTTORATO DI RICERCA IN

SCIENZE CARDIO NEFRO TORACICHE

Ciclo 33

Settore Concorsuale: 06/E1 - CHIRURGIA CARDIO - TORACO - VASCOLARE

Settore Scientifico Disciplinare: MED/03 - GENETICA MEDICA

TUMOR HETEROGENEITY IN ESOPHAGEAL ADENOCARCINOMA: A GENOMIC APPROACH

Presentata da: Isotta Bozzarelli

Coordinatore Dottorato

Gaetano Domenico Gargiulo

Supervisore

Elena Bonora

Esame finale anno 2021

ABSTRACT

INTRODUCTION: Esophageal adenocarcinoma (EAC) is a severe malignancy in terms of prognosis and mortality rate. Because its great genetic heterogeneity, disputes regarding classification, prevention and treatments are still unsolved.

AIM: We investigated intra- and inter-EAC heterogeneity by defining EAC's somatic mutational profile and the role of candidate microRNAs, to correlate the molecular profile of tumors to clinical outcomes and to identify biomarkers for classification.

METHODS: 38 EAC cases were analyzed via high-throughput cell sorting technology combined with targeted sequencing and whole genome low-pass sequencing. Targeted sequencing of further 169 cases was performed to widen the study. miR221 and miR483-3p expression was profiled via qPCR in 112 EACs and correlation with clinical outcomes was investigated.

RESULTS: 35/38 EACs carried at least one somatic mutation absent in stromal cells. *TP53* was found mutated in 73.7% of cases. Selective sorting revealed tumor subclones with different mutational loads and copy number alterations, confirming the high intra-tumor heterogeneity of EAC. Mutations were in most cases at homozygous state, and we identified alterations that were missed with the whole-tumor analysis. Mutations in *HNF1A* gene, not previously associated with EAC, were identified in both cohorts. Higher expression of miR483-3p and miR221 was associated with poorer cancer specific survival (P=0.0293 and P=0.0059), and recurrence in the Lauren intestinal subtype (P=0.0459 and P=0.0002). Median expression levels of miRNAs were higher in patients with advanced tumor stages. The loss of SMAD4 immunoreactivity was significantly associated with poorer cancer specific survival and recurrence (P=0.0452; P=0.022 respectively).

CONCLUSION: Combining selective sorting technology and next generation sequencing allowed to better define EAC inter- and intra-tumor heterogeneity. We identified *HNF1A* as a new mutated gene associated to EAC that could be involved in tumor progression and promising biomarkers such as SMAD4, miR221 and miR483-3p to identify patients at higher risk for more aggressive tumors.

1. INTRODUCTION 1
1.1 Epidemiology of Esophageal Cancer 1
1.2 ESCC and EAC are characterized by a different molecular landscape 3
1.3 Risk factors 4
1.3.1 Non genetic risk factors 4
1.3.2 Genetic risk factors 8
1.4 The classifications of EAC 10
1.4.1 The Siewert classification 10
1.4.2 The Lauren classification 12
1.4.3 Immunohistological classification of esophageal adenocarcinoma 13
1.4.4 The EACSGE histological classification 14
1.5 Unraveling the genomic signature of EAC 16
1.6 Investigating the genetic heterogeneity in EAC 21
1.7 The role of MicroRNAs in Esophageal Adenocarcinoma 25
1.7.1 MiRNAs regulate gene expression 25
1.7.2 miRNAs biogenesis and mechanism of action 26
1.7.3 MicroRNA and cancer 28
1.7.4 MiRNA profile in EAC 28
1.8 Prognosis and treatment of EAC 32
1.8.1 Prognosis 32
1.8.2 Surgery and neoadjuvant therapy 32
1.8.3 Targeted therapies 33
1.8.4 Immunotherapy 35
2. AIMS 36
3. MATERIALS AND METHODS 38
3.1 Genetic analysis of esophageal adenocarcinoma with DEPArray 38
3.1.1 Sample recruitment 38
3.1.2 Cells dissociation, DNA quality control and cell sorting with DEPArray™ 38
3.1.3 OncoSeek panel genetic analysis 41
3.1.4 CNA analysis through Whole-Genome Low-Pass sequencing 41

3.1.5 Whole Exome Sequencing (WES) 42
3.1.6 Bioinformatics analysis of WES data 43
3.1.7 Variants confirmation through Sanger sequencing 44
3.1.8 Droplet digital PCR (ddPCR) 44
3.1.9 Statistical analysis 45
3.2 EAC sequencing with an NGS custom panel enriching for cancer-related genes 46
3.2.1 Sample recruitment 46
3.2.2 Custom EAC Panel: library preparation, hybridization and sequencing 46
3.3 Analysis of the profile and functional studies of specific microRNA: miR483-3p and miR221 47
3.3.1 Sample recruitment 47
3.3.2 Cell lines 48
3.3.3 RNA isolation 49
3.3.4 Reverse transcription PCR and real-time quantitative PCR analysis (qPCR) for miRNA validation 49
3.3.5 MiR483-3p mimic transfection with Lipofectamine 3000 51
3.3.6 Reverse transcription PCR and qPCR analysis for genes of interest expression levels in cell lines 51
3.3.7 Western blot 52
3.3.8 Statistical analysis 53
4. RESULTS 54
4.1 High-throughput sorting and targeted sequencing of Esophageal Adenocarcinoma subpopulations unveil a complex mutational landscape 54
4.1.1 The landscape of somatic mutation in sorted populations 54
4.1.2 Different tumor populations are present in the same EAC specimen 57
4.1.3 *TP53* is the most frequently mutated gene 59
4.1.4 *HNF1A* is mutated in EAC 62
4.1.5 Identification of additional mutations through Whole Exome Sequencing (WES) 63
4.1.6 Correlation between *TP53* mutations and clinical outcomes 65
4.2 Expanding the genetic analysis to a wider cohort of patients 67

4.2.1 Mutational landscape in 169 EACs cases 67
4.2.2 *TP53* mutational spectrum 68
4.2.3 Mutations in the *HNF1A* gene: a further player in EAC 69
4.2.4 Statistical analysis 71
4.3 Analysis of deregulated miR483-3p and miR221 in esophageal adenocarcinomas 72
4.3.1 Expression analysis via single assays confirms an up-regulation of miR221 and miR483-3p in EACs 72
4.3.2 Correlation between miRNAs expression and clinical-pathological features in EAC 73
4.3.3 MiRNAs expression analysis in EAC cell lines 77
4.3.4 miR483-3p: evaluating its effect on gene expression levels using a miRNA mimic 78
4.3.5 Correlation between miR483-3p and *SMAD4* immunoreactivity 80
5. DISCUSSION 83
6. CONCLUSIONS 96
7. TABLES 97
8. REFERENCES 114

1. INTRODUCTION

1.1 Epidemiology of Esophageal Cancer

Esophageal Cancer (EC) is the seventh most common cancer worldwide, ranking sixth in terms of mortality [1]. It was estimated that 572,034 newly diagnosed cases occurred in 2018, with 508,585 deaths (Figure 1 and 2). EC can be classified into two main distinct histological subtypes: Squamous Cell Carcinoma (ESCC) and AdenoCarcinoma (EAC) [2].

The differences in geographical distribution of EC subtypes are remarkable: ESCC is the predominant esophageal cancer subtype in Southeastern and Central Asia (the so-called esophageal cancer belt), in Southern and Eastern Africa, in South America and among African Americans in North America. The Asian countries alone contribute to nearly 80% of the global ESCC cases [3]. In contrast, EAC is the main histologic subtype in Western countries, constituting around 46% of global adenocarcinoma (AC) cases [4].

ESCC incidence is broadly declining, while since 1970s we have witnessed to a rapid increase in EAC cases in many Western countries, including Europe, North America, and Australia, where the incidence and mortality rates associated with esophageal adenocarcinoma have overtaken those of ESCC in several regions [5]. EAC is the most rapidly increasing form of cancer in some populations; its incidence has increased 4-10% each year; in the US, the incidence of EAC among men surpassed that for ESCC around 1990 and continues to increase [6].

EAC increases in incidence with age, peaking in the seventh and eighth decades of life [6], and it is characterized by a striking male predominance in incidence, stronger than that of any other non–sex-specific cancer in

several populations, reaching, in the US, a male to female ratio as high as 9:1 [7].

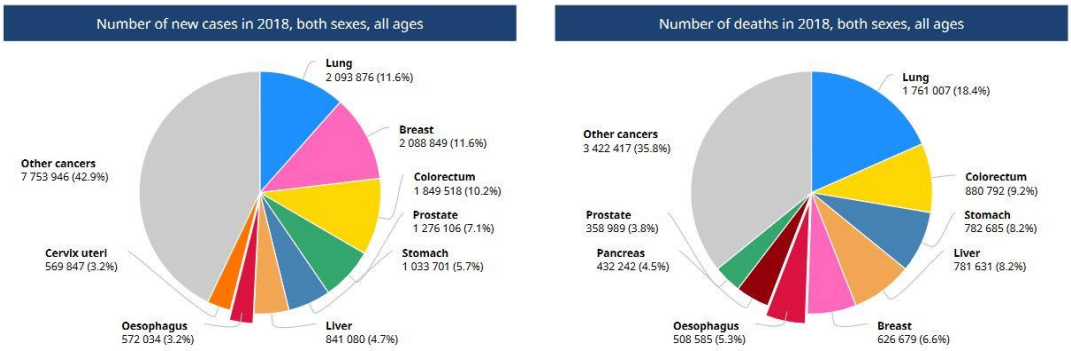

Figure 1: Worldwide incidence and mortality for esophageal cancer in 2018. Image from GLOBOCAN, aviable on http://globocan.iarc.fr/).

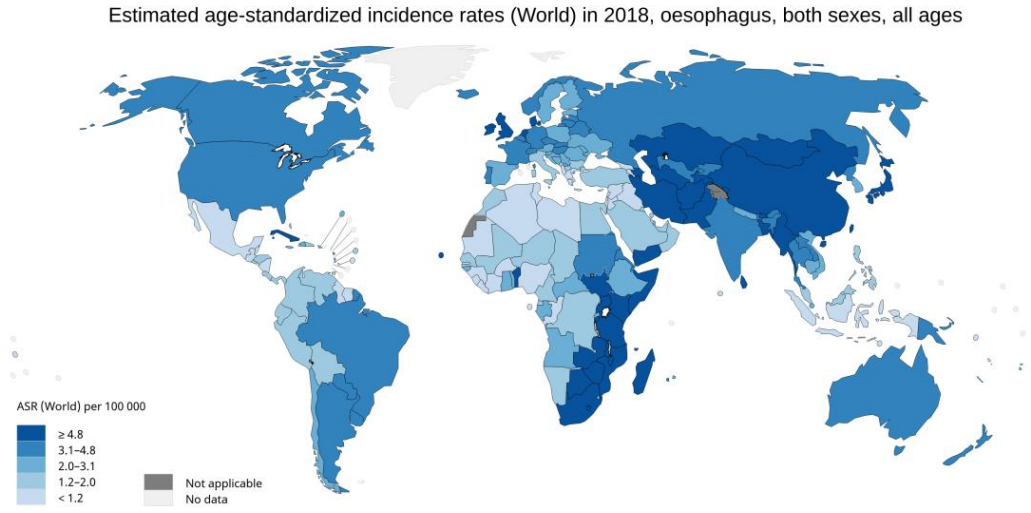

Figure 2: Worldwide rates of esophageal cancer incidence. Image from GLOBOCAN, aviable on http://globocan.iarc.fr/).

1.2 ESCC and EAC are characterized by a different molecular landscape

Although ESCC and EAC have been grouped together based on their anatomic location, molecular studies clearly defined the two cancer subtypes as distinct entities, in terms of cell of origin, epidemiology, risk factors and molecular features [2]. Squamous cell carcinoma is often localized in the proximal to mid-esophagus, and originates from squamous epithelial cells, whereas EAC occurs from glandular cells in the distal portion of the esophagus, in proximity to the gastro-esophageal junction (GEJ) [8], [9].

Other evidence based on recent genomic analysis also confirms that EAC and ESCC are different cancer entities [10]. In the molecular study by the Cancer Genome Atlas Research Network (TCGARN), 164 ECs derived from Western and Eastern populations were analyzed, providing further evidence that ESCC and EAC differentiate at molecular level [11]. Indeed, while ESCC resembles the head and neck squamous cancer, EAC is closer to the chromosomal instable subtype (CIN) gastric cancer (Figure 3). With the exception of *TP53*, which is the most commonly altered gene in both EAC and ESCC, the genomic profile of these subtypes of EC is considerably different. ESCC bears frequent alterations in *PIK3CA*, *CCND1, PTEN, NFE2L2, NOTCH1, MLL2, SOX2, FGFR1* and *MDM2*. In EAC the most frequently somatic alterations have been found in *ERBB2, KRAS, EGFR, SMAD4, ARID1A, VEGFA, CCNE1* and *GATA4/6* [11].

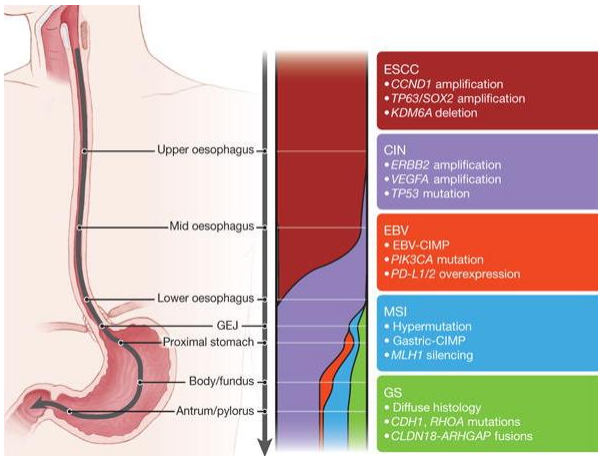

Figure 3: Molecular subtypes of gastroesophageal tumors. Each subtype is present in different proportions in different anatomic regions (as highlighted by the widths of the colour bands). Key features of subtypes are indicated in associated text. Image from The Cancer Genome Atlas Research Network, 2017 [11].

1.3 Risk factors

1.3.1 Non genetic risk factors

EAC has a complex etiology, with the involvement of genetic, behavioral and environmental factors. One of the most prominent risk factors linked to the development of esophageal adenocarcinoma is gastro-esophageal reflux disease (GERD) [12], where the esophageal epithelial cells are exposed to gastroduodenal acid and bile in a constant loop of damage and regeneration of esophageal tissue, that causes histologic and genetic changes [13], [14], directly but also indirectly through chronic inflammatory reactions [15], [16]. Studies have shown that there is a strong association between the 2 most common GERD symptoms (heartburn and regurgitation) and EAC risk, which increases with increased duration and/or frequency, arriving to a 6 fold higher risk in patients having heartburn for more than 20 years [17].

Chronic GERD can lead to the onset of Barrett's esophagus (BE), a metaplastic condition characterized by changes in the lining of the distal esophagus, where the normal squamous epithelium is replaced by an intestinal columnar type [18]. Barrett's esophagus is considered a premalignant condition and one of the common risk factors of EAC [19], that can lead to its development through consecutive steps, from erosive esophagitis to non-dysplastic BE, low-grade and high-grade dysplasia, to adenocarcinoma [20] (Figure 4). Retrospective population-based studies found that the risk of progression from BE to EAC is 0.13%-0.40% per patient per year [21], [22], and the likelihood of developing EAC is increased 1.7 times with GERD and 10.6 times in patients diagnosed with BE [23].

However, the reason why some cases of BE progress into EAC and some do not is still unclear. EAC can arise with neither GERD or BE being present: up to 40% of patients diagnosed with EAC do not report GERD symptoms [24] and a systematic review found that only 24% to 64% of resected EAC specimens had histological evidence of BE at the time of surgery [25], [26].

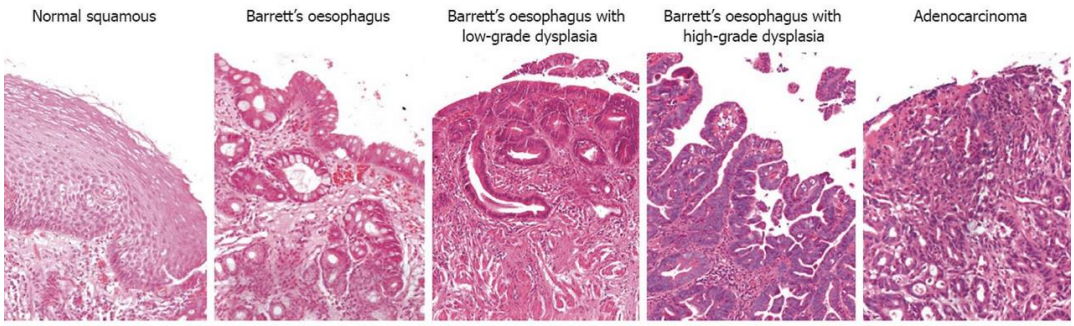

Figure 4: Barrett's esophagus progression: Transition from squamous epithelium to intestinal metaplasia, low-grade and high-grade dysplasia, and adenocarcinoma. Image from: Ong et al., 2010 [27].

The rising incidence of esophageal adenocarcinoma in Western populations could be related either to the increasing prevalence of GERD alone and to obesity plus GERD, in combination with the declining prevalence of Helicobacter pylori infection [4].

Even though the increasing incidence of EAC seems to have started before the start of the obesity epidemic [28], [29], obesity is another important risk factor in EAC onset [30], and it is associated with a risk of EAC that is increased by a factor of 2.4 to 2.8 [31], [32]. In particular, visceral abdominal obesity is associated with an increased risk of BE and cancer [33], possibly through a mechanical contribution given that intra-gastric pressure can disrupt the lower esophageal sphincter leading to hiatal hernia, and promoting and exacerbating GERD [34], [35]. Obesity is a systemic disease that may increase EAC risk through inflammatory and metabolic alterations [36]. Studies have shown associations between serum leptin and insulin levels, as well as metabolic syndrome components, and an altered risk of BE [37], [38]. Also, hypertrophied adipocytes and inflammatory cells within fat deposits create a low-grade inflammation environment that promotes tumor development through the release of adipokines and cytokines [33]. Abdominal adiposity is more common in men, which has led to speculation that it could explain some sex-related differences in cancer risk. However, comparing lean and overweight individuals, the male predominance seems to persist at a similar level [39], [40].

There is an inverse correlation between infection with the gastric bacterium *Helicobacter pylori* and EAC incidence: meta-analysis of observational studies have reported a 40%–60% reduced risk of EAC among persons with *H. pylori* infection [41], [42]. The prevalence of *H. pylori* infection has started to decrease in Western regions since the

middle of the 20th century, and may have contributed to the rising EAC incidence in Western populations [43].
A possible mechanism of this inverse association may be related to a reduced acid production because of atrophic gastritis following *H. pylori* infection, so decreasing reflux and thereby reduce the risk of EAC [44], [45].
Few studies have been conducted on the roles of bacteria other than *H. pylori* in development of EAC. There is a complex but conserved population of resident microbes in the esophagus, and it was shown that the esophageal microbiome changes in patients with GERD or BE compared to healthy individuals, decreasing in diversity and with an altered community composition in patients with EAC; however, it is not clear how the intestinal microbiome affects risk of EAC and further studies are needed [46], [47].

Tobacco smoking is a well-established and moderately strong risk factor for EAC. A study from the International Barrett's and Esophageal Adenocarcinoma Consortium (BEACON) showed that the risk of EAC is approximately twice as high among current smokers as it is among people who have never smoked, and that there is a dose-response association, rising to a 2.7-fold increased risk for individuals who had 45 or more pack-years of smoking history and 30% reduced risk individuals who have stopped smoking for at least 10 years compared with current smokers [48].
Instead, although alcohol is a recognized risk factor for the development of many cancers [49], pooled analysis studies have shown no significant association between alcohol consumption and esophageal adenocarcinoma [50], or the risk of progression from BE to EAC [51].

In a large prospective study in the USA high intake of red meats, fats, and processed foods seem to be positively associated with EAC whereas high

intake of fiber, fresh fruit, and vegetables is associated with a lower risk [52], [53].

Given the strong male predominance in EAC [6], the involvement of sex hormones in the etiology of EAC was investigated. A meta-analysis of 5 observational studies found a reduced risk of EAC in post-menopausal women who use menopause hormone therapy compared with non-users [54].

1.3.2 Genetic risk factors

Genetic susceptibility to EAC has been studied in depth. Approximately 7% of cases of Barrett's esophagus (BE) or EAC occur within families [55], [56]. A whole-exome sequencing study in 2016, of a multi-generational family in which 14 members were affected by BE or EAC, identified a variant in the V-set and immunoglobulin domain containing 10 like gene (*VSIG10L*), encoding S631G, as a possible cause of familial EAC [57].

Genome-wide association studies (GWAS) from various consortia led to the identification of genetic variants for BE and EAC susceptibility. These studies analyzed thousands of germline DNA specimens in order to identify single nucleotide polymorphisms (SNPs) that can be recognized as a genotypic marker, which is more likely to be associated to a specific phenotype, therefore more frequent in patients with a particular disease compared with healthy individuals. Many of the SNPs have been found in loci at or close to genes that regulate development and differentiation of the esophagogastric tract.

The first GWAS analysis to identify BE's predisposing variants was conducted by Su and colleagues. Two SNPs were identified: one was detected in the telomeric region of the *MHC* (O.R. 1.21), the other found close to the *FOXF1* gene (O.R. 1.14), belonging to a family of transcription factors that regulate gastrointestinal and esophageal development [58].

Levine and colleagues evaluated genetic variants in BE but also EAC patients, finding SNPs associated to *CRTC1* gene (CREB-regulated transcription factor; O.R. 1.18); *FOXP1* (O.R. 1.18), and *BARX1* (O.R. 0.83, involved in esophageal differentiation) [59].

Palles and colleagues identified new BE-associated SNPs, close to *GDF7* gene (OR 1.14, encoding a ligand in the BMP pathway); and SNPs in *TXB* (O.R. 0.90, a transcription factors involved esophageal and cardiac development), and *ALDHIA* (O.R. 0.90, involved in retinoic acid synthesis and alcohol metabolism) that showed a protective effect [60].

These associations have been validated in further studies [61]–[64].

The meta-analysis conducted by Gharahkhani and colleagues, not only confirmed the loci already identified in the previous studies, but detected other new risk variants. Among them, the one having the strongest association with Barrett's metaplasia and EAC was an intronic variant within *CFTR* (OR 0.84) ,which is mutated in cystic fibrosis. Considering that patients with cystic fibrosis have increased incidence of GERD, the authors suggest that *CFTR* could play an important role in the process of GERD, common to cystic fibrosis, BE, and EAC [63].

They also identified a risk variant near *HTR3C/ABCC5* that was associated with EAC and not with BE (OR 1.17). *ABCC5* encodes for an ATP-binding cassette membrane protein that is involved in transport and has been implicated in cancer development and progression; furthermore, it has a role in the embryonal development of the intestine [63].

Researchers also investigated germline variants in genes that regulate inflammation, androgen signaling, and cancer-related processes for their association with risk of Barrett and EAC. Variants associated with BE and EAC risk were identified at the *MGST1* locus (a gene with roles in the cellular response to oxidative stress) [65], in the androgen-related genes *CYP17A1* and *JMJD1C* [66], and at the *CDKN2A* locus [67], but further studies in larger sample sizes are needed to replicate these findings.

In a recent linkage analysis the Y-chromosome F haplogroup was found to be a risk factor for EAC with an OR 1.5, while the R1a and the K haplogroups were significantly underrepresented in the BE/EAC group compared to the GERD group (O.R. of 0.63 and 0.56 respectively) and seems to confer a protective effect against the development of BE [68].
The risk of BE and EA onset is influenced by a combination of germline genetic variants of small effect, with a shared polygenic effect [69].

1.4 The classifications of EAC

An accurate classification is a main requisite for the diagnosis, treatment and prognosis of cancer. Historically tumor classification was based on the anatomic location and histologic features, assuming that cancers from the same site of origin shared comparable pathogenic processes and treatment results.

1.4.1 The Siewert classification

Siewert and colleagues introduced a classification to separate gastro-esophageal-junction (EGJ) adenocarcinomas into three types based on the relationship between the EGJ location and the epicenter of the tumor (Figure 5) [70]–[72]. In particular:

- Type I tumors (or distal esophageal tumors): have their epicenter (or more than two-thirds of their bulk) located 1–5 cm above the EGJ, and they may infiltrate the esophago-gastric junction from above;
- Type II tumors (or true carcinomas of the cardia): the tumor epicenter arises within 1 cm above to 2 cm below the EGJ;
- Type III tumors (or subcardial gastric carcinoma): those where the epicenter is located 2–5 cm distal to the GEJ, and infiltrates the EG junction and distal esophagus from below.

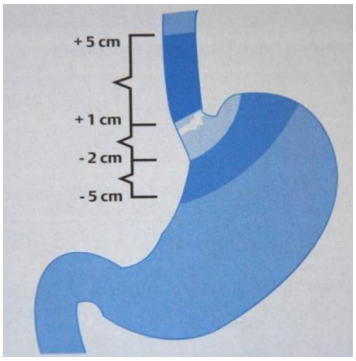

Figure 5: The Siewert classification. Image from Chevallay et al., 2018 [73].

The Siewert classification is widely used for preoperative assessment of the tumor location in order to plan the best surgical approach related to the fact these three types of tumor show different patterns of lymphatic dissemination [71], [74], [75].

The current 8th edition of American Joint Committee on Cancer (AJCC) staging manual guidelines [76] has introduced simplified categories including adenocarcinomas of the esophagus and esophagogastric junction in a single section [10] comprehending all tumors located in the distal thoracic esophagus, esophagogastric junction and within the first 5 cm of the stomach [77].
In the 5th edition of the World Health Organization (WHO) classification of digestive system [78] there is a change in anatomical definition of junctional esophageal adenocarcinoma which now are defined as all tumors with the epicenter within 20 mm (instead of 50 mm) proximal or distal the esophagogastric junction. Cancers whose epicenter is more than 2 cm distal from the GEJ are staged using the stomach cancer TNM staging, even if the GEJ is involved [79].
This approach for classification is still controversial, since it does not take into account the molecular profiles and different biological behaviors imply that EAC may be consistently heterogeneous [75], [80]–[82].

1.4.2 The Lauren classification

The Lauren classification is a commonly used histopathological classification system originally designed for gastric adenocarcinomas [83], [84], whose prognostic value has been expanded to EACs too to stratify patients [85].

According to the Lauren classification EAC are divided into three subtypes (Figure 6):

- Intestinal type, which is mostly well to moderately differentiated and it forms glandular structures reminiscent of adenocarcinoma of the large intestine;
- Diffuse type, which is composed of poorly cohesive tumor cells with little or no gland formation, often containing various proportions of signet ring cells;
- Mixed type, which exhibits features of both intestinal and diffuse type carcinomas.

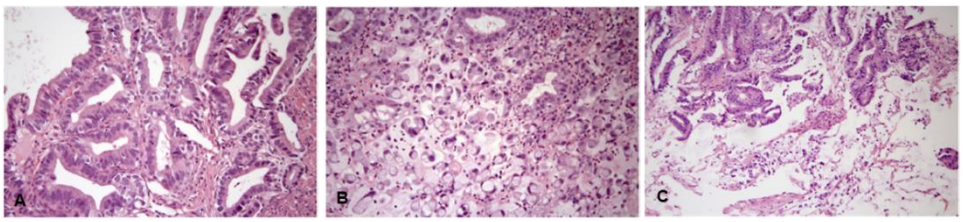

Figure 6: The three different subtypes of EAC according to the Lauren classification. **A.** Intestinal type; **B.** Diffuse type; **C.** Mixed type. Image from van der Kaaij et al., 2017 [85].

The majority of tumors can be classified as intestinal and it was shown a correlation between the histological subtype and overall survival: the EAC diffuse type has a more aggressive nature, has a higher risk of lymph node metastases and it is associated with a significantly worse prognosis compared with intestinal type tumors [85], [86]. Moreover, neo-adjuvant

chemo-radiotherapy appeared to be more effective in intestinal type carcinomas than diffuse/mixed type carcinomas [87].

1.4.3 Immunohistological classification of esophageal adenocarcinoma

A classification for EAC is based on the presence (+) /absence (-) of Barrett intestinal metaplasia (BIM) and gastric intestinal metaplasia (GIM) and on different immunoprofiles [75]. By assessing the presence or absence of BIM and GIM, three groups were defined for the esophageal and cardia adenocarcinomas: a Barrett's like type (BIM+GIM-), a gastric cancer–like (BIM-GIM+) and a cardiopyloric like type (BIM-GIM-). The BIM/ GIM subtypes categorization was further validated by the immunohistochemical IHC profile of these three groups: indeed, the expression pattern of tumor cytokeratin 7 (CK7) and cytokeratin 20 (CK20) was found to be related to the presence or absence of intestinal or gastric metaplasia [75].

Thus, three different immunoprofiles were identified:

- The greater expression of the Ck7 intestinal markers (CK7+/CK20-) in BIM+/GIM- defines the Barrett's esophagus-like type;
- The gastric cancer–like type (BIM-GIM+) is characterized by a CK7-/CK20+ pattern;
- The cardiopyloric like type (BIM-GIM-) has a mixed profile (CK7+/CK20+).

As described in the literature, different immunoprofiles have consequences on the tumor behavior: according to the presence or absence of BIM and GIM in the esophagus and cardia, EAC show different patterns of lymph nodes metastatic spread [82].

Also, the BIM-/GIM- group includes patients with higher stage (III-IV) tumors and a more aggressive disease compared to the BIM+/GIM- ones. This is in agreement with the idea that EACs cannot always be treated as

unique pathological entity and always a GERD-related tumor and other pathogenic pathways should be taken into consideration [82].

1.4.4 The EACSGE histological classification

Recently, a novel histological classification based on morphologic features of esophageal/esophagogastric junction adenocarcinomas was developed by the anatomo-pathologists of our research group.

Seven morphologic subtypes were identified, based on the growth pattern and cytostructural characteristics, showing different degrees of aggressiveness (Unpublished data):

- Glandular Well Differentiated (GL-WD): the entire tumor has a glandular structure and no significant loss of intercellular cohesion is seen;
- Glandular Poorly Differentiated (GL-PD): glandular structure is lost in more than 10% of the tumor but intercellular cohesion is maintained;
- Mucinous Well Differentiated (M-WD): the mucinous component is present in at least 50% of the tumor and the growth pattern is exclusively expanding;
- Mucinous Poorly Differentiated (M-PD): characterized by the presence of poorly cohesive tumor cells, floating in extracellular mucin lakes; infiltrative growth pattern, it may have signet ring features;
- Diffuse Desmoplastic (D-D): poorly-cohesive cells infiltrating the wall and producing marked fibroblast-rich desmoplasia; signet ring cells are often limited to the most superficial part of the tumor;
- Diffuse Anaplastic (D-A): poorly-cohesive cells which with an infiltrative growth pattern and frequent angioinvasion; no signet ring features;

- Mixed (Mix): admixture of glandular aspects and poorly-cohesive cellular components.

Based on survival curves this classification allows the discrimination of two major prognostic groups the Low grade carcinomas group (including GL-WD, M-WD and D-D subtypes) (FIGURE) and the High grade carcinomas group (which includes GL-PD, M-PD, DA and Mix subtypes) (Figure 7).

This classification has proved to have a statistically significant prognostic impact, especially if coupled with stage. Indeed, the stage plus histotype combination shows a high discriminating power for cancer specific survival, ranging from 86.9% to 0% at 5 years, depending on histologic subtype.

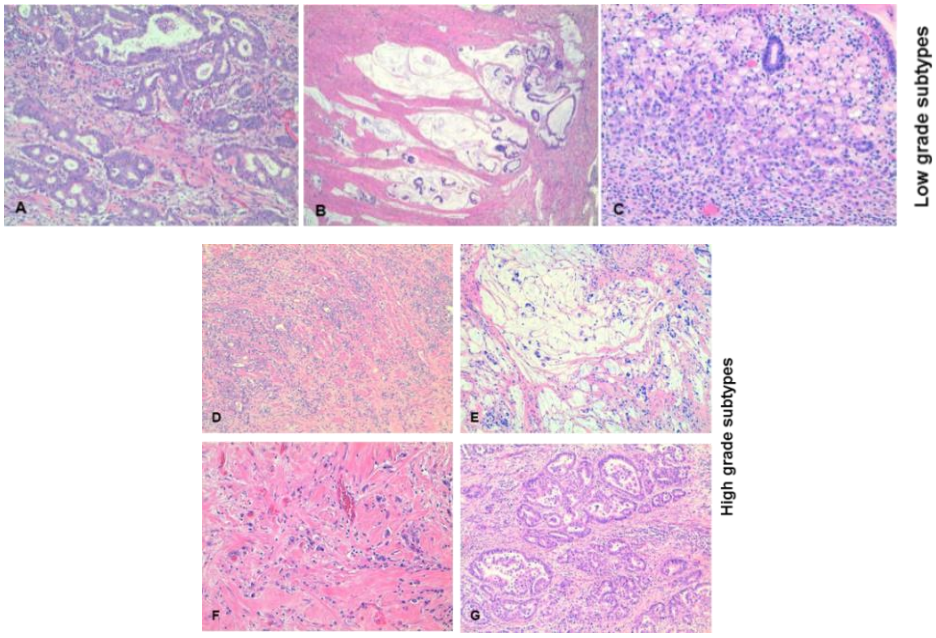

Figure 7: The EACSGE histologic classification. Haematoxylin eosin stain of EAC histotypes assigned according to the EACSGE classification. **A.** Glandular well differentiated; **B.** Mucinous well differentiated; **C.** Diffuse desmoplastic; **D.** Glandular poorly differentiated; **E.** Mucinous poorly differentiated; **F.** Diffuse anaplastic; **G.** Mixed. By kind permission of Professor Roberto Fiocca.

1.5 Unraveling the genomic signature of EAC

As cancer is a highly heterogeneous disease that arises from complex genetic and epigenetic alterations, it is crucial to identify the molecular events underlying each cancer, for the optimization of treatment decisions and the improvement of patient outcomes. The advent of high throughput molecular tools in the past two decades has enabled us to visualize the most relevant molecular features, in order to better understand the behavior of each cancer and then categorize them in sub-types based on genetics and expression characteristics in addition to the classical histologic classification in a perspective of "personalized oncology".

With a next generation sequencing (NGS) approach, genomic analysis performed on EAC samples provided a deeper understanding of the tumorigenic process, enabling the identification of recurrent genetic alterations and specific signaling pathways associated with EAC.
Whole exome (WES) and whole genome (WGS) sequencing allowed the identification of somatic structural rearrangements, copy number alterations (CNA) and single-nucleotide mutations, suggesting a high heterogeneity in EAC, with chromosomal instability and subsequent genome doubling constituting a defining characteristic of EAC. Genome instability is proposed to occur as an early event in EAC tumorigenesis [11], [88].
Chromosomal instability is characterized by DNA aneuploidy, structural changes of chromosomes (i.e. translocations) and mutations in various proto-oncogenes and tumor suppressor genes [89]. Based on a study where more than 3000 cancers and 27 tumor types were compared, EAC was included in a group of tumors with the most frequent CNA [90], [91].
In EAC the median frequency of chromosomal rearrangements was reported at 172 per tumor (range of 77-402). Approximately 20% of these

rearrangements were classified as inter-chromosomal translocations [92] These studies outlined complex structural and whole chromosome abnormalities in EAC.

In the initial systematic WES study that included 149 paired samples of EAC tumor and normal tissue, Dulak and colleagues identified 26 genes with significantly recurring mutations among which *TP53* (72%), *ELMO1* (25%), *DOCK2* (12%), *CDKN2A*(12%), *ARID1A* (9%), *SMAD4* (8%) and *PIK3CA* (6%); they also found amplifications in *KRAS* (21%), *HER2* (19%), *EGFR* (16%), *CCND1* (10%) and *MET* (6%), and loss of *SMAD4* (34%), *CDKN2A* (32%) and *ARID1A* (10%) [92].
A pattern of A>C transversions at AA dinucleotides was the most frequent type of mutation in EAC [92], [93].

Secrier and colleagues reported a WGS analysis on 129 EAC samples, proposing a mutational signatures classification with potential therapeutic relevance [94]:

- mutagenic: characterized by a dominant T>G mutational pattern associated with a high mutational load and neoantigen burden;
- DNA damage repair (DDR)-impaired: with enrichment for BRCA signatures with prevalent defects in the homologous recombination pathway;
- C>A/T mutational pattern: with evidence of aging imprint.

Receptor tyrosine kinases (RTKs) were frequently found co-amplified in EAC (potentially explaining the low success rate of RTK monotherapies) and these events showed a higher prevalence in the C>A/T dominant subgroup. Very few genes are recurrently altered by point mutations, supporting the idea that most gene alterations are the result of chromosomal instability [94].

Although the considerable level of genetic heterogeneity, *TP53* is the most frequently mutated gene in EACs, as reported in the study conducted by The Cancer Genome Atlas (TCGA) Research Network. The study also revealed high frequency of mutation in *CDKN2A,* whose level of inactivation increased up to 76% when considering also epigenetic silencing [11]. The cell cycle pathway is also affected by amplification of *CDK6, CCNE1* and *CCND1* genes, that encode for protein kinases and cyclins involved in cell cycle regulation [11], [95].

Among other frequently amplified genes, we can find *MYC* (in approximately 30% EACs), which regulates proliferation [96] and receptor tyrosine kinases (RTKs) of the *EGFR* family and their downstream mediators. Amplification of the *ERBB2* gene (32% of EACs) and *EGFR* gene (15% cases) [92] can activate the phosphatidylinositol-3-kinase (PI3K) pathway [96] which can be further altered by mutations in *PI3KCA*, *PI3KR1* and *PTEN* [88]. In addition, EACs shows amplifications of *KRAS VEGFA*, *FGFR2*, *IGF1R*, and *MET* genes [11], [88]. Another major dysregulated pathway in EAC is the is the transforming growth factor beta (TGFβ), which is involved in cell growth, development, differentiation, apoptosis, and inhibition of proliferation and inflammation in normal tissues [97], [98]. The TGFβ pathway can promote epithelial to mesenchimal transition, invasion and metastasis during EAC development [99]. EAC is characterized by increased expression levels of BMP4 that is thought to promote invasive phenotype. Bone morphogenetic proteins (BMPs) belong to the TGFβ superfamily, and are involved in a wide range of biological processes [100], [101]. During esophageal embryogenesis BMP4 is involved in the columnar epithelial stage but it is not present in the adult esophagus [102]. Serial analysis of gene expression (SAGE) of Barrett's sections from patients compared to normal controls revealed that BMP4 is highly up-regulated in BE [103] and that BMP4 signaling is activated as demonstrated by the presence of its downstream targets, pSMAD1/5/8 and ID2 [104]. BMP4 and its targets are also present in the

GERD inflamed squamous epithelium [104], [105]. Notably, exposure to proinflammatory factors, such as bile salts, lead to an increased expression of *BMP4* [104], [106] and *TGFβ1* [107]. *TGFβ1* expression is also increased in advanced stages [108].
In contrast, TGFβ signal transducers (SMADs) are commonly lost in EAC, with *SMAD4* as one of the most altered gene [88]. The product of this gene forms transcription complexes with other members of the SMAD protein family and regulates TGFβ-mediated transcription [109] Loss of *SMAD4* is associated with a poorer outcome and propensity to cancer recurrence [110]. Although mutations in *SMAD4* are quite common events in EAC, the principal causes of reduced SMAD4 expression are represented by promoter hypermethylation or deletion and protein modifications [111].

Frequent loss of heterozygosity (LOH) events occur at 17p and 9p, that harbor *TP53* and *CDKN2A* tumor suppressor genes, and *TP53* LOH is associated to genomic doubling, circumstance that Stachler and colleagues observed to precede BE-EAC progression in the 62.5% of cases [112]. Nones and colleagues also showed that genomic catastrophes are frequent in EAC, with almost a third of cases undergoing chromothriptic events [93]. This disruptive process results in a sudden accumulation of chromosomal rearrangements, gains losses and breaks involving large regions of the genome, and may be explained by the high frequency of loss of wild-type *TP53* and the great impact that it has on genomic instability [93].

These events could also explain why BE progression oftentimes does not fit into the classical linear multistep process. BE was found to be polyclonal and highly mutated even in the absence of dysplasia [93]. At the same time, comparing adjacent EAC and BE, less than 20% of the mutational profiles overlap [96]. This seems conflicting with studies showing that many mutations in EAC are already present in BE [113]. The reason for

this discrepancy may possibly be attributable to clonal variations and the presence of dysplastic cells in analyzed specimens. There are different pathways through which BE can progress to EAC, but suddenly tumor evolution can dramatically accelerate [93], [114]. This may be attributable to the loss of *TP53* [112], genome doubling and chromosomal instability. The fast progression of EAC in some BE patients may be potentially explained by a high frequency of chromothripsis events that may cause catastrophic genome rearrangements at any stage [93], [114] (Figure 8).

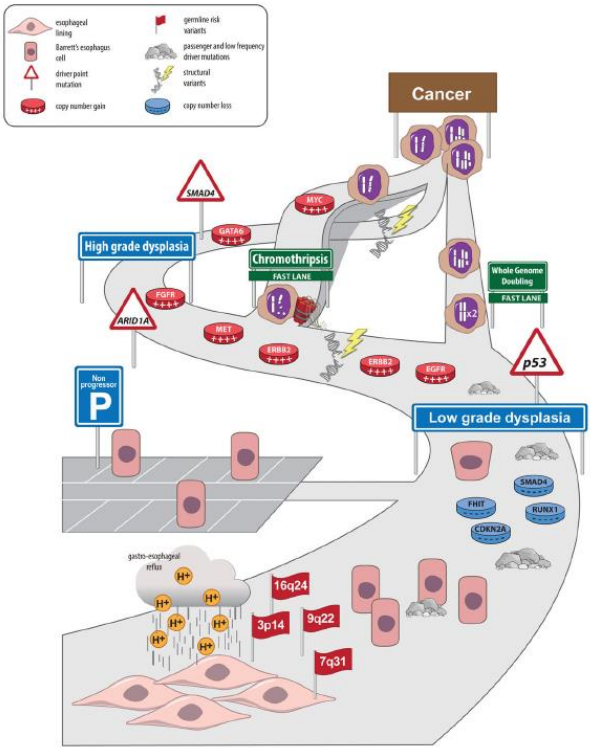

Figure 8: Paths of BE progression to EAC. Findings from next-generation sequencing studies indicate BE progression can accelerate via genome doubling, genome catastrophes, and other unknown mechanisms, even at early stages of tumor progression. Image from: Contino et al., 2017 [114].

Genetic alterations in EAC are accompanied by significant changes of the epigenome. Hypermethylation is present in 70% of EACs [11]. Epigenetic silencing through promoter methylation was found for the *CDKN2A* gene,

and also in *MGMT* and *CHFR* genes, for which methylation has been associated with responses to alkylating agents and microtubule inhibitors, respectively [11].
Tumorigenic process in the esophagus is characterized not only by hypermethylation of the CpG islands in BE compared to normal squamous epithelium, but also by decreasing DNA methylation outside of the CpG islands [115]. These two coexisting epigenetic phenomena force global transcriptome alterations that play significant roles in the development and progression of EAC [116]. Although promising, clinical application of these epigenetic biomarkers requires additional investigation.

The high degree of heterogeneity in EAC landscape may be responsible for its aggressiveness and its poor outcome, and also for the difficulty to date in finding targets for tailored therapies [88].

1.6 Investigating the genetic heterogeneity in EAC

The technological improvement that allowed to enter the Next Generation Sequencing era (NGS) has been with no doubt a significant revolution in the genetics field.
However, so far the NGS analyses carried out in EAC studies analyzed the DNA derived from the tumor sample as a whole, composed not only of tumor cells, but also of stromal and infiltrating immune cells. Therefore, loss of heterozygosity, copy number alterations and the true zygosity of somatic mutations in tumor cells could be masked by the presence of stromal cells and/or subclones with different mutational profile.
In order to solve this limitation, our research group combined NGS with high-throughput cell sorting technology that enables the recovery of

individual cells or specific subpopulation of interest from mixture samples and even from low cell count samples.

Taking advantage of one of these cell-sorting systems, called DEPArray™ (Menarini Silicon Biosystems) [117], a pilot study was conduct to assess the feasibility of the system to better investigate the genome complexity in FFPE EAC samples. The case analyzed in this study was a 53-year-old woman who underwent primary radical resection of a 2B HER-2-positive Barrett's type EAC, adjuvant chemo-radiotherapy, targeted HER-2 therapy and two-stage resection of chest metastases.

The selective sorting technology is based on fluorescence for vimentin and pan-cytokeratin in combination with the intensity of the DAPI signal (to evaluate cellular ploidy) and allowed to discriminate 9 cancer (CK+/VIM-) populations from 9 stromal cells populations (VIM+/CK-) present in the tumor tissue section.

Targeted NGS on tumor and stromal populations, performed using the OncoSeek panel, revealed that *TP53* was completely mutated in the EAC and metastatic clusters, while wild-type in the stromal cells, suggesting an early event of loss of heterozygosity (LOH) at the *TP53* locus.

Several LOH events were detected thanks to the purity of the sorted samples, involving *PDGFRA* and *KIT* on chromosome 4 and *CDK6* and *MET* on chromosome 7 in the primary EAC and metastases (Figure 9A).

Copy-number analysis of the sorted cell populations revealed a high level of *ERBB2* amplification in all tumor subpopulations, whose fold-change significantly decreased from the primary tumor to the two chest metastases developed after Trastuzumab therapy ($p < 0.01$ M2/PT, $p < 0.05$ M1/PT) (Figure 9B).

The parallel Whole Exome Sequencing (WES) performed on the primary EAC and the two metastases identified the somatic *TP53* missense mutation but at heterozygous state. Despite the "diluting" effect due to stromal cells, *ERBB2* amplification was revealed, even if at much lower rate due to normal cells contamination. It was also observed a focal

amplification in the second metastasis spanning *RNF146* and *ECHDC1* genes.

Thus, the synergic use of high-throughput sorting technology and NGS allowed to reveal the true tumor cell mutational status of the somatic mutations and CNVs, without a "diluting" effect due to the presence of stromal cells; and the progressive reduction of *ERBB2* copy-gains in the two recurrent metastases compared to the primary tumor, not detectable by immunohistochemistry. This is an important aspect from a therapeutic point of view because the lower copy number in the metastases indicates a selection of sub-clones more resistant to treatment.

Genomic information derived from cancer cell sub-populations could help understanding tumor progression and somatic phylogenesis. Combining these data with available clinical variables could further stratify patients, in order to select the ones with highest risk of malignant progression or for targeted therapies.

The data obtained from this research work were recently published [118].

A

				EAC primary site							
				stromal			tumor			gDNA	unsrt
	gene	var	event	L2057	L2065	L2612	L2056	L2066	L2613	L1839	L2058
1	PDGFRA	chr4:55149258:G:A	LOH	25.6	55.4	60.4	0.0	0.0	0.0	24.0	15.3
2	PDGFRA	chr4:55152040:C:T	LOH	60.3	41.4	94.6	100.0	100.0	0.0	94.3	90.1
3	KIT	chr4:55526615:C:T	LOH	63.6	67.7	63.8	100.0	100.0	100.0	75.9	83.9
4	KIT	chr4:55563683:T:G	LOH	11.2	40.4	71.2	100.0	100.0	100.0	67.5	91.3
5	KIT	chr4:55579081:G:A	LOH	65.2	70.6	59.5	0.0	0.0	0.0	36.4	66.7
6	KIT	chr4:55605075:A:G	LOH	0.0	42.3	100.0	75.0	100.0	100.0	34.0	71.6
7	CDK6	chr7:92285123:A:G	LOH	75.0	69.6	16.6	100.0	100.0	100.0	79.1	83.3
8	CDK6	chr7:92313733:A:G	LOH	38.3	82.6	56.6	0.0	0.0	0.0	38.7	17.8
9	CDK6	chr7:92333408:A:G	LOH	47.8	50.6	32.8	0.0	5.3	0.0	26.7	18.9
10	MET	chr7:116336947:C:T	LOH	80.5	34.7	10.4	100.0	100.0	100.0	79.9	64.6
11	MET	chr7:116336948:G:A	LOH	20.3	65.2	89.5	0.0	0.0	0.0	20.1	35.4
12	MET	chr7:116379094:C:T	LOH	84.6	55.6	23.7	100.0	100.0	100.0	83.5	50.0
13	TP53	chr17:7577094:G:A	SOM_HOM	0.0	0.0	0.0	100.0	99.4	90.9	49.9	55.8
14	ERBB2	chr17:37858678:A:G	amplification	76.1	53.0	38.8	99.3	99.0	99.4	97.8	98.2

B

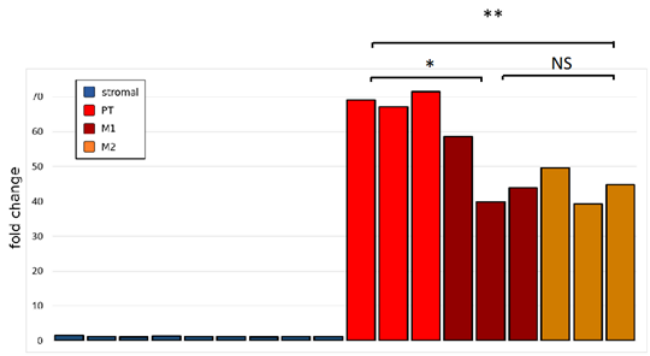

Figure 9: A. Variant identification in tumor (blue) and stromal (red) sorted cell populations from primary tumor, compared to unsorted sample (violet). Numeric values represent the alternative allele frequency. Several loss of heterozygosity (LOH) events were detected thanks to the purity of the sorted samples. **B.** Her-2 fold-change in all sorted pure populations (stromal and tumor) from primary tumor and the two metastases. CNV differences in the primary EAC and metastases. * = $p < 0.05$,** = $p < 0.001$, NS = not significant. Image modified from Isidori et al., 2018 [118].

1.7 The role of MicroRNAs in Esophageal Adenocarcinoma

1.7.1 MiRNAs regulate gene expression

Gene expression is the process through which the information carried by a gene is converted into functional macromolecules that allow the cell to differentiate, perform its functions and modify them in response to specific stimuli. Different systems in every step ensure a fine-tuned regulation of gene expression, during transcription, mRNA processing, translation, compartmentalization and activity of the synthesized protein. MicroRNAs (miRNAs) are a large class of single-stranded, non-coding RNAs of about 18-25 nucleotides length that, by binding a target mRNA in its 3'-UTR (UnTranslated Region), negatively regulate gene expression at post–transcriptional level, either inducing mRNA degradation or preventing translation [119], [120].

To date, 1917 miRNAs have been identified in humans (http://www.mirbase.org November 2020) and it is estimated that they are involved in the regulation in up of 60% genes [121]. A single miRNA is able to regulate the expression of different genes and the same gene can be regulated by different miRNAs.

MiRNA regulation of gene expression influences several cellular processes such as apoptosis, proliferation, cell differentiation, embryonic development, hematopoiesis, development and function of the nervous and immune systems [119], [122]. Each tissue is characterized by a specific set of miRNAs, based on the type of tissue and stage of development [123], [124].

1.7.2 MiRNAs biogenesis and mechanism of action

The production of a mature miRNA is divided into three phases: transcription and processing of larger ribonucleotide sequences in the nucleus, translocation into the cytoplasm, and maturation (Figure 10). miRNAs can be located either in intronic regions of a “host” gene [125], or in intragenic independent units with specific promoter elements and polyadenylation signals [126]. They can be encoded individually or in clusters, with formation of polycistronic transcripts.

A long precursor (pri-miRNA) is transcribed by RNA polymerase II [127]. It has a 5′ CAP, a 3′ polyadenylated tail and a "hairpin" secondary structure. Then the microprocessor complex, made up of the RNase III Drosha and the cofactor DGCR8, cuts the pri-miRNA to form a precursor called pre-miRNA [128], a double-stranded sequence of about 60-70 nucleotides also characterized by a hairpin structure [129].

The pre-miRNA is exported to the cytoplasm by the Ran-GTPase exportin-5 [130], where another type III RNase, DICER, cuts the hairpin generating a dsRNA molecule of 19-22 bp that contains the mature miRNA (guide strand) and its complementary miRNA* [131]. Mature miRNAs can be found on both strands of duplex RNA, but because of thermodynamic properties, only one strand (mature miRNA) is loaded on the RNA-Induced Silencing Complex (RISC) whereas the other strand is degraded [132]. If both strands of the duplex are functional miRNA, they are denoted with a -3p or -5p suffix.

The RISC complex directs mature miRNA to its target mRNA to allow direct repression [133]. The recognition between a miRNA and its target mRNA occurs through the 5′ end "seed region" of the miRNA (of about 2-8 nucleotides) that pairs with the binding site on the 3′ UTR of the target mRNA, inducing its degradation or inhibiting its translation [119], [134].

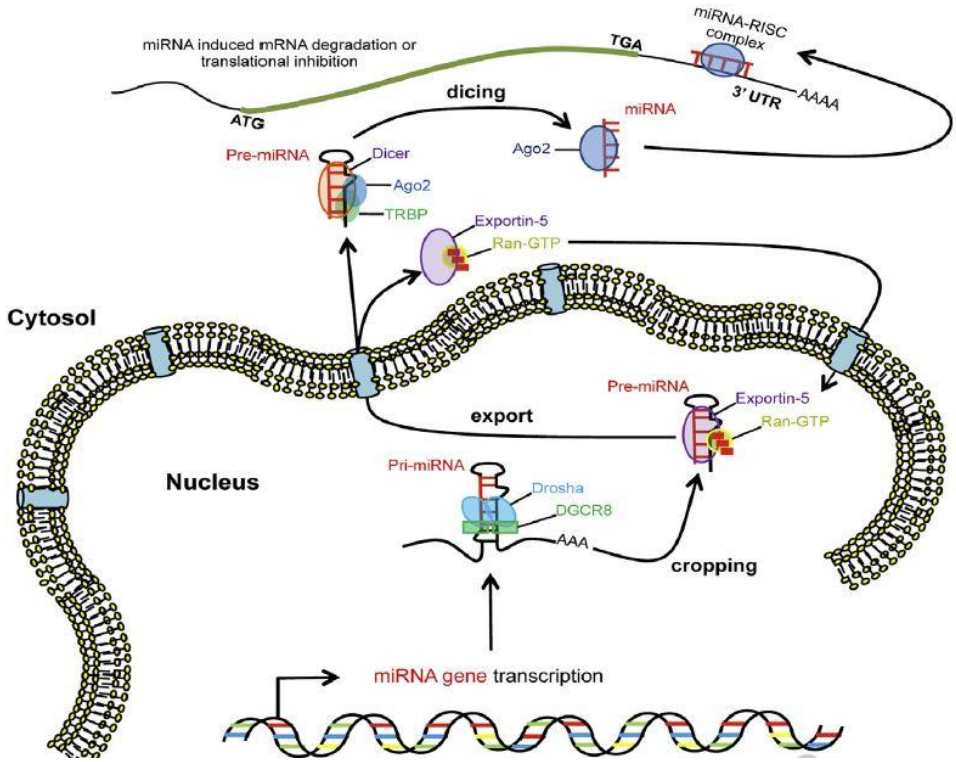

Figure 10: Schematic representation of miRNA biogenesis and miR-RISC activity. Image from Acunzo et al., 2015 [135].

1.7.3 MicroRNA and cancer

The first clue that linked miRNAs and cancer derived from a study on Chronic Lymphocytic Leukemia (CLL) [136]. It was discovered that the miR15a/16-1 cluster is frequently deleted in CLL, concluding that these two microRNAs have a tumor suppressor activity. This finding triggered numerous studies that revealed a differential miRNA expression not only between normal and tumor tissue, but also between primary and metastatic tumor. These differences are tumor-specific and in some cases associated with prognosis [135].

It is the function performed by the target transcripts that determines whether a miRNA is to be considered oncogene or tumor suppressor [137], [138]. miRNAs will be more and more exploited as biological markers for diagnosis, prognosis, early detection of the origin of a tumor and as a target for therapeutic monitoring [135].

1.7.4 MiRNA profile in EAC

In the last years, the discovery of miRNAs that come into play at different steps of tumor progression has been an important topic in esophageal cancer research, however many studies focused on ESCC or esophageal cancer in general.

Investigating miRNAs in BE and EAC revealed a different expression of miRNAs among healthy, premalignant and tumor tissue in EAC. Feber and colleagues showed that miRNA expression profiles distinguished normal esophagus from EAC and that miR-21 expression was 3-5 folds increased in EAC compared to normal epithelia [139]. Smith and colleagues performed qPCR and microarrays analyses for miRNA expressions in healthy gastric and squamous esophageal epithelia, BE and EAC, identifying several differently expressed miRNAs in BE development and progression to EAC, including miR-215, miR-205, 203 194 145 143 and miR21 [140].

The study by Garman and colleagues indicated that miRNAs differ between squamous esophageal epithelium and BE/EAC but could not differentiate between BE and EAC patients [141].

Using miRNA sequencing analysis, another study identified 23 miRNAs involved in BE progression, four of them (miR-192, miR-194, miR-196a and miR-196b) with higher expression in BE patients who progressed to cancer compared to those who did not progress [142].

Several studies reported that many miRNAs were aberrantly expressed in BE/EAC tissues: among them miR-21, miR-25, miR-143, miR-145, miR-192, miR-194, miR-196a, miR-215,and miR-223 are found to be up-regulated, while miR-136, miR-203, and miR-205 are down-regulated compared to normal esophageal tissue [143], [144]. An increased expression of miR-194-5p and miR-215-5p appear to be specific for intestinal-type BE epithelia and has a high accuracy for BE detection, thus could be tested for non-endoscopic molecular diagnosis of BE [145].

A recent meta-analysis has shown that aberrant expression of specific miRNAs correlated with prognosis in EC, the presence of metastasis and tumor response to neoadjuvant therapies; in particular high tissue levels of miR-21, one of the most studied miRNA, seemed to correlate with poorer overall survival times in EC patients [146]. Other miRNA that seemed to have significantly prognostic value were miR-133a, miR-133b, miR-138, miR-203, and miR-655 [146]. However, this meta-analysis included both ESCC and EAC.

No data are available regarding specific miRNAs that could discriminate among different subtypes of EAC (i.e. different histological subgroups, or according to Lauren classification).

MicroRNAs might play an important role in the onset of BE and EAC, and it would be of great interest the identification of a miRNA signature specific for each disease stage, in order to identify diagnostic and prognostic biomarkers. Also, shedding light on their mechanisms of action

and targets will help understanding EAC pathogenesis and the identification of therapeutic targets.

Nonetheless, the research in EAC miRNA pathophysiology had to face many challenges. As an example, a recent systematic review evaluated that at least 105 miRNA were found to be dysregulated in BE onset and progression to EAC. However, only 24 of the 105 miRNAs have been identified in more than one study and validated with different techniques [147]. Interestingly, two miRNAs (miR127-3p and miR200) were reported as both up-regulated and down-regulated in BE. The lack of consistent studies and these discrepancies can be due to technical factors, i.e. a low miRNA yield obtained from serum samples or the lack of suitable endogenous miRNA controls, but also due to differences in samples type or a different microenvironment [147].

Moreover, a single miRNA can regulate a large number of genes, so it is not a surprise that in some circumstances they appear to have a diversity of functions, also contrasting. Indeed, certain miRNAs have been described as oncogenic in one scenario, but tumor suppressive in anothers [148], [149].

As an example, miR-125b is described to act as an oncomiR in the vast majority of hematologic malignancies and as a tumor suppressor in many solid tumors [148]. Therefore the classification of a miRNA as oncogenic or tumor suppressive is not straightforward, but it may depend on the context.

Only a deeper understanding of miRNA signaling network will help to overcome these issues and allow to take advantage of their great potential as clinical biomarkers and targets for tailored therapies.

In order to identity differential miRNAs profiles, our research group conducted a preliminary study microRNA expression in EAC. miRNA expression levels were evaluated in 8 EAC cases and two pools of 8 normal gastric tissues, using TaqMan MicroRNA Array card A2.1/B3 (Thermo

Fisher Scientific). A total of 754 human different miRNAs was screened, 26 miRNAs were accepted as significantly over expressed and 72 miRNAs were found significantly down-regulated (Figure 11A). Among them, miR-221 and miR-483-3p were selected based on public data available (miRBase: http://www.mirbase.org/). Both miR221 and miR483-3p resulted significantly up-regulated in our screening of EAC cases (Figure 11B), respectively showing a mean fold increase of 2.746 and 11.33.

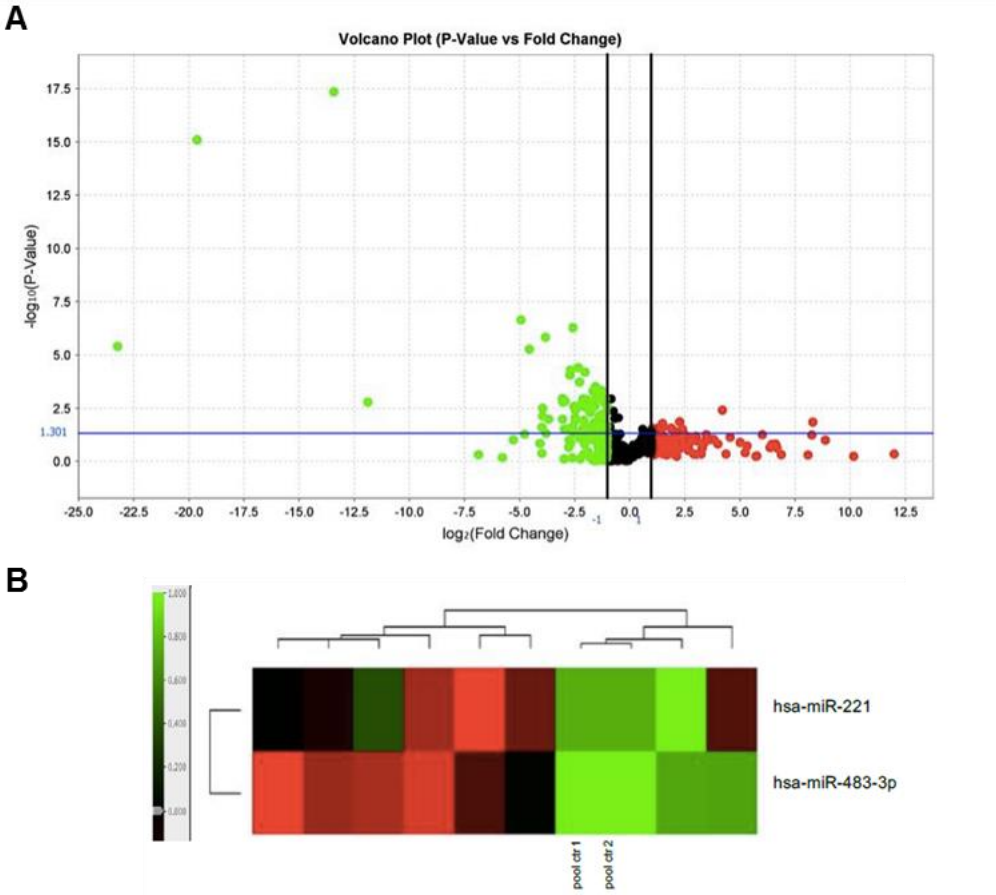

Figure 11: A. MicroRNA Array analysis shows deregulated miRNAs in EAC tissues versus healthy controls; miRNAs with down-regulated expression are shown in green, up-regulated ones in red. **B.** Differential expression of miR221 and miR483-3p in EAC samples versus controls. Unpublished data.

1.8 Prognosis and treatment of EAC

1.8.1 Prognosis

Esophageal adenocarcinoma is characterized by poor prognosis [150] Thanks to earlier tumor detection, BE surveillance, better surgical therapy, and the addition of neo-adjuvant chemotherapy or chemoradiotherapy, the 5-year survival has improved [151]–[153] from less than 5% in the 1960s to about 20%, but this value has not changed significantly over the past 20 years [150], [154].

This is in part related to late clinical presentation: indeed, due to the late presentation of symptoms and the aggressiveness of this malignancy, most patients present when regional metastases (30% of cases) or distant metastases (40% of cases) have already occurred [155], at which point the 5-year survival rate declines from 80.5% in the small proportion of EAC patients with stage I tumors, to 45.1%, 17.6% and, 2.1% for patients with stage II, III, and IV tumors, respectively [47]. Even with early stage cancer patients, often there is a high rate of lymphatic spread (due to the extensive lymphatic network in submucosa): 17% of Tb1 tumors have positive lymph-nodes on resection, so there is high rate of local and distant recurrence [154].

1.8.2 Surgery and neoadjuvant therapy

Surgical resection is still the first-line therapy of the overall treatment regimen of EAC. Based on tumor characteristics and location, endoscopic mucosal resection should be preferred for patients with BE, Tis (high-grade dysplasia, carcinoma in situ), T1a and T1b tumors without lymphovascular invasion [156], [157]. For T1b tumors that have entered the submucosa, there is a 20% risk of lymph-node spreading, so radical esophagectomy is the method of election [158]. The standard of care for

advanced tumors instead is a multimodal treatment combining esophagectomy with neoadjuvant therapy [159]–[161].
Numerous phase III randomized clinical trials have established the utility of combining perioperative chemotherapy to surgery compared with surgery alone, among them the MAGIC (Medical Research Council (MRC) Adjuvant Gastric Infusional Chemotherapy) [162], ACCORD (Actions Concertées dans les Cancer Colorectaux et Digestifs) [163], and OE02 (MRC oesophageal working group) [164] trials were landmark studies that demonstrated a significant survival advantage in the perioperative chemotherapy group. Subsequent studies have shown similar results in the FLOT-4 (fluorouracil, leucovorin, oxaliplatin, and docetaxel) trial [87], [165], which reported a superior advantage of a docetaxol-based regimen.

Many U.S. institutions are now adopting neoadjuvant chemo-radiotherapy as the standard approach. The Dutch Chemoradiotherapy for Oesophageal Cancer Followed by Surgery Study (CROSS) trial was the reference study, in which randomized patients with resectable lesions of the esophagus or GE junction received carboplatin and paclitaxel with concurrent radiotherapy followed by surgery or surgery alone [160]. This was the first study to demonstrate the potential benefit of concomitant chemo and radiotherapy to improve loco-regional control and improve the rate of complete resection. Long-term results have showed a statistically significant increase in survival. On the basis of these results, the CROSS regimen is now a standard treatment in many countries [166].

1.8.3 Targeted therapies

Targeted therapies are based on the idea of using drugs that can inhibit specific molecules that are overexpressed in an individual patient's tumor. EAC is molecularly heterogeneous [92], making targeted therapies problematic. Many agents have been trialled in the EAC, but so far only

two molecules have been approved for treatment in the metastatic setting, Trastuzumab and Ramucirumab [167].

Trastuzumab is a humanized monoclonal antibody against HER2, and it is the standard of care for patients with HER2 positive breast cancer [168]. HER2, (also known as ERBB2) is a member of the human epidermal growth factor receptor (EGFR) family of proteins and a transmembrane tyrosine-kinase receptor involved in cell proliferation, differentiation, and survival [169].
HER2 amplification has been reported in 20-30% of EAC cases, and it is a poor prognostic indicator [170], [171].
The ToGA (Trastuzumab for Gastric Cancer) trial demonstrated that Trastuzumab, combined with chemotherapy, increased overall survival and progression-free survival [172] in patients with advanced gastroesophageal adenocarcinoma and confirmed overexpression of HER2 [173]. Unfortunately, Trastuzumab clinical effect is limited as primary resistance is common and acquired resistance develops quickly [174].
The second FDA-approved biological agent is Ramucirumab, an igG1 monoclonal antibody targeting human vascular endothelial growth factor receptor 2 (VEGFR-2). Ramucirumab showed survival advantage in two randomized phase-III trials, REGARD (Ramucirumab monotherapy for previously treated advanced gastric or gastro-oesophageal junction adenocarcinoma) and RAINBOW (Ramucirumab plus paclitaxel versus placebo plus paclitaxel in patients with previously treated advanced gastric or gastro-oesophageal junction adenocarcinoma) and it was approved in combination with paclitaxel in the second-line setting [175].

Crizotinib is a small molecule inhibitor that showed a promising response in MET-amplified gastroesophageal adenocarcinoma patients [176]. The selective inhibition of MET using AMG-337 also showed anti-tumor activity in MET-positive patients [177], [178].

Given its essential role in tumor suppression and chemotherapeutic drug response, targeting mutant p53 is another major approach in therapies. This could be achieved by restoring wild-type p53 activity, inhibiting the gain of function of p53 mutants, or targeting p53 mutant stability. Among the most investigated compounds there are PRIMA-1 and its derivative PRIMA-1met APR-246, tested to restore activity of mutant p53 [179]–[181]. APR-246 has been tested on EAC cells and seems either to induce apoptosis and to reduce chemoresistance, selectively targeting cancer cells with p53 accumulation, thus having a limited cytotoxic effect on normal cells [182], [183]

Both PRIMA-1 and APR246 are being evaluated in clinical trials [184]. An initial phase I clinical trial has shown APR-246 to be safe in humans. Phase Ib/II study evaluating the efficacy of APR-246 in the treatment of advanced and metastatic esophageal or gastro-esophageal junction cancers is currently ongoing [185].

1.8.4 Immunotherapy

A big step forward in EAC treatment is immunotherapy. Cancer immunotherapy uses monoclonal antibodies direct against immune checkpoint proteins to enable T-cell recognition of tumor cells, and delivers the antitumor immune response [186].

Under physiological conditions, PD-1 (programmed cell death 1) suppresses the function of T-cells, thus preventing autoimmunity. Tumor cells are able to overexpress PD-1, decreasing T-cell-driven anti-tumor response [187]. Pembrolizumab is a monoclonal antibody approved by the FDA that binds T-cell surface receptor PD1. The KEYNOTE-028 trial showed promising outcomes for patients with advanced gastric and gastroesophageal cancers treated with Pembrolizumab, with manageable toxicity and durable antitumor activity in 40% of EAC [188].

2. AIMS

Esophageal adenocarcinoma is one of the cancers with the highest mutation rate [92], and data sequencing of multiple regions from the same tumor revealed that EAC is characterized by a high level of spatial and temporal heterogeneity [189].

However, unlike other types of cancers, where the characterization of specific subtypes with therapeutic implications has been possible, we still have a poor understanding of the clinical significance of EAC heterogeneity. Hence, a major key question is still open: what can we learn from the genetic and epigenetic diversity of EACs in order to make a clinically useful classification, ameliorate the response to conventional therapies and boost tailored targeted therapies?

Only a deep molecular characterization will allow clarifying these unresolved controversies.

In order to resolve the high intra- and inter-tumor heterogeneity and to correlate the molecular profile of tumors to clinical outcomes, such as histotype, recurrence and survival, the aims of this research project were:

- to define the somatic mutational profile of EAC, analyzing inter- and intra- tumor heterogeneity;
- to evaluate EAC at epigenetic level, focusing on the expression profile of some candidate microRNAs (miRNAs) identified in previous studies,

in the attempt to identify biological markers that allow to classify types of homogeneous neoplasms.

Therefore, given the results of the pilot study performed, a **first aim** of this research project was to expand the genetic analysis to a wider cohort:

through separation of normal and tumor cells with high-throughput sorting systems in combination with NGS technology, the main goal is to evaluate intra and inter tumor heterogeneity and deeply characterize different cancer cell populations, that can be linked to different clinical outcomes, i.e. recurrence and survival. A cohort of 37 EAC patients who underwent primary surgical resection without neoadjuvant therapy has been screened, in the attempt to better understand the genetic landscape in such heterogenic type of cancer.

The **second aim** of this project was to evaluate the expression of miRNA483-3p and miRNA221, found aberrantly expressed in a previous study, in a larger cohort of EAC cases. Then, we checked for any correlation with different histological subtypes and/or clinical outcomes, and tried to identify specific targets and pathways of action.

3. MATERIALS AND METHODS

All the studies were approved (# L3P1223) by the Ethical Committee "Comitato Etico IRST IRCCS AVR (CEIIAV)"- Italy (Reg. Sper. 109/2016 Protocol 7353/51/2016) and written informed consent was obtained from all patients.

3.1 Genetic analysis of esophageal adenocarcinoma with DEPArray

3.1.1 Sample recruitment

The formalin fixed paraffin embedded (FFPE) surgical specimens used for the analysis derived from 38 EAC patients who underwent primary esophagectomy, with no neoadjuvant therapy. Tumor area was defined through hematoxylin-eosin stain. Clinical features are summarized in Table 1, Chapter 7.

3.1.2 Cells dissociation, DNA quality control and cell sorting with DEPArray™

According to manufacturer's protocol, to obtain the cell suspension to load on the DEPArray (Menarini Silicon Biosystems) a 50-µm FFPE section was collected in a nylon biopsy bag and inside a 50-ml conical tube, dewaxed and rehydrated. After 5 min at room Temperature (RT) in 10 mM sodium citrate buffer (pH 6.4) the section was heat-treated in the same pre-warmed buffer for 1 h at 80°C. The section was cooled down at RT and washed three times in RPMI medium (Life Technologies, Carlsbad, CA, USA) for 5 minutes. Dissociation was performed incubating the section in

10 ml of a 0.1% collagenase I-A (Sigma-Aldrich, St. Louis, MO, USA), 0.1% dispase (Life Technologies) solution at 37°C for 45 minutes. The resuspended cells were transferred through a 30-µm mesh nylon filter into a 15-ml conical tube. After two washes in ice-cold PBATw (PBS 1% BSA 0.05% Tween20 buffer) and centrifugation at 1000 g for 5 min, the pellet was resuspended in 1 ml of ice-cold PBATw. An aliquot of 5×10^5 cells was incubated 30 minutes at 4°C with 100 µl of the primary monoclonal antibody mixture made up of anti-keratin (CK) MNF116, IgG1 (DAKO, Glostrup, Denmark) (final concentration 3.2 µg/ml), anti-keratin (CK) AE1/AE3, IgG1 (Millipore–Chemicon, Burlington, Massachusetts, USA) (final concentration 10 µg/ml) and anti-vimentin (VIM) 3B4, IgG2a (DAKO) (final concentration = 3.1 µg/ml) in PBATw. Cells were washed twice with ice-cold PBATw and incubated with 60 min in the dark at 4°C in 100 µl of premixed secondary reagents made up of: Alexa Fluor® 488 Goat Anti-Mouse IgG1 (Life Technologies), for keratin detection and Alexa Fluor® 647 Goat Anti-Mouse IgG2a (Life Technologies) for vimentin detection, both to a final concentration of 2.5 µg/ml. Cells were washed twice and incubated in a DNA staining solution containing 10 µM DAPI (Sigma-Aldrich) in PBATw, for 30 min at 37°C. After two washes and 5 min centrifugation at 1000 g, the pellet was resuspended in PBATw.

Before cell sorting, the DNA integrity was assessed using the DEPArray™ FFPE QC Kit (Menarini Silicon Biosystems), a qPCR-based assay that provides a QC score to evaluate the sample quality. QC score should be ≥0.20 for optimal NGS analysis. This value was used to determine, after cell sorting, the effectively amplifiable template (EAT), calculated multiplying the QC score times ploidy, times number of cells recovered.

The DEPArray™ technology (Menarini Silicon Biosystems) takes advantage of a non-uniform electric field to wield neutral, polarizable particles.

For the sorting, labeled cell suspension was washed twice with 1 ml of SB115 buffer (Menarini Silicon Biosystems) and approximately 24000 cells were loaded into the DEPArray™ A300K cartridge (Menarini Silicon Biosystems) and trapped in dielectrophoretic (DEP) cages. Different cells are discriminated using immunofluorescent staining, DNA content and LED optical imaging and then are driven to a collection tube by mobilizing DEP cages.

Homogeneous tumor cell populations (CK+/VIM-) stromal populations (VIM+/CK-), and a pool of unsorted cell were recovered (Figure 12).

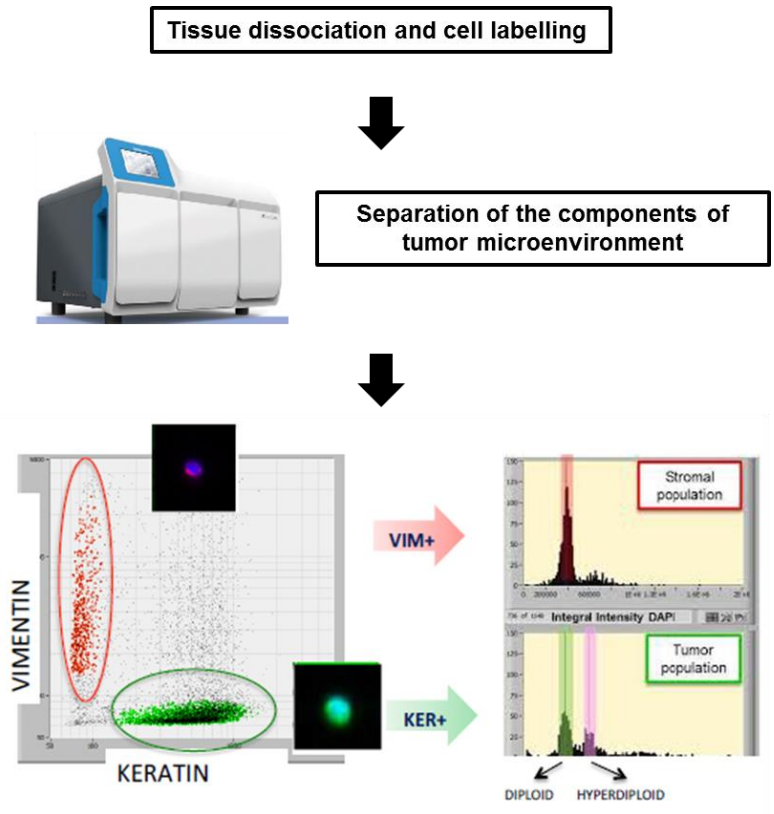

Figure 12: Schemating representation of DEPArray Digital Cell Sorting workflow. After a step of dissociation of the FFPE tissue and the labelling of the resuspended cells, the obtained material was processed using the DEPArray platform. Stromal and tumor cell populations were sorted based on their DNA content and on fluorescence of antibodies against vimentin/pan-cytokeratin.

3.1.3 OncoSeek panel genetic analysis

The DEPArray™ OncoSeek Panel (Menarini Silicon Biosystems) generated Illumina-compatible, targeted libraries from sorted cell lysates, for the detection of single nucleotide variants (SNVs), indels and copy number alterations (CNAs) from 63 oncology-related genes (Table 2 Chapter 7). According to the manufacturer's protocol, libraries were diluted 1:10,000, quantified in triplicate using the KAPA Library Quantification Kit (Hoffmann-La Roche, Basilea, Switzerland), then pooled together and loaded on a MiSeq instrument (Illumina Inc., San Diego, CA, USA).

The bioinformatics analysis, either for SNVs and CNAa detection, was performed according to pipeline, either on sorted (stromal and tumor) cell population and on unsorted cells (whole tumor) [118].

3.1.4 CNA analysis through Whole-Genome Low-Pass sequencing

Recovered cells were lysed according SB LysePrep™ Kit (Menarini Silicon Biosystems) and the obtained sample underwent fragmentation by Covaris M220 (Covaris, Woburn, Massachusetts, USA) for 3 min and 52 sec (pick power:50, duty factor:20,cycles/burst:200) to obtain a 150–200 bp fragment size.

Libraries were prepared using Accel-NGS® 2S PCR-Free DNA Library kit (Swift Biosciences, Ann Arbor, MI, USA) according to the manufacturer's instructions. 20 µl of library were amplified with 2×KAPA HiFi HotStart Ready Mix (Hoffman-La Roche), 6 µM each of Amplicon PCR Forward and Reverse primers (primers sequence reported in Chapter 7, Table 3) under the following conditions:

Hold	98 °C	45”
15 cycles	98 °C	15”
	60 °C	30”
	72 °C	1’
Hold	72 °C	1’

After a clean-up with 0.75X Agencourt AMPure XP beads (Beckman Coulter Genomics, Chaska, USA), the libraries were eluted in 20 µl Low TE (Swift Biosciences), normalized and pooled to 4 nM based on qPCR quantification. Pooled libraries were denatured and brought to a 12 pM final concentration. Sequencing was performed on the MiSeq instrument using 2 × 100 bp paired-end sequencing with the MiSeq Reagent Kit V3 (Illumina).

Bioinformatics data analysis was performed according to pipeline [118].

3.1.5 Whole Exome Sequencing (WES)

Whole Exome Sequencing was performed on 8 EAC samples of the previous cohort described.

DNA was extracted from 3, 10-µm thick, FFPE sections using the QIAMP DNA Mini Kit (Qiagen, Hilden, Germany) according to manufacturer’s protocol.

Dual-index, paired-end libraries were prepared using the Nextera Rapid Capture Exome Kit (Illumina), according to protocol. The first step was the enzymatic preparation, where 150 ng of genomic DNA were tagmented to obtain 250-300 bp DNA fragments with adapter sequences added. A step of PCR amplification (10 cycles) incorporated unique index for each sample. After purification, the single DNA libraries were run on 2100 Bioanalyzer DNA 1000 chip (Agilent Technologies, Santa Clara, California, USA) to confirm the appropriate size and quantified using Qubit dsDNA BR Assay Kit (ThermoFisher Scientific, Waltham, Massachusetts, USA).

For exome enrichment, 500 ng of each library preparation was pooled in groups of 8 samples to perform hybridization with capture probes for 16 hours at 58°C. The hybridized regions were separated from the non-bound products through streptavidin magnetic beads-capture and wash and elution steps. The enriched library pools were checked for quantity and size with Qubit dsDNA HS Assay kit (ThermoFisher Scientific) and 2100 Bioanalyzer High Sensitivity DNA (Agilent Technologies) respectively.
Each pool was normalized to 1.3 pM and then sequenced on an Illumina NextSeq500 platform (Illumina) at 150 bp paired ends.

3.1.6 Bioinformatics analysis of WES data

The bioinformatics analysis of retrieved data was performed according to the internal pipeline available in our research laboratory [190].
Through a process called annotation, for each variant key information was reported, such as: the genomic position with respect to the reference sequence of the hg19 human genome, the gene harboring the variant, the nucleotide sequence change, the type of mutation (insertion, deletion, SNP) and the consequence (missense, non-sense, synonym, frameshift), the frequency in the population and a prediction of pathogenicity based on in-silico programs such as Poly-phen-2 and SIFT.
To identify candidate mutations for EAC, the annotated variants were then filtered using few parameters:

- PASS variant
- Minor Allele Frequency (MAF) < 0.01
- Type of variant (intronic and UTR variants were excluded)
- Prediction of pathogenicity based on in-silico programs, in particular Poly-phen-2 (http://genetics.bwh.harvard.edu/pph2/) and SIFT (https://sift.bii.a-star.edu.sg/) for missense variants, Provean (http://provean.jcvi.org/index.php) for inframe variants and ESEfinder3.0 (http://krainer01.cshl.edu/cgi-

bin/tools/ESE3/esefinder.cgi?process=home) for splicing or synonym variants.

All the variants were individually checked using Integrative Genomics Viewer (IGV) software to exclude false positives [191].

3.1.7 Variants confirmation through Sanger sequencing

To validate our result with an independent technique, Sanger sequencing was performed for few identified variants. Starting from the extracted genomic DNA, PCR amplification was performed using KAPA HiFi HotStart (Hoffman-La Roche) according to the manufacturer's protocol. The used primers are reported in Table 3, Chapter 7. After purification with 96-well multiscreen PCR (Millipore) PCR products were sequenced according to protocol using the BigDye v1.1 kit (ThermoFisher Scientific), in the 2720 Thermal Cycler (ThermoFisher Scientific) under the following conditions:

Hold	96°C	1'
35 cycles	96°C	10"
	60°C	4'

Sequencing reaction product were purified with Montage SEQ 96 plate (Millipore) and run on 3730 DNA Analyzer (Thermo Fisher Scientific). Electropherograms were visualized with Sequencer 4.7 (Gene Codes Corporation, Ann Arbor, MI, USA) or Chromas 2.0 (Chromas, Technelysium, South Brisbane, Australia).

3.1.8 Droplet digital PCR (ddPCR)

Assays for TP53_R273H (dHsaMDV2010109) and CDKN2A_R58* (dHsaMDS2512016) were set using the QX100/QX200 Droplet Digital

PCR (ddPCR) system (Bio-Rad, Hercules, California, USA) combining 50 ng of DNA from unsorted material with 2X ddPCR Supermix for Probes no dUTP (Bio-Rad), and 20X primer/probe mix in a final volume of 20 µl. Target mutant probe was FAM dyed, wild-type was HEX labeled and they were provided together in a single tube. Negative control, no-template reactions were performed for each experiment.

The reaction was loaded into a DG8 cartridge well (Bio-Rad) together with 70 µl of droplet generation oil (Bio-Rad) and placed in the droplet generator (Bio-Rad). The obtained product was transferred to a 96-well plate, heat-sealed with a foil seal and run with the following thermal cycling conditions:

Hold	95°C	10’
40 cycles	94°C	30”
	55°C	1’
Hold	98°C	10’
Ramp rate for each step: 2°C/sec		

Droplets were read using QX100/QX200 Droplet Reader (Bio-Rad), and the data were analyzed using QuantaSoft software (Bio-Rad).

3.1.9 Statistical analysis

Data were analyzed using SPSS (version 15.0; SPSS Inc., Chicago, IL, USA) or Prism (GraphPad Software Ins., California, USA).

Differences in frequency data were analyzed using Chi-square (χ^2) or Fisher’s tests as appropriate. Mann-Whitney test was used to analyze continuous variables. *P*-values <0.05 were considered significant. Cancer-specific survival was assessed using the Kaplan-Meier method and log-rank test. Comparison between histological subtypes and distribution of *TP53* mutations was performed with the Chi-square test for given

probabilities (R software package; R Project for Statistical Computing, Vienna, Austria), Bonferroni's correction was applied, and *P*-values <0.025 were considered significant.

3.2 EAC sequencing with an NGS custom panel enriching for cancer-related genes

3.2.1 Sample recruitment

The DNA samples analyzed were selected from those of EAC patients, surgically treated in 3 Italian Centers: Istituto Europeo di Oncologia (IEO), Milano, (14 cases); IRCCS Ospedale San Raffaele, Milano, (131 cases); Ospedale di Verona, Verona (24 cases) for a total of 169 samples. The inclusion criteria consisted in the presence of adenocarcinoma of the esophagogastric junction; no neoadjuvant treatment (chemioradiotherapy-naïve EACs). All surgical resections were formalin fixed, paraffin embedded (FFPE), examined by gastrointestinal pathologists and classified according to Lauren and the EACSGE histological classification (detailed clinical features are summarized in Table 1, Chapter 7).

3.2.2 Custom EAC Panel: library preparation, hybridization and sequencing

DNA was extracted from 2, 40-µm thick, FFPE sections using the QIAMP DNA Mini Kit (Qiagen) according to manufacturer's protocol.

Dual-index paired-end libraries were prepared using the lotus DNA library prep kit (IDT, Integrated DNA Technologies Inc. Coralville, Iowa, USA) according to manufacturer's instruction. The protocol followed 3 major steps: an enzymatic preparation, where fragmentation to obtain 300-350 bp DNA fragments, end –repair and dA tailing were performed; the ligation of stubby adapters, and PCR amplification for 11 cycles with indexing primers, in order to incorporate sample-unique indexing

sequences and P5 and P7 sequences to attach to stick to the flow-cell. After purification, the single DNA libraries were run on 3% agarose gel to confirm the appropriate size and quantified using Qubit dsDNA BR Assay Kit (ThermoFisher Scientific). 500 ng of each library preparation was pooled in groups of 16 samples to perform hybridization and enrichment for selected gene regions. This step was performed using xGen Lockdown probe pool and xGen hybridization capture of DNA libraries kit (IDT, Integrated DNA Technologies), according to protocol. Each pool of 16 samples was hybridized to the capture probes for 16 hours at 65°C. xGen Lockdown Probes are individually synthesized, 5′ biotinylated oligos, and were assembled in a custom panel of 28 genes for target capture. The genes selected for this study are listed in Table 4, Chapter 7.

The hybridized regions were then captured with streptavidin magnetic beads and, after the non-bound products removal, a post-capture PCR of 11 cycles was performed.

The enriched library pools were checked for quantity and size with Qubit dsDNA HS Assay kit (Thermo Fisher Scientific) and 2100 Bioanalyzer High Sensitivity DNA (Agilent Technologies) respectively.

Each pool was normalized to 1.3 pM and then sequenced on an Illumina NextSeq 500 platform (Illumina) at 150 bp paired ends. Bioinformatics and statistical analysis were performed as described above.

3.3 Analysis of the profile and functional studies of specific microRNA: miR483-3p and miR221

3.3.1 Sample recruitment

FFPE surgical resections from 112 patients diagnosed with esophageal adenocarcinoma but not treated with neoadjuvant therapy were collected (47 cases from Maria Cecilia Hospital, Cotignola, Italy; 8 cases from IRCCS Policlinico San Martino, Genova, Italy, 10 cases from Helsinki University

Central Hospital, Helsinki, Finland and 47 cases from The Academic Medical Center Hospital, Amsterdam, Netherlands). All tumors had full clinical and pathological data and were classified according to Lauren. 8 FFPE healthy gastric mucosa were used as control samples. Clinical features of all subjects are summed up in Table 1 Chapter 7.

3.3.2 Cell lines

OE19, OE33 and FLO-1 cell lines (Figure 13) were used to evaluate expression profiles of both miR483-3p and miR221 and perform functional studies.

Cell lines were provided by Professor Kausilia K. Krishnadath (Academic Medical Center Hospital, Amsterdam, Netherlands).

The OE19 cell line was established from an adenocarcinoma of gastric cardia/esophageal junction of a 72 year old male patient. The tumor, at pathological stage III (UICC), showed moderate differentiation [192], [193].

The OE33 cell line derived from a 73 year old female patient diagnosed with adenocarcinoma of the lower esophagus (Barrett's metaplasia). The tumor was identified as pathological stage IIA (UICC) and showed poor differentiation [192], [193].

The FLO-1 cell line was established from a primary distal esophageal adenocarcinoma (classified as pathological stage III, poorly differentiated) of a 68 years old Caucasian male [193], [194].

All cells were cultured in a 5% CO_2 incubator at 37°C.

Growth medium and storage conditions are described in Chapter 7 Table 5.

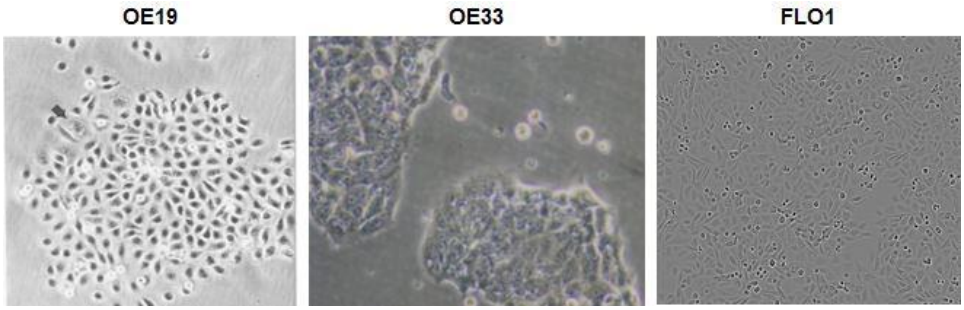

Figure 13: Three EAC cell lines (OE19, OE33, FLO1) were used for miRNAs analysis.

3.3.3 RNA isolation

Total RNA was extracted under RNase free conditions starting from 2, 10 μm thick FFPE sections enriched in tumor area, using Recover All Total Nucleic Acid Isolation for FFPE Kit (Thermo Fisher Scientific) and treated with *DNase I* (Thermo Fisher Scientific) following manufacturer's protocol.

Total RNA from cell lines was isolated using Invitrogen™ RiboPure™ RNA Purification Kit (Thermo Fisher Scientific) according to protocol.

RNA was stored at -80 °C; the yield was assessed through NanoDrop spectrophotometer reading (Thermo Fisher Scientific) and to ensure RNA good quality an aliquot was run on a 1% agarose gel.

3.3.4 Reverse transcription PCR and real-time quantitative PCR analysis (qPCR) for miRNA validation

The validation of miR221 and miR483-3p expression levels was performed through qPCR single assays using single TaqMan probes (Thermo Fisher Scientific).

Starting from 150 ng of total RNA from FFPE sections or cell lines, reverse transcription was performed using 5X miRNA primers (TaqMan MicroRNA Assay, Thermo Fisher Scientific) for miR221, miR483-3p and RNU44 (endogenous control), and using TaqMan MicroRNA Reverse

Transcription Kit according to manufacturer's instructions (Thermo Fisher Scientific).

A step of preamplification was performed combining 2.5 µl of the RT reaction, 20X specific primer pool for miR221, miR483-3p and RNU44 (#000524, #002339, #001094) and TaqMan PreAmp Master Mix in a final volume of 25 µl and run on the 2720 Thermal Cycler (Thermo Fisher Scientific) under the following conditions:

Hold	95°C	10'
Hold	55°C	2'
Hold	72°C	2'
12 cycles	95°C	15"
	60°C	4'
Hold	99°C	10'

The preamplification product was diluted 1:8 in TE 0.1X and 2 µl were combined with TaqMan Universal Master Mix II, No AmpErase UNG (2X) and the specific 20X TaqMan MicroRNA primers (described above). qPCR was run on 7500 Fast Real-Time PCR Systems (Thermo Fisher Scientific) using universal cycling conditions:

Hold	95°C	10'
40 cycles	95°C	15"
	60°C	1'

RNU44 was used as control to normalize the target miRNAs abundance in each sample. Each sample was run in triplicate. Relative miRNA expression levels were calculated using the ΔΔCT method, comparing FFPE tumor cases versus the pool of 8 tissues of healthy gastric mucosa, or

comparing cell lines versus a commercial pool of normal esophagus RNAs from 5 different donors (BioChain, Newark, CA, USA).

3.3.5 MiR483-3p mimic transfection with Lipofectamine 3000

mirVana™ miRNA mimics (Thermo Fisher Scientific) are small, chemically modified, double-stranded RNAs that mimic endogenous miRNAs and enable miRNA functional analysis by up-regulation of miRNA activity. To mimic and evaluate the effects of miR483-3p up-regulation, 0.25-0.3 $*10^6$ cells were seeded in a 6 well plate to be 80% confluent at transfection. 100 nM of either mirVana™ miR483-3p mimic or scramble control were transfected using Lipofectamine 3000 reagent (Thermo Fisher Scientific) according to protocol. Cells were incubated at 37°C at different time points then RNA was extracted as described in paragraph 3.3.3. To confirm that transfection successfully occurred the expression of miR483-3p was evaluated through qPCR single assays using single miR483-3p TaqMan probes (Thermo Fisher Scientific) as described in paragraph 3.3.4.

3.3.6 Reverse transcription PCR and qPCR analysis for genes of interest expression levels in cell lines

To evaluate expression level of the genes of interest *PUMA*, *SMAD4* and *CTNNB1* in EAC cell lines, 200 ng of total RNA, extracted from either tranfected or normal cells, was retrotranscribed with Maxima H Minus First Strand cDNA Synthesis Kit (Thermo Fisher Scientific). 10 ng of cDNA were used as template for qPCR reaction with PowerUp SYBR Green Master Mix (Thermo Fisher Scientific) and 500 nM of each Forward and Reverse specific primer, according to protocol. β-actin was used as endogenous control for abundance normalization in each sample. Primer sequences for each gene are reported in Table 3, Chapter 7. Each reaction

was performed in triplicate, and run on the 7500 Fast Real-Time PCR Systems (Thermo Fisher Scientific) under the following conditions:

Hold	50°C	2’
Hold	95°C	2’
40 cycles	95°C	3”
	60°C	30”

Relative gene expression levels were calculated using the ΔΔCT method using as normal control a commercial pool of normal esophagus RNAs from 5 different donors (BioChain, Newark, CA, USA).

3.3.7 Western blot

Cells were lysed in ice cold RIPA buffer: 50 mM HEPES (EuroClone S.P.A. Milan, Italy), 1 mM EDTA (Sigma-Aldrich), 10% glycerol (Thermo Fisher Scientific), 1% Triton X-100 (Sigma-Aldrich), 50 mM NaCl in presence of proteases and phosphatases inhibitors (Sigma-Aldrich). The Lowry assay (Bio-Rad) was used, according to protocol, to evaluate total proteins and 20 μg of protein sample were loaded onto 10% TGX Stain-Free™ Fastcast™ acrylamide gel (Bio-Rad). The gel was electrotransferred onto nitrocellulose membrane using Trans-Blot Turbo Transfer System (Bio-Rad). The membrane was subsequently blocked in Tris Buffered Saline (TBS), 1% Casein-TBS (Bio-Rad) for 1 hour at room temperature and incubated at 4°C 16 hours with anti-SMAD4 (mouse, 1:200, Santa Cruz Biotechnology, Dallas, Texas, USA) and anti-vinculin (mouse, 1:10,000; Cell Signalling, Leiden, Netherlands) primary antibodies. Membranes were washed three times in TBS 0.1% Tween and incubated with peroxidase-conjugated secondary antibodies (1:25000, Sigma-Aldrich) for 45 minutes at room temperature. Bands were revealed using WESTAR Supernova

(Cyanagen, Bologna, Italy) and detected with ChemiDoc™ XRS+ (Bio-Rad).

3.3.8 Statistical analysis

The ROC method was used to optimize cut-off values for miRNAs classification into a “high expression” and “low expression” groups.

qPCR analysis, correlations between miRNA expression and histological classification or clinical outcomes were investigated using Mann-Whitney and Kruskall-Wallis tests, t-Student’s test and Kaplan-Meier method, using Prism (GraphPad, San Diego, CA, USA). A *P*-value <0.05 was considered statistically significant.

4. RESULTS

4.1 High-throughput sorting and targeted sequencing of Esophageal Adenocarcinoma subpopulations unveil a complex mutational landscape

In order to characterize the genetic heterogeneity of esophageal adenocarcinoma, we started from archival material of 38 EAC patients, treated with surgery alone (Table 1, Chapter 7), to obtain different cell populations from the FFPE block using a high-throughput cell sorting technology [117], [195]. Immunoreactivity to antibodies against vimentin/pan-cytokeratin and DAPI fluorescence were used to separate tumor cell populations (CK+/VIM-) from the normal stromal one (VIM+/CK-). DNA was extracted from the sorted cell populations and the unsorted sample, and target sequencing was performed on 63 cancer-related genes using the OncoSeek Panel (Menarini Silicon Biosystems).

4.1.1 The landscape of somatic mutation in sorted populations

Data analysis revealed a total of 61 point mutations (missense, nonsense and frameshift) detected in the unsorted samples, while 9 additional somatic mutations were revealed by targeted sequencing of the sorted tumor populations (Figure 14).

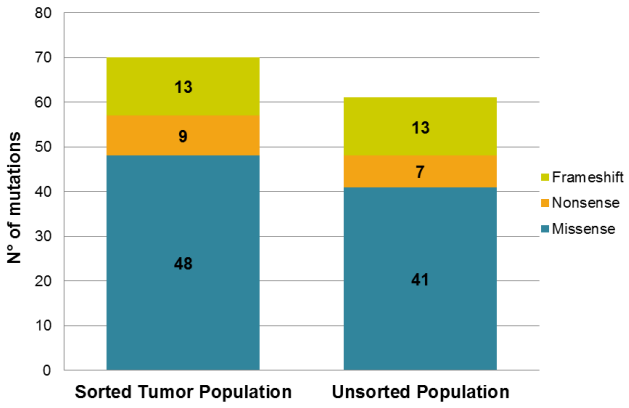

Figure 14: Using high throughput sorting and targeted sequencing, a different number of point mutations were detected in tumor sorted and unsorted cells (Blue: missense; Orange: nonsense; Green: frameshift).

In 35 out of 38 EACs, at least one somatic alteration (point mutation or CNA) was present in the sorted tumor population but not in the corresponding sorted stromal cells. Only 5 cases carried a single somatic alteration, whereas multiple genes were altered in the remaining cases (Figure 15).

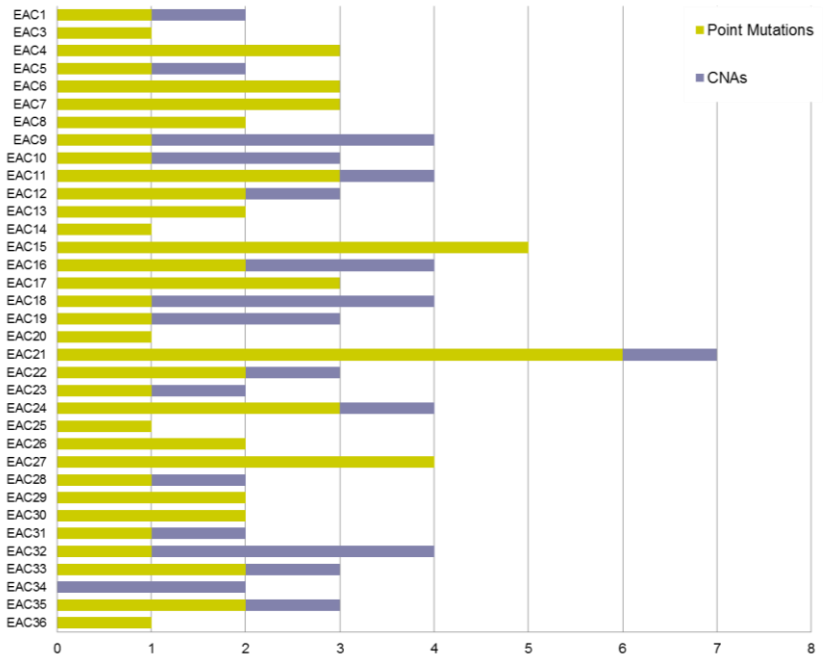

Figure15: Mutation detection through high throughput sorting and targeted sequencing: For each sample, total number of mutation detected, both point mutation (green) and copy number alterations (violet).

The cell sorting analysis revealed that, in most cases, the mutations were almost homozygous in tumor population (the number of reads supporting the alternative allele was >80%). Conversely, in the unsorted specimen, most mutations were detected with a much lower allele frequency (reads supporting the alternative allele were under 20%) and were below the limit of detection for a conventional NGS analysis at lower coverage (below 4,000X) (Figure 16).

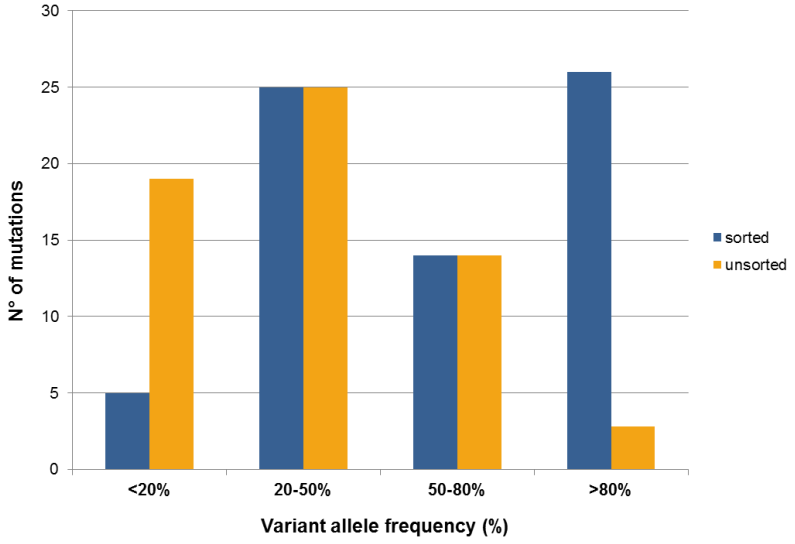

Figure 16: Mutation detection through high throughput sorting and targeted sequencing:
Number of point mutations identified in sorted (dark blue) and unsorted (orange) populations, in relation to the number of reads supporting the alternative allele.

All the somatic mutations and CNAs identified in sorted tumor populations with the OncoSeek panel analysis are described in Table 6, Chapter 7. The value of the alternative allele frequency is reported.

4.1.2 Different tumor populations are present in the same EAC specimen

The DAPI signal is proportional to DNA content and allows to assign a DNA index (D.I.) at each population. Stromal populations have a normal diploid DNA, thus D.I. equal 1. Tumor populations instead usually show a D.I. higher than 1, characteristic of a hyperdiploid DNA content; sometimes they can present a pseudodiploid D.I. (~1), resembling of a normal DNA profile.

Using DAPI staining, both hyperdiploid and pseudodiploid tumor populations were isolated in 13 EACs, and 9 of them where further profiled by low-pass whole genome in order to verify whether cytokeratin positive pseudodiploid cells were truly tumor clones. In 2 cases (EAC10 and EAC18) the pseudodiploid cell populations presented a normal copy number profile, whereas in 7 cases the aberrant copy number profile distinctive of neoplastic population was confirmed (Figure 17A). Comparison of hyperdiploid and pseudodiploid populations in these 7 cases displayed different single-nucleotide mutational loads, and in 2 cases (EAC19 and EAC4) additional CNAs were detected within hyperdiploid populations. This suggests that different subclones might have developed at different stages of tumor progression (Figure 17B, C).

A

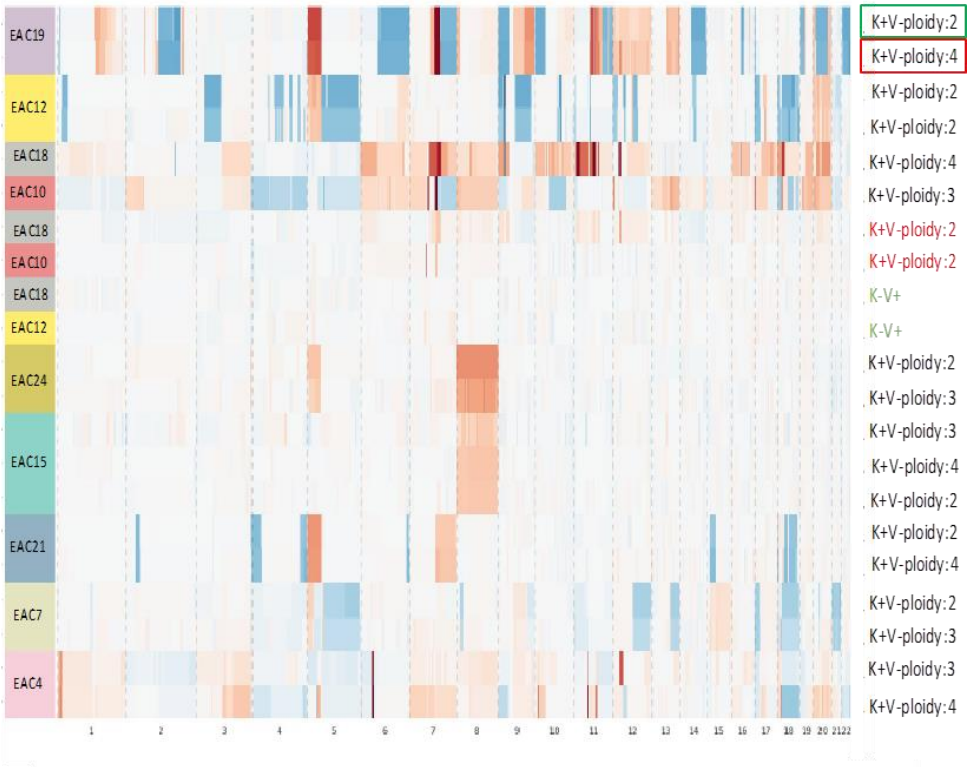

B

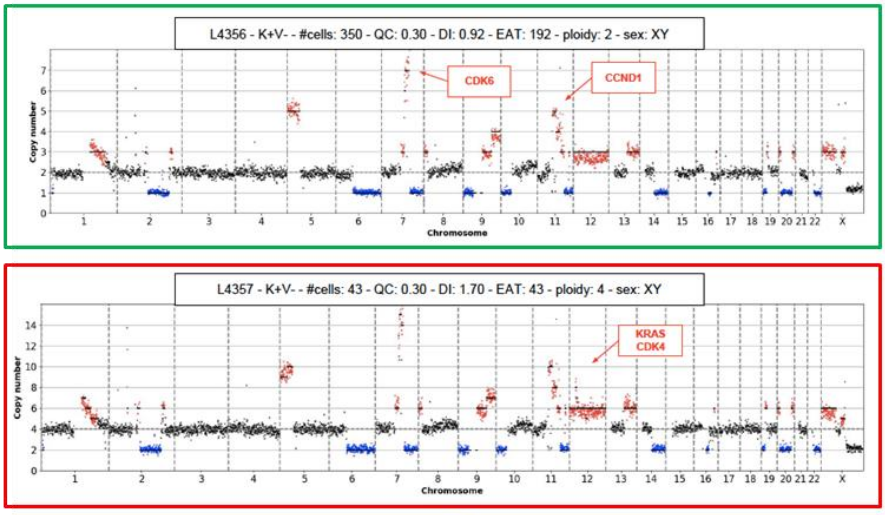

C

	method	LowPass	
	lib ID	L4356	L4357
	cell type	K+V-	K+V-
	DNA index	0.92	1.70
	ploidy	2	4
gene	profile	aberrant	aberrant
CDK6		amplification (8)	amplification (17)
CCND1		gains (5)	amplification (8)
KRAS			amplification (8)
CDK4			gains (5)

Figure 17: Tumor population with different ploidy can be resolved with high-throughput sorting and low pass whole genome sequencing. A. CNV profile of different subpopulations in 9 EACs. Gains and amplifications are shown in red, losses are in blue. **B.** An example is reported for EAC19: the low pass analysis shows CNAs in the chromosomes profile of keratin-positive pseudodiploid (L4356) and hyperdiploid (L4357) subpopulations (x-axis: chromosomes are plotted; y-axis: ploidy values). **C.** The table describes the main CNAs identified in the two subpopulations, with approximate copy number values indicated in brackets. As we can see, additional CNAs were detected within hyperdiploid population.

4.1.3 *TP53* is the most frequently mutated gene

TP53 mutations were detected in 28/38 cases (73.7%), for a total of 16 different *TP53* missense changes (two of which classified as functional in IARC *TP53* Database (http://p53.iarc.fr/) and 8 loss of function (stop codon/frameshift) changes (Figure 18).

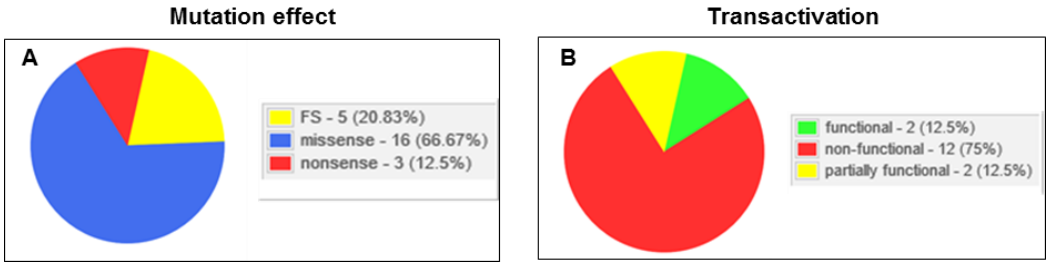

Figure 18: A. *TP53* mutation effect: mutations are classified as missense, nonsense, frameshift, based on the consequence on protein sequence. The proportion of each class in our cohort is shown as percentage. **B. Transactivation:** based on IARC *TP53* information, missense mutations are classified according to their experimentally measured transactivation activity.

Both missense and loss of function changes were present in 2 cases (Table 6, Chapter 7). In 64.3% of cases (18/28) *TP53* variant were detected as homozygous, while 35.7% (10/28) of EACs presented heterozygous *TP53* mutations.

In 5 of the cases having two tumor populations, the hyperdiploid tumor clones completely lost the *TP53* wild-type allele, presenting a homozygous profile; instead in the pseudodiploid population the mutations were

detected as heterozygous. This is a further evidence of multiple tumor clones at different progression times and high frequency of loss of heterozigosity events at *TP53* locus during EAC evolution.
The mutations are located across the whole *TP53* coding region, but they occurred preferentially in the DNA-binding domain (Figure 19).

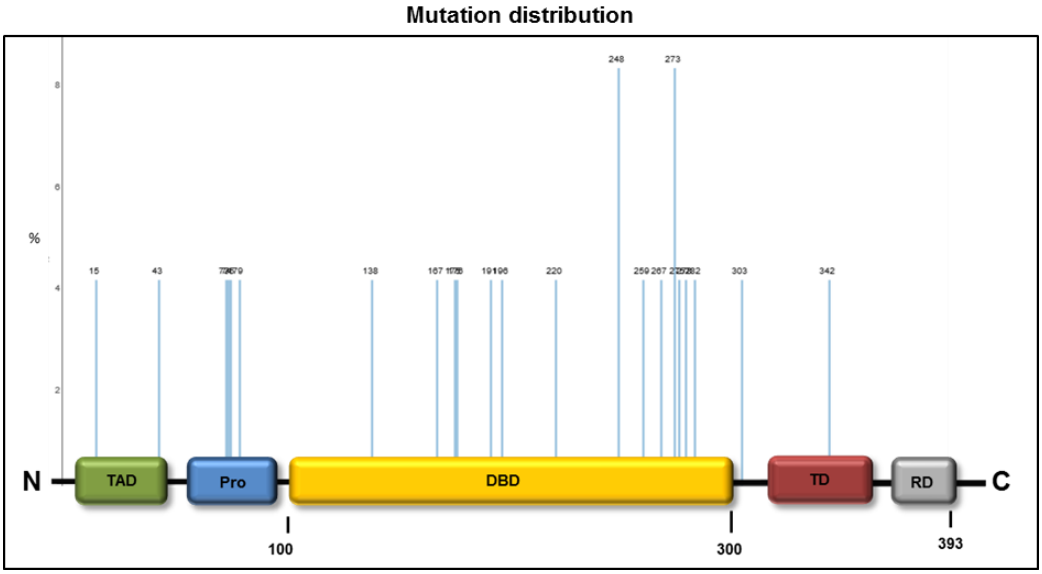

Figure 19: *TP53* mutation distribution. Distribution of point mutations across the p53 protein sequence. Numbers correspond to aminoacidic position. The y-axis represents the frequency (percentage) of representation of each mutation. TAD: transactivation domain; Pro: proline rich domain; DBD: DNA binding domain; TD: tetramerization domain; RD: regulation domain.

Mutations in *CDKN2A,* a p53-regulated target, were found in 4 cases. Digital Droplet PCR (ddPCR) was used as an independent technique to validate few detected variants. Among the available and validated probes for ddPCR, we selected *TP53* p.R273H, a hotspot mutation detected in 3 different patients (EAC6, EAC11 and EAC26), and the *CDKN2A* p.R58* nonsense mutation observed in EAC4. All of the variants were present at low allele frequency in the unsorted sample (<20%) but trough ddPCR we were able to validate their presence. In figure 20, for each sample the fractional abundance of the mutant allele in unsorted material is reported

(expressed as percentage). A wild-type and a no-template samples were used as controls.

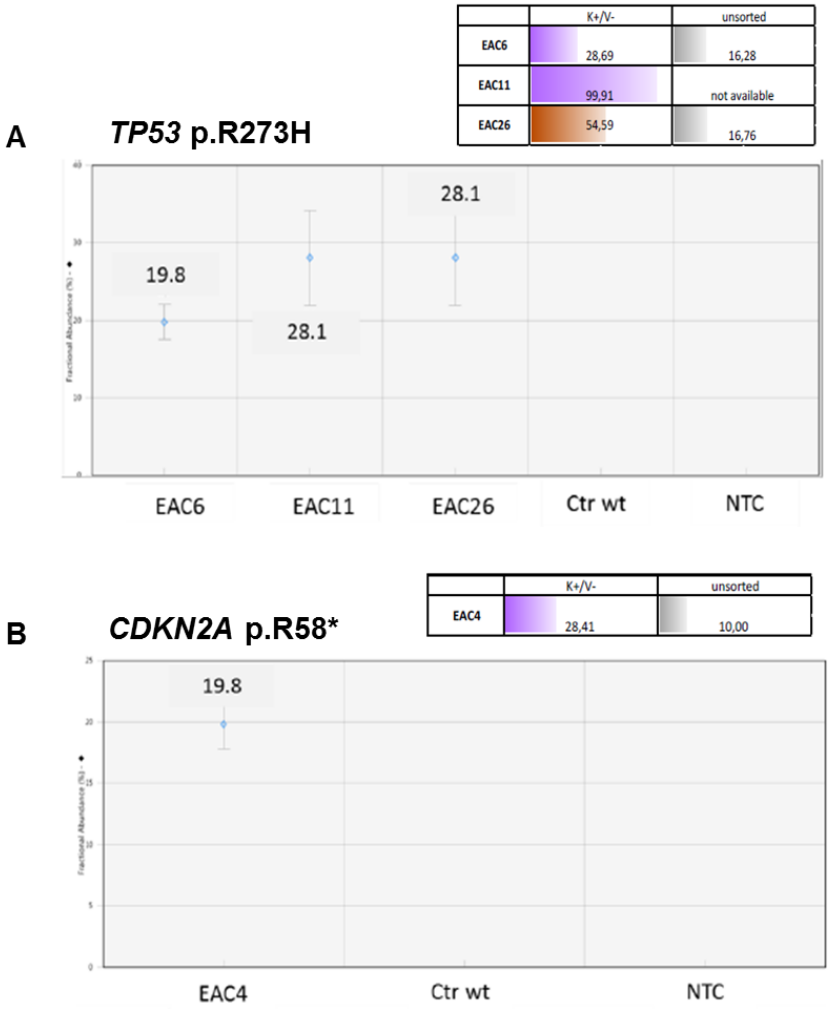

Figure 20: Validation of *TP53* and *CDKN2A* mutations by Droplet Digital PCR (ddPCR) assays. ddPCR was used as an independent technique to validate two of the mutation identified with the Oncoseek panel. **A.** *TP53* p.R273H mutation is evaluated in 3 EAC samples (EAC6, EAC11, EAC26), a *TP53* wild-type control (Ctr wt) and a no-template control (NTC). **B.** *CDKN2A* p.R58* mutation is evaluated in EAC4 sample, a *CDKN2A* wild-type control (Ctr wt) and a no-template control (NTC). The values represent the mutant allele fractional abundance, from the DNA of unsorted material, and are expressed as percentage. In the tables, the alternative allele frequency for the mutation in each patient is expressed as percentage in the sorted tumoral (purple, hyperdyploid; brown, pseudodiploid) and unsorted (gray) populations.

4.1.4 *HNF1A* is mutated in EAC

In EAC13 and EAC15 2 variants in *HNF1A* gene were detected: respectively, the missense change p.R263C, mapping to a region of the DNA binding domain, and predicted deleterious in PROVEAN, and the deletion c.864delG that causes a frameshift with the insertion of a premature stop codon (Figures 21 A, B).

The latter was confirmed through Sanger sequencing from the unsorted tumor tissue (Figure 21C).

HNF1A encodes for a transcription factor that acts as a tumor suppressor in pancreatic cancer, and it is involved in epithelia-to-mesenchimal transformation (EMT) [196]. This was the first time that mutations in this gene were reported in EAC.

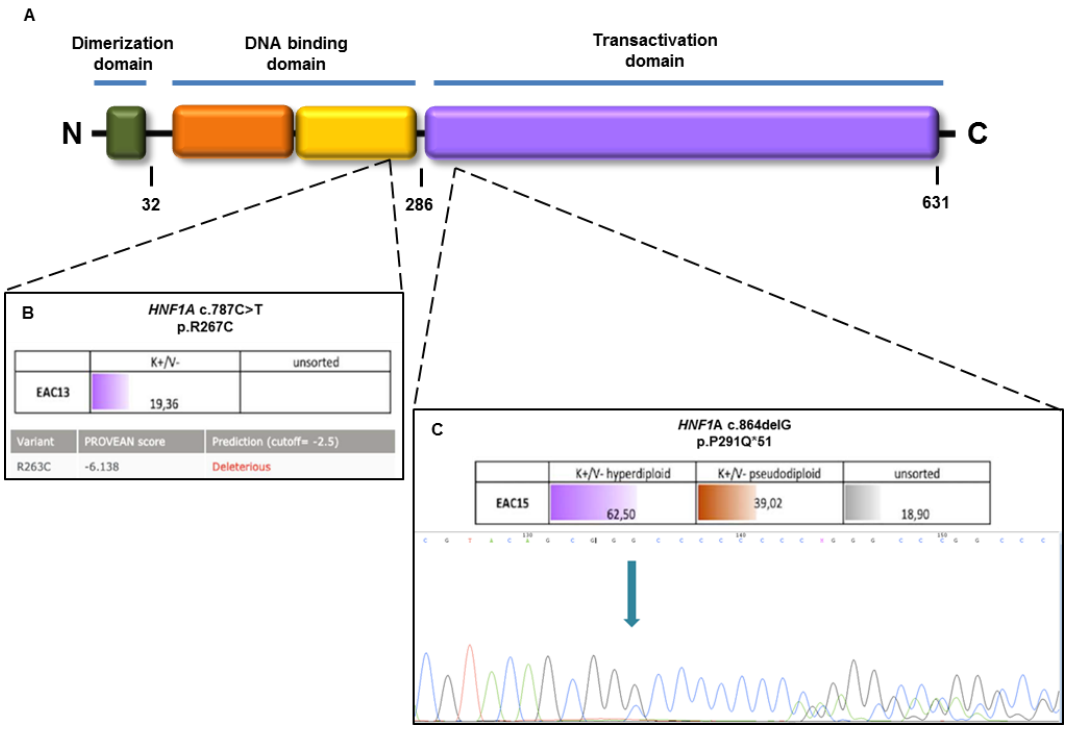

Figure 21: Mutations in *HNF1A* gene have been identified in EAC. A. Schematic representation of HNF1A protein sequence, characterized by a dimerization domain, a DNA binding domain and a transactivation domain. **B.** The *HNF1A* p.R267C missense mutation occurs in a region belonging to the DNA binding domain. The panel shows the frequency of the alternative

allele identified in the sorted tumor population in EAC13 sample. It is also reported the prediction analysis performed with the online tool PROVEAN. **C.** The *HNF1A* p.P219Q*51 frameshift mutation causes the formation of a premature stop codon. The panel shows the frequency of the alternative allele identified in the sorted hyperdiplod and pseudodiploid tumor populations and in the unsorted cells of EAC15 sample. It is also shown the electropherogram of the variant (blue arrow) observed wuth Sanger sequencing.

HNF1A mutations were present in conjunction with mutations in other genes: the missense one was associated with somatic mutations of *PIK3CA, CDH1, SMARCB1*, and the frameshift mutation was found with *TP53, EGFR, FLT3* and *IDH2* mutations.

4.1.5 Identification of additional mutations through Whole Exome Sequencing (WES)

WES was performed on the DNA extracted from the tumor in toto in 8 EAC cases. Cases were selected among those who reported none or only few variants, in example in EAC3 only one variant in *TP53* was detected, EAC35 showed 2 variants at low allele frequency, and EAC34 and EAC37 resulted negative at the OncoSeek Panel analysis.

In Figure22A it is shown, for each sample, the distribution of sequencing depth on exome targets: this parameter varies depending on the quality of FFPE samples, however from 40% to 80% of the targeted region was covered at least 10X. All the relevant variants detected are reported in Figure 22B (in green those already identified with the OncoSeek Panel and confirmed via WES, such as *CDKN2A* p.L63Q, *APC* p.R876* and *TP53* p.Y220C, p.R267G, p.C176F, p.A138V, p.V73RfsTer76). However, WES analysis allowed the detection of additional variants compared to the target panel, involving other tumor related genes: *ARID2* p.T148K, *ATM* p.R924W*, MSH6* p.C1145F in EAC33, *FLT3* p.E776K and *ERBB2* p.R648Q in EAC8, and *ALK* p.G35R in EAC3.

A

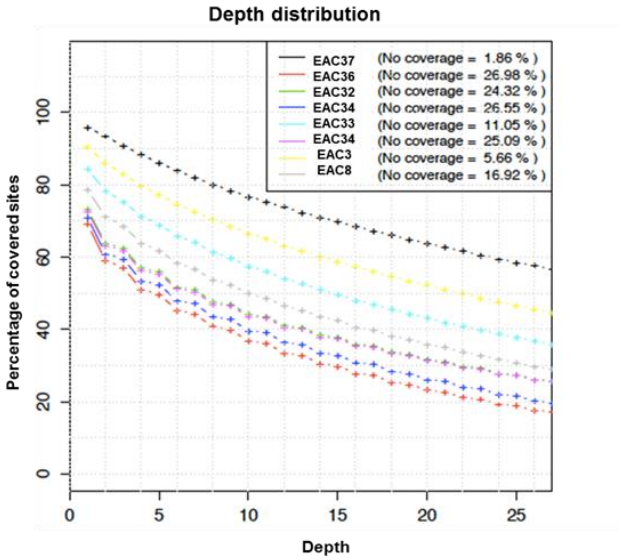

B

EAC_ID	Gene	Mutations
EAC3	*TP53* *ALK* *LRRK2*	ENST00000269305:p.C176F ENST00000453137:p.G35R ENSP00000298910.7:p.M2521I
EAC8	*TP53* *APC* *ERBB2* *FLT3* *NOTCH1* *RASAL1*	ENST00000269305:p.A138V ENST00000269305:p.V73RfsTer76 ENST00000512211:p.R876* ENST00000584601:p.R648Q ENST00000537084:p.E776K ENST00000277541:p.G2299S ENST00000548055:p.W53*
EAC32	*TP53* *ERBB4* *RHBDF2*	ENST00000269305:p.R267G ENST00000436443:p.E215K ENST00000591885:p.R320C
EAC33	*MSH6* *ARID2* *ATM* *CDH1*	ENST00000540021:p.C1145F ENST00000457135:p.T148K ENST00000527805:p.R924W ENST00000422392:p.T217K
EAC35	*CDKN2A* *NOTCH1*	ENST00000498124:p.L63Q ENST00000277541:p.T984M
EAC36	*TP53* *INO80D*	ENST00000269305:p.Y220C ENST00000424117:p.W241*
EAC37	*MYLK* *TMBIM4*	ENST00000475616:p.I512V ENST00000556010:c.464+2T>C

Figure 22: A. Sequencing-depth distribution on exome targets per sample. In the legend for each color is reported the referring sample. **B.** Mutations identified through WES performed on DNA extracted from unsorted material of 8 EAC cases. In green, the mutations already identified through targeted sequencing.

4.1.6 Correlation between *TP53* mutations and clinical outcomes

A preliminary statistical analysis was performed in order to correlate the results of the genetic investigation with clinical outcomes. The most mutated gene in our samples, *TP53*, shows a different mutation distribution according to the histological subtype: in our cohort the 77.4% of the Lauren's intestinal cases carried *TP53* mutations, with a statistically significant difference in frequency distribution (χ^2 test: P=0.002263) that was not observed for the diffuse histological subtype (χ^2 test: P= 0.7055), even though only a few cases were diffuse (Table 1).

	TP53		**Total**	**P**
Lauren	**Wild-type**	**Mutant**		
Intestinal	7 (22.6%)	24 (77.4%)	31 (100%)	0.002263
Diffuse	3 (42.9%)	4 (57.1%)	7 (100%)	0.7055
Total	10 (26.3%)	28 (73.7%)	38 (100%)	

Table 1: *TP53* mutational status and Lauren's classification. There is a difference in frequency distribution of mutated *TP53* in Lauren intestinal subtype (chi-squared test for given probabilities and Bonferroni's correction P=0.002263).

We evaluated the influence of *TP53* on survival and the analysis highlighted that *TP53* mutational status seems to correlate with a better cancer specific survival, compared with patients with wild-type *TP53* (Kaplan-Meier method, Log-Rank *P* = 0.0276; Figure 23). This could be related to the absence of treatment with neoadjuvant therapy in the cohort (naïve patients). Surgery alone could be more beneficial in a subset of patients that, because of their genetic status, can have a worse response to some of the drugs used for the neoadjuvant therapy.

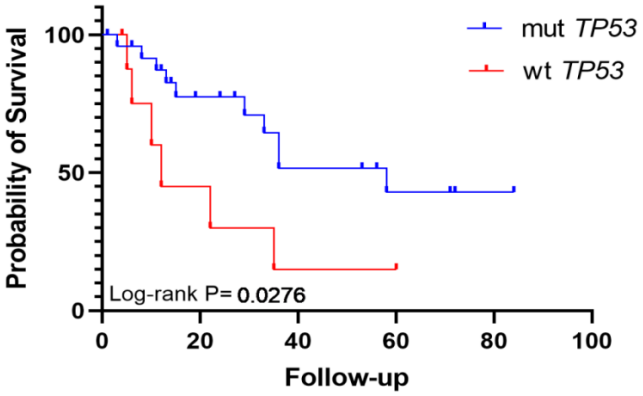

Figure 23: Mutated *TP53* seems to be correlated with better cancer specific survival. The figure shows the results of Kaplan-Meier test for cancer-specific survival comparing patients with mutated (mut) or wild-type (wt) *TP53* (log-rank *P* = 0.0276).

4.2 Expanding the genetic analysis to a wider cohort of patients

Given the small number of cases enrolled in the first analysis, we decided to expand our research to a wider group of EAC patients in order to evaluate the genetic profile. We gathered FFPE archival material from 169 EACs patients, none of them subjected to neoadjuvant therapy (naïve patients). All the samples were classified according to Lauren and to the novel EACSGE histologic classification developed by our research group. Targeted sequencing with a panel of 28 cancer related genes was performed of DNA extracted from the whole tumor specimen.

4.2.1 Mutational landscape in 169 EACs cases

Data analysis revealed a total of 346 mutations (single nucleotide point mutations, small insertions and deletions) across the whole cohort. 17 samples did not carry any variant of interest in the targeted genes, 62 cases showed only one somatic alteration, while the remaining EACs were found to carry mutations in multiple genes. *TP53* was once again the most frequently mutated gene, with 106 cases carrying at least one mutation. Among other highly mutated genes, *ATM* (31 cases), *APC* (21 cases), and *MSH6* (18 cases) were found. *CDKN2A* was altered in 17 patients (Figure 24A). Considering the effect determined by these mutations, 74% of them were missense, 19% were loss of function (frameshift 13%; nonsense 6%) and in a small proportion splicing and inframe changes were present (5% and 2% respectively) (Figure 24B).

A

Gene	Number of mutations
TP53	106
ATM	31
APC	21
MSH6	18
CDKN2S	17
ERBB2	16
PIK3CA	14
SMAD4	13
SMARCA4	12

B

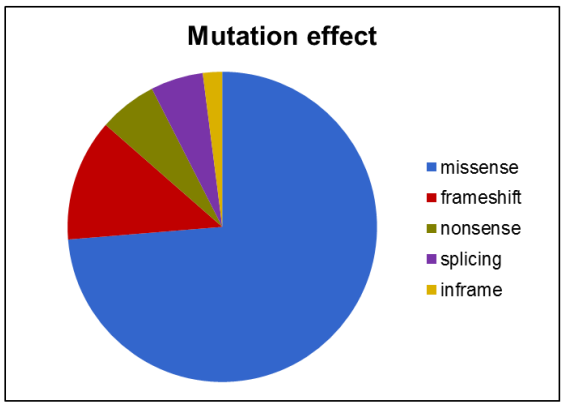

Figure 24: Overview of the molecular landscape in targeted sequenced EAC samples. A. List of the most mutated genes identified in our cohort, with the corresponding number of variants in which the gene was found altered. **B.** Pie chart synthesizes the percentage of mutations having a specific effect: 74% of mutations provoke a missense change, 19% are loss of function (frameshift and stop gain), 5% and 2% are related to splicing and inframe variants respectively.

4.2.2 *TP53* mutational spectrum

TP53 mutations were detected in 106/169 cases (62.7%), for a total of 51 missense mutation, 21 loss of function (nonsense/frameshift) changes and 10 mutations involving splicing (Figure 25A). One missense variant is classified as functional in the IARC *TP53* Database (http://p53.iarc.fr/) (Figure 25B).

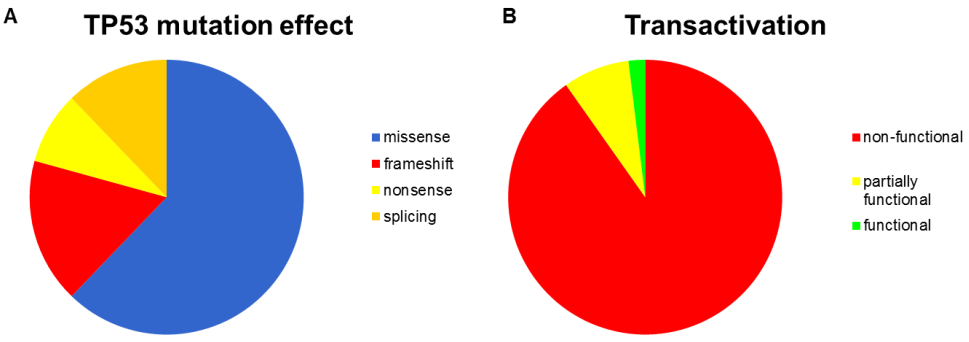

Figure 25: A. *TP53* mutation effect: mutations are classified as missense, nonsense, frameshift, and splicing based on the consequence on protein sequence. **B. Transactivation:** based on IARC

TP53 information, missense mutations are classified according to their experimentally measured transactivation activity.

Figure 26 shows the mutation distribution for missense and loss of function changes across the p53 proteins sequence. The vast majority of mutations occurred in the region corresponding to the DNA-binding domain (Figure 26), with recurrent mutations in "hotspot" regions, for example at codons 193, 213 and 278.

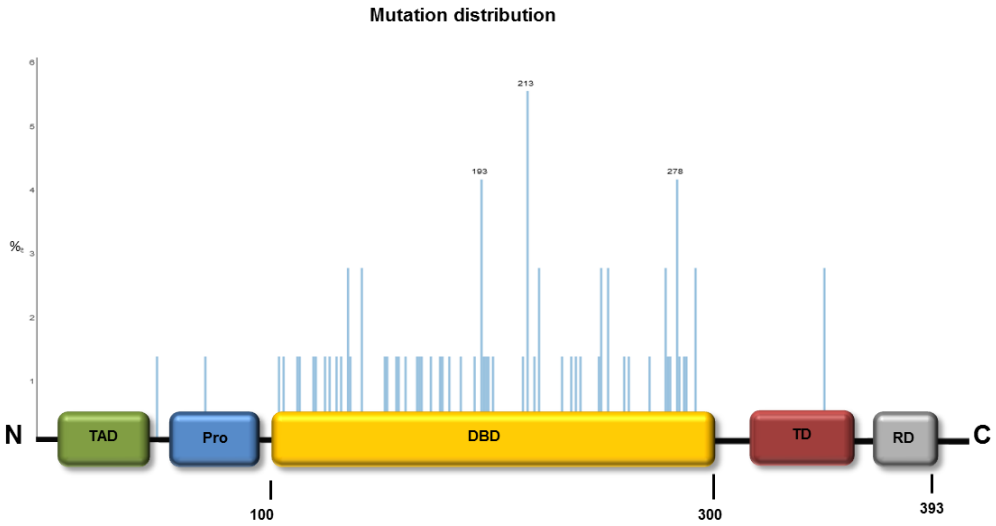

Figure 26: *TP53* mutation distribution. Distribution of point mutations across the p53 protein sequence. Numbers correspond to aminoacidic position. On y-axis the frequency (in percentage) of each mutation is shown. TAD: transactivation domain; Pro: proline rich domain; DBD: DNA binding domain; TD: tetramerization domain; RD: regulation domain.

4.2.3 Mutations in the *HNF1A* gene: a further player in EAC

HNF1A is a transcriptional activator that regulates the tissue specific expression of multiple genes. In pancreatic cancer is considered to be a possible tumor suppressor [196]. The analysis of our former cohort of cases reported, for the first time, *HNF1A* mutations occurring in esophageal adenocarcinomas. This data was confirmed by the findings in

the 169 patients, where mutations in *HNF1A* were detected in 7 samples (one of them carrying 2 mutations in this gene) (Table 2). Five different missense changes and 2 frameshifts were identified, with 2 patients carrying the same variant (p.Ala161Thr).

ID	Nucleotide change at genomic position	Mutation effect	Protein change
EAC143	12:121432117G>GC	Frameshift	p.Gly292ArgfsTer25
EAC188	12:121434597C>T	Missense	p.Pro454Leu
EAC189	12:121426790G>A	Missense	p.Ala161Thr
EAC200	12:121426790G>A	Missense	p.Ala161Thr
EAC201	12:121426776C>T 12:121434366TC>T	Missense Frameshift	p.Thr156Met p.Pro379LeufsTer5
EAC224	12:121426812G>A	Missense	p.Arg168His
EAC234	12:121437082C>A	Missense	p.His505Asn

Table 2: List of the variants identified in *HNF1A* in the 169 patients analysis. For each sample, it is reported the nucleotide change at the genomic position, the effect of the mutation and the change at protein level.

The mutations were distributed along the DNA-binding and the transactivation regions; the 2 frameshifts were predicted to generate a truncated protein missing a major portion of the transactivation domain (Figure 27).

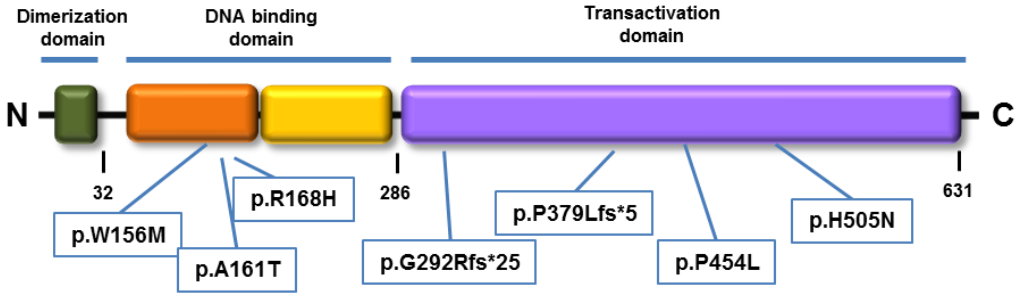

Figure 27: New mutations in *HNF1A* gene identified in EAC. Schematic representation of HNF1A protein sequence and the relative position of the mutations identified.

In 6/7 cases, *HNF1A* mutations co-occurred with other variants. The only variant found not to be associated with mutations in other genes was the

frameshift p.G292Rfs*25. Several variants were associated to variants in genes already found associated with the first two *HNF1A* mutations identified with the OncoSeek Panel, i.e. *TP53, EGFR, FLT3 IDH2* and *PIK3CA*. The other variants detected in association with *HNF1A* mutations were in *ATM*, *SMAD4*, *ERBB2*, *RET1*, *CTNNB1* and *MSH6* genes. Mutations in *PIK3CA* co-occurred with *HNF1A* mutations 3/7 times. Interestingly, the *HNF1A* p.A161T, identified in 2 cases, in both cases co-occurred with mutations in *PIK3CA*.

4.2.4 Statistical analysis

In this dataset no statistical difference in survival was observed comparing patients with mutated versus wild-type *TP53* gene, neither in the overall cohort or considering histological subtypes according to EACSGE classification. Mutations in some genes might be correlated to recurrence: in particular, variants in *MSH6* (Fisher's exact test, P=0.0439) (Figure 28A), and variants in *APC* in the EACSGE Low grade group (Fisher's exact test, P=0.0183) (Figure 28B).

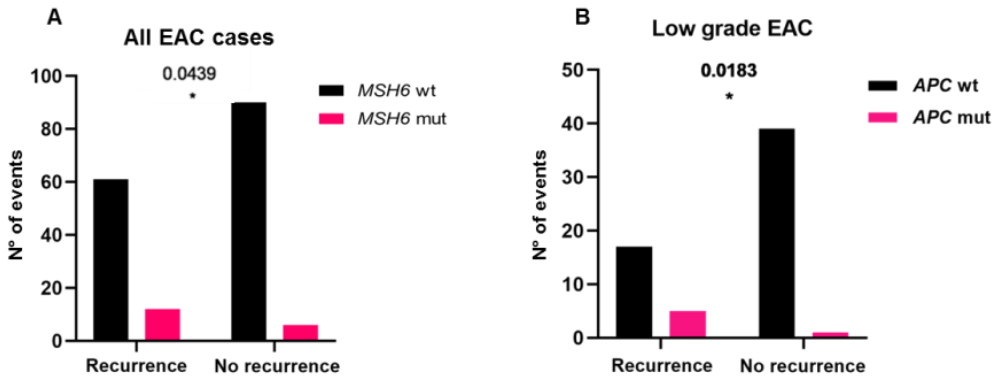

Figure 28: Mutations in *MSH6* and *APC* seems to be related to recurrence. Fisher's exact test showed a statistically significant correlation between recurrence and: **A.** mutated *MSH6*, in all EAC cases (P=0.0439); **B.** mutated *APC* in the Low grade histological subtype (P=0.0183).

4.3 Analysis of deregulated miR483-3p and miR221 in esophageal adenocarcinomas

In order to identity a differential expression of miRNAs in esophageal adenocarcinoma, a preliminary study conducted by our research group profiled 8 EAC cases and two pools of 8 normal gastric tissues using TaqMan MicroRNA Array cards A2.1/B3 and the analysis revealed 26 overexpressed miRNAs and 72 downregulated ones. Among them, the two overexpressed miR221 (fold increase: 2.746) and miR-483-3p (fold increase:11,33) were selected based on public data available (miRBase: http://www.mirbase.org/).

4.3.1 Expression analysis via single assays confirms an up-regulation of miR221 and miR483-3p in EACs

To validate this association, miRNA 221 and miRNA 483-3p expression levels were evaluated in a cohort of 112 FFPE surgical specimens of EAC naive patients via Real-time PCR single assays (clinical features are reported in Table 1 Chapter 7). Fold changes were obtained comparing EAC cases versus a pool of 8 RNAs isolated from FFPE samples of healthy gastric mucosa and RNU44 was used as endogenous control.

In accordance with our preliminary array data, these two miRNAs were significantly overexpressed in EAC cases compared to normal gastric tissues (miR221 mean fold increase 2.276, Wilcoxon Signed Rank test: $P<0.0001$; miR483-3p mean fold increase 5.964 $P<0.0001$) (Figure 29).

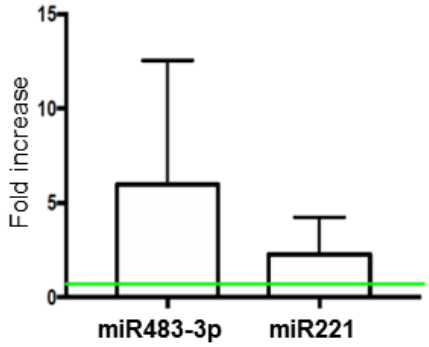

Figure 29: miR483-3p and miR221 expression levels in EAC cases. The values are expressed as fold increase and compared to a control pool of FFPE healthy gastric tissues (green base line).

4.3.2 Correlation between miRNAs expression and clinical-pathological features in EAC

To investigate further the role of miR221 and miR483-3p in EAC, we evaluated possible correlations between miRNAs expression in relation with tumor recurrence, cancer specific death, stage, Lauren classification and the EACSGE dichotomous histologic classification.

In order to divide patients into a high- and a low- miRNAs expression groups, an optimal cut-off value was elaborated using ROC (Receiver Operating Characteristic) curve analysis and Youden index. A cut-off of 1.32 fold-change distinguished patients in miR221-high or -low expression level groups, while a cut off of 3.15 was calculated for miR483.

Higher expression of both miR483-3p and miR221 was associated with poorer cancer specific survival (Kaplan-Meier; Log-Rank P=0.0293 and P=0.0059 respectively) (Figure 30 A and C). This correlation was more notable in the Lauren intestinal subtype of cancers (miR483-3p Log-Rank P=0.0059; miR221 Log-Rank P=0.0024; Figure 30 B and D).

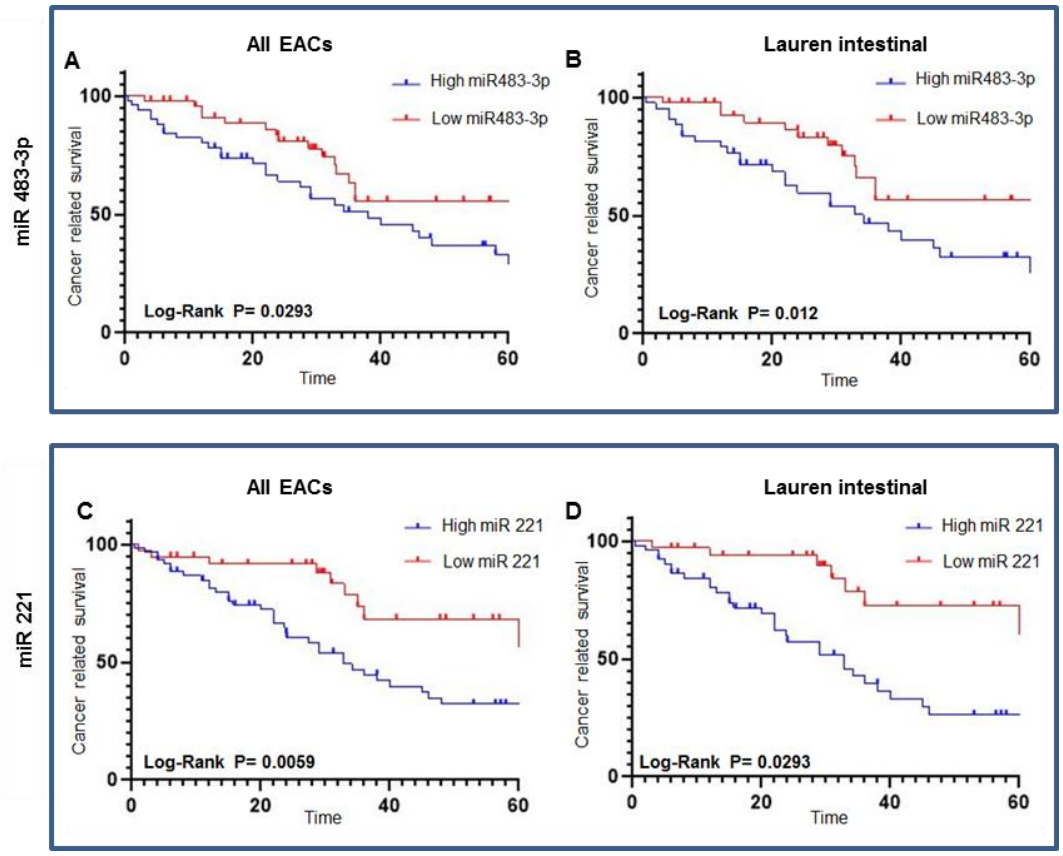

Figure 30: MiRNAs expression levels and cancer related survival Kaplan-Meier curves illustrate cancer-related survival for groups of patients divided on high or low expression levels of miRNA 483-3p and 221; in all EACs (**A and C**) and only in Lauren intestinal subtype (**B and D**) respectively.

While for miR483-3p no differences were seen comparing High and Low grade cases, patients with up-regulated miR221 show poorer survival in Low grade subtype (P=0.0110) (Figure 31).

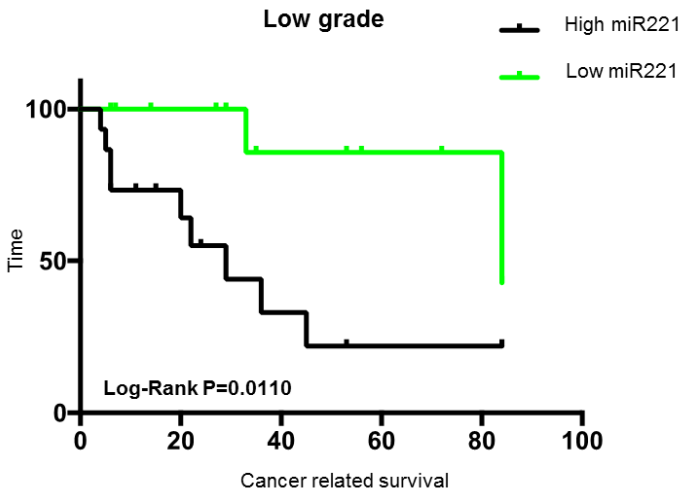

Figure 31: MiR221 expression levels and cancer related survival Kaplan-Meier curve illustrates cancer-related survival for Low grade subtype, stratified on miR221 expression level (High or Low).

Mann-Whitney test revealed a correlation with miR483-3p expression levels and recurrence in the Lauren subtype (P=0.0459) (Figure 32A). MiR221 shows a correlation with the event of recurrence in all EAC cohort, (P=0.0002), in the Lauren intestinal subtype (P=0.0003) and in the Low grade histological subgroup (P=0.0079) (Figure 32 B, C, D).

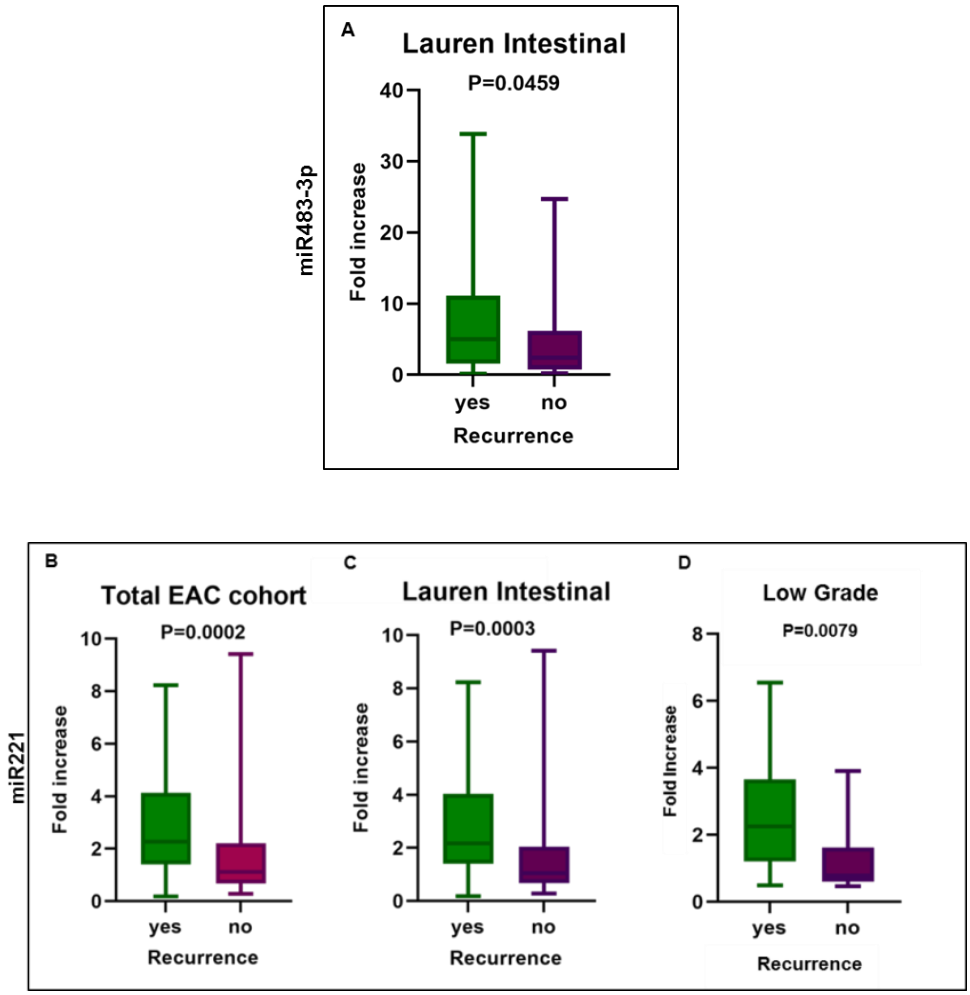

Figure 32: Correlations between miRNAs and recurrence using Mann-Whitney test. A. Correlation between miR483-3p and recurrence in Lauren intestinal subgroup P=0.0459. Correlation between miR221 and recurrence in **B.** total EAC cohort P=0.0002; **C.** Lauren intestinal subtype (P=0.0341); **D.** Low grade subtype (P=0.0255).

Patients with advanced tumor stages show higher median expression levels of miRNAs 483-3p and 221. In our cohort, TNM stages 2 and 3 tumors showed an up-regulated miR483-3p expression (Mann-Whitney test *P*=0.0532 (stages 1-2); *P*=0.0174 (stages 1-3); Figure 33 A and B). Also, stage 3 and 4 tumors had significantly higher median expression levels of miR221 (Mann-Whitey test P=0.0257 stages 1-3, P=0.0134 stages 1-4; Figure 33 C and D).

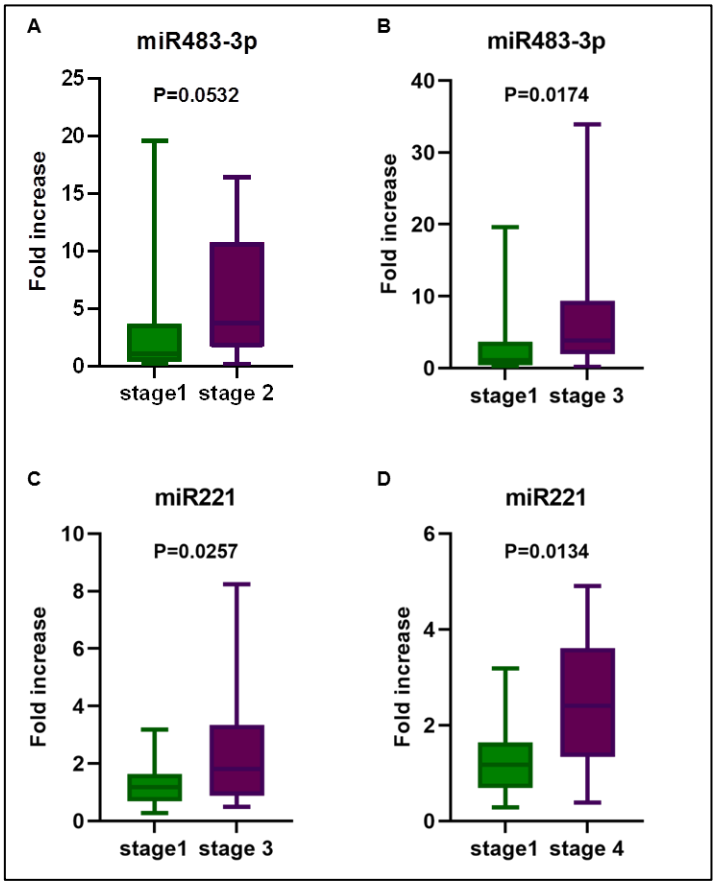

Figure 33: Correlation between miRNAs and tumor stages, using Mann-Whitney test. **A.** miR483-3p, stage 1 vs stage 2 (*P*=0.0532); **B.** miR483-3p, stage 1 vs stage 3(*P*=0.0174); **C.** miR221, stage 1 vs stage 3 (P=0.0257); **D.** miR221, stage 1 vs stage 4 (P=0.0134).

4.3.3 MiRNAs expression analysis in EAC cell lines

The expression of miR483-3p and miR221 was evaluated in 3 different EAC cell lines, OE19, OE33 and FLO-1, via single qPCR assays as described above. While no significant differences were detected in miR221 levels among the cell lines, FLO-1 showed a significantly increased expression of miR 483-3p (P=0.01), compared with OE-19 and OE-33 (fold-change=2.7; Figure 34).

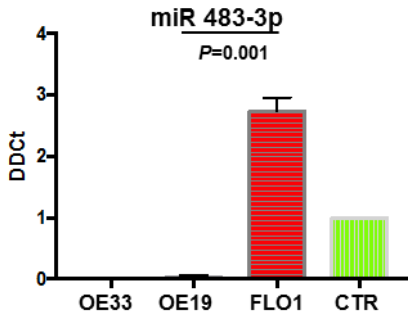

Figure 34: Expression of miR 483-3p in 3 EAC cell lines (OE33, OE19, FLO1) and esophageal control tissue. FLO-1 showed a significantly increased expression of miR 483-3p (P=0.001), compared with OE-19 and OE-33.

4.3.4 miR483-3p: evaluating its effect on gene expression levels using a miRNA mimic

From a review of the literature, *SMAD4*, *PUMA* and *CTNNB1* were identified as three of the major genes modulated by miR483-3p. We therefore evaluated their expression levels within our 3 cell lines through qPCR, using *β-actin* as endogenous control. Relative gene expression levels are reported in figure 35 as ΔΔCt, normalized versus a commercial control RNA pool of esophageal tissue derived from 5 different healthy donors. SMAD4 was also evaluated via Western Blot, confirming its presence at a protein level.

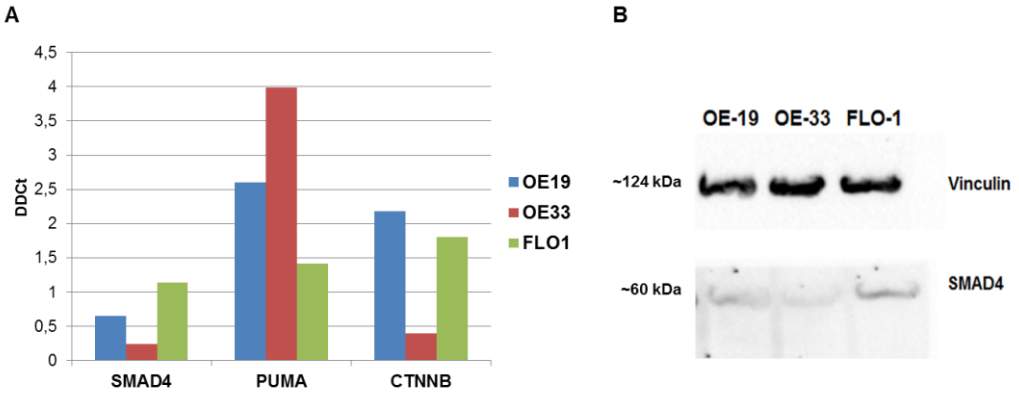

Figure 35: Expression of *SMAD4*, *PUMA*, *CTNNB1* A. Expression was evaluated in 3 EAC cell lines (OE33, OE19, FLO1). The values are expressed as fold increase with respect to a commercial control RNAs pool. **B.** SMAD4 expression at protein level via Western blot. Vinculin was used as endogenous reference control.

In order to evaluate the effects of miR483-3p up-regulation, we used a miRNA mimic, i.e. a small molecule that mimics the role of endogenous miR483-3p with an up-regulation of miRNA activity. OE19 cell line was transfected with either miR483-3p mimic or a scramble control using Lipofectamine 3000 reagent. Cells were incubated at 37°C then RNA was extracted at 24, 48 and 72 hours. qPCR with single assays for miR483-3p was used to evaluate the successful transfection of cells (fold change mimic: 791.12; Figure 37).

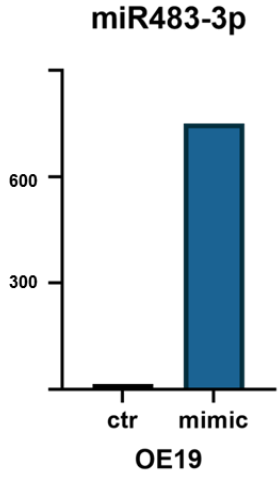

Figure 36: Expression of miR 483-3p was evaluated in OE19 cell lines transfected either with miR483-3p mimic or a scramble control (ctr).

The expression levels of *SMAD4*, *PUMA* and *CTNNB1* were determined via qPCR. *β-actin* was used as endogenous control. Compared with cells transfected with the scramble vector, expression of *SMAD4* significantly decreased post transfection with miRNA mimic (Kruskall-Wallis test:

P=0.0343; Figure 38). No significant differences were observed in the levels of *PUMA* or *CTNNB1*.

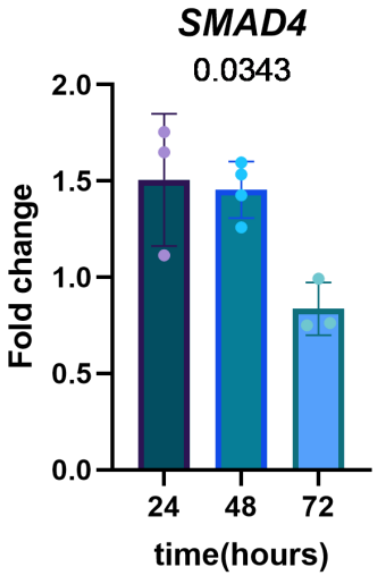

Figure 38: *SMAD4* expression significantly decreased post transfection with miR483-3p mimic. mRNA expression levels of *SMAD4* in OE19 were assessed at 24, 48,72 hours post transfection of the miR483-3p mimic. The transfection with the scramble was used as control. β-actin expression levels were used for normalization. Kruskall-Wallis test: P=0.0343.

This result seems in line with previous studies in pancreatic cancer, where it was demonstrated that miR483-3p can target *SMAD4*, leading to its reduced expression [197].

4.3.5 Correlation between miR483-3p and *SMAD4* immunoreactivity

In order to evaluate a correlation between miR483-3p and the reduction of *SMAD4*, we compared miR483-3p expression levels with immunohistochemical data of 55 FFPE EAC samples (in collaboration with Prof. R. Fiocca and Prof. L. Mastracci). Based on previous works on colon

cancer [198], [199] a cut-off of 30% of complete loss of SMAD4 expression was set to classify samples.

SMAD4 immunoreactivity was lost in 28/55 EAC cases (50.9%), but no correlation was observed with miR483-3p expression (Table 8, Chapter 7). Therefore additional mechanisms, such as promoter hypermethylation, might explain SMAD4 loss, independently of miR483-3p expression and in absence of gene mutations, as previous data indicated [111].

However, since loss of SMAD4 expression was found in half of EAC samples, its effect on clinical outcome was evaluated.
The loss of SMAD4 immunoreactivity was significantly associated with cancer specific survival (Kaplan-Meier analysis Log-Rank: P=0.0452; Figure 39)

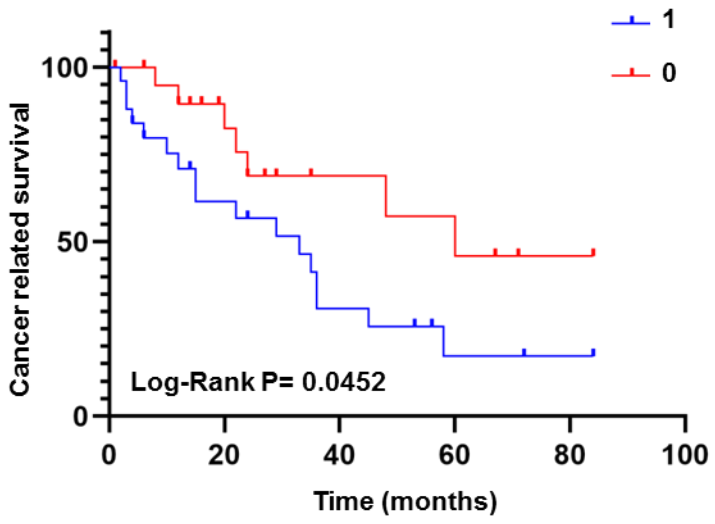

Figure 39: SMAD4 protein expression level and cancer related survival Kaplan-Meier curve illustrates cancer-related survival for EAC cases, grouped according to cancer with (0): high SMAD4 (<30% loss of protein expression) and (1): low SMAD4 (>30% loss of protein expression) (Log-Rank: *P*=0.0452).

We also observed a significant correlation between SMAD4 loss and recurrence (Kaplan-Meier analysis Log-Rank: P=0.0284; Figure 40).

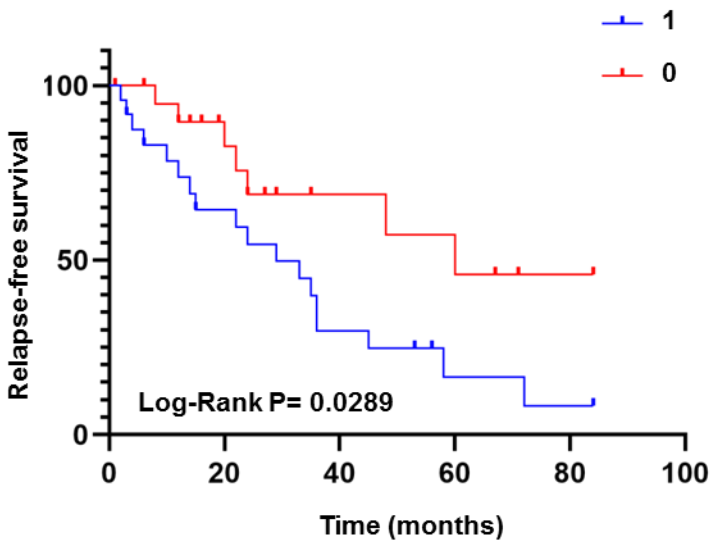

Figure 40: SMAD4 protein expression level and relapse-free survival Kaplan-Meier curve illustrates relapse-free survival for EAC cases, grouped according to cancer with (0): high SMAD4 (<30% loss of protein expression) and (1): low SMAD4 (>30% loss of protein expression) (Log-Rank: *P*=0.0289).

This result suggests that SMAD4 expression could be a potential prognostic biomarker in esophageal adenocarcinoma.

5. DISCUSSION

Exome and whole genome sequencing studies revealed that EAC is characterized by a high mutation burden, a preponderance of copy number alterations and large-scale chromosomal rearrangements, often due to genomic catastrophes, such as chromothripsis [92]–[94].
Tumor heterogeneity, referring to both inter- and intra-tumor forms, is an important attribute of cancer and a major contributor to tumor progression [200]–[202]. It can be observed not only at genomic but also at the epigenomic level, and it can affect the efficacy of tumor biopsy, cancer diagnosis, and treatment planning [203].
Even though advances in sequencing technology deepened the understanding of EAC heterogeneity, it is still challenging to translate this knowledge into clinical practice.

In order to provide novel insights into the pathogenesis of EAC, this research project aimed to better define EAC inter- and intra- tumor heterogeneity, at a genetic level, analyzing EACs somatic mutational profiles using a high throughput sorting system, but also at epigenetic level, focusing on the expression profile of some candidate microRNAs, in order to correlate the molecular profile of tumors to clinical outcomes, such as histotype, recurrence and survival and identify biological markers that allow to classify types of homogeneous neoplasms.

In the first part of the project we combined NGS techniques with DEPArray cell sorting technology (Silicon Biosystems) to perform a screening of 38 FFPE EAC samples, derived from patients who underwent esophageal-gastric resection without neoadjuvant chemotherapy. Based on

the fluorescence for vimentin and pan-cytokeratin in combination with the intensity of the DAPI signal, the cell sorting system accurately discriminated the tumor cell population from the stromal one, allowing a precise NGS genetic analysis of the somatic tumor alterations without the "diluting" effect due to the presence of normal stromal cells.

All stromal populations were characterized by a normal diploid profile. Instead, the analysis of the sorted cell populations highlighted the great inter and intra heterogeneity of tumor cells, not only in the mutation profiles, but also in terms of cellular ploidy: in seven cases, tumor subpopulations were discriminated on the basis of DNA content, hyperdiploid or pseudodiploid, and showed different copy number variant (CNV) profiles at low pass whole-genome analysis, different percentages of the alternative allele and different somatic mutational loads. This suggests the existence of multiple tumor subclones in the same tumor, at different stages of progression, which may have a different response to conventional radio-chemotherapy, and which may be specifically targets for targeted drug therapy.

The sorting of tumor cells allowed also to visualize the real allelic frequencies of the mutations, which in most cases were observed as homozygous. These mutations were absent in the corresponding stromal cells recovered with the same technology and, when analyzing the DNA extracted from the specimen in toto (unsorted), due to the contamination of the stromal cells in the tumor area, several mutations were detected with a much lower allelic frequency, despite a high coverage.

This was especially true for the tumor suppressor gene *TP53*, whose mutations were mainly shifted to homozygosity in the sorted tumor populations. This result confirms that *TP53* mutations and loss of heterozygosity are early events in EAC tumorigenesis, in agreement with previous findings [114].

TP53 gene maps on the short arm of chromosome 17 [204] and it is one of most important tumor suppressor gene, encoding for a transcription factor with key role in the maintenance of genetic stability [205], [206].

In normal cells, p53 protein is maintained at low levels by a series of regulators including MDM2 [207], but it can be stabilized in response to various stresses, to promote an adequate cellular response, including cell-cycle arrest of damaged cells, DNA repair and apoptosis [208], [209].

Mutations in the *TP53* gene consist primarily in missense substitutions, the majority of them occurring in the central DNA-binding-domain and affecting *TP53* transcriptional activity [210]. Multiple reports indicate the presence of six preferred mutational hotspot-sites, in codons 175, 245, 248, 249, 273, and 282 [211].

TP53 mutations can have different effects: loss of function mutations determine the inability to activate the transcription of p53 target genes [212]; a dominant negative effect can be present in heterozygous cancer cells and it is associated with hetero-oligomerization: replacing one or more wild-type p53 molecules in the tetramer, the mutant p53 compromises the activity of the protein [213], [214]; mutant p53 can also play an oncogenic activity through a gain-of-function effect (Figure 41), where p53 mutants can bind to novel protein partners, including transcription factors, thereby affecting the regulation of novel target genes [215].

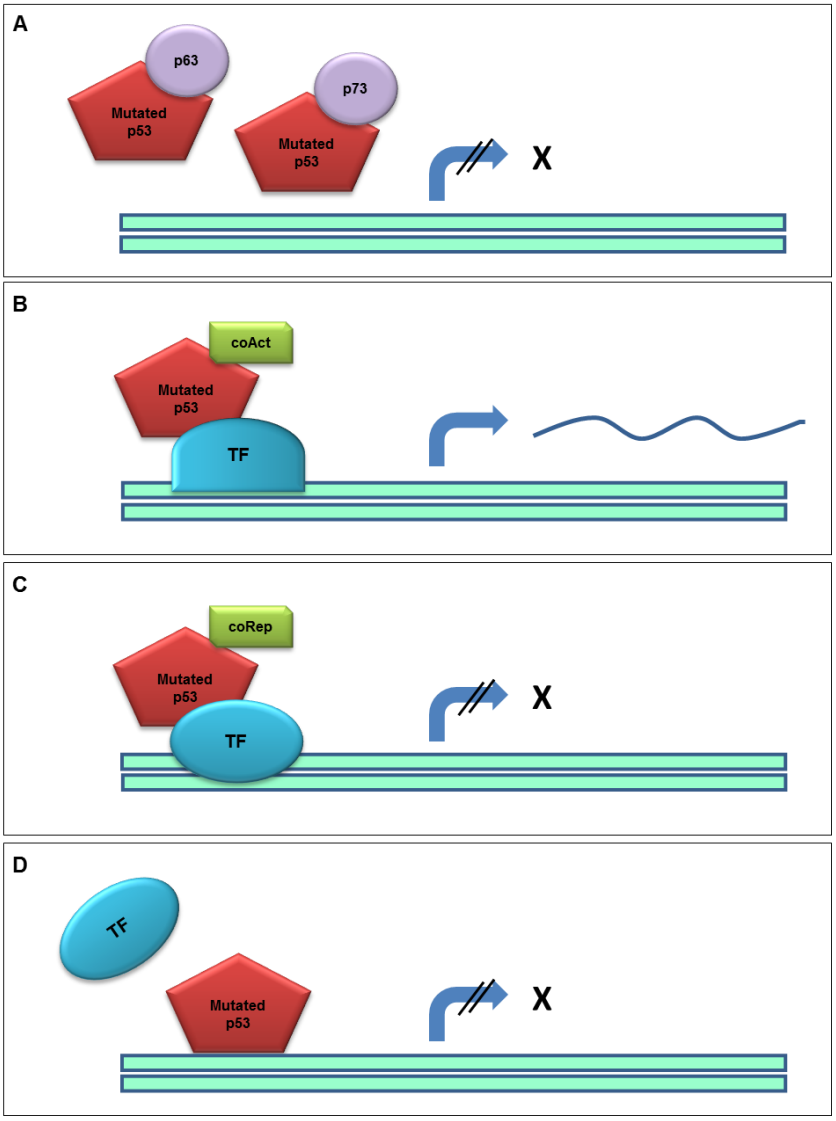

Figure 41: Gain of function mutated p53 transcriptional effects [215]. **A.** Mutated p53 can interact with p53-related proteins p63 and p73 isoforms, making them transcriptionally inactive. **B. and C.** Mutated p53 can modulate both positively and negatively transcription factors activity, engaging protein–protein interactions and recruiting coactivators and corepressors. **D.** Mutated p53 can displace a positively acting TF leading to repression of adjacent genes.

Somatic mutations in *TP53* were predominant in our cohort, in accordance with literature data [11], [88] (Figure 42). The striking preponderance of *TP53* mutations in EAC patients suggests that a molecular analysis of the *TP53* mutational status could be compelling for an accurate diagnosis, for prognosis and for evaluating the best therapeutic options.

p53 immunohistochemistry is not always correlated to the mutation status, especially in presence of loss of function mutations, where p53 immunostaining cannot help to discriminate wild-type from mutant forms [216], [217].

Therefore, a molecular analysis performed through sequencing technologies could be of critical importance for the early assessment of *TP53* mutational status, especially in a perspective of selecting the most efficient approach in target therapies. Targeting mutant p53 is a promising strategy. Different methods have been studied to reactivate p53 activity. Some compounds, such as PRIMA-1met APR-246 can restore the activity of mutant p53 in presence of missense mutations [179]–[181]. Other molecules instead, in example Nutlin-3, act by inhibiting the interaction between p53 and MDM2, then the effect of Nutlin-3 treatment can be effective only in cancer cells with wild-type p53 protein [218], [219]. Performing a mutation analysis of sorted tumor cells as we did in this study, to determine not only the type of variant, but also the real zigosity of *TP53* could be very valuable to select patients more suitable for selected therapies [220].

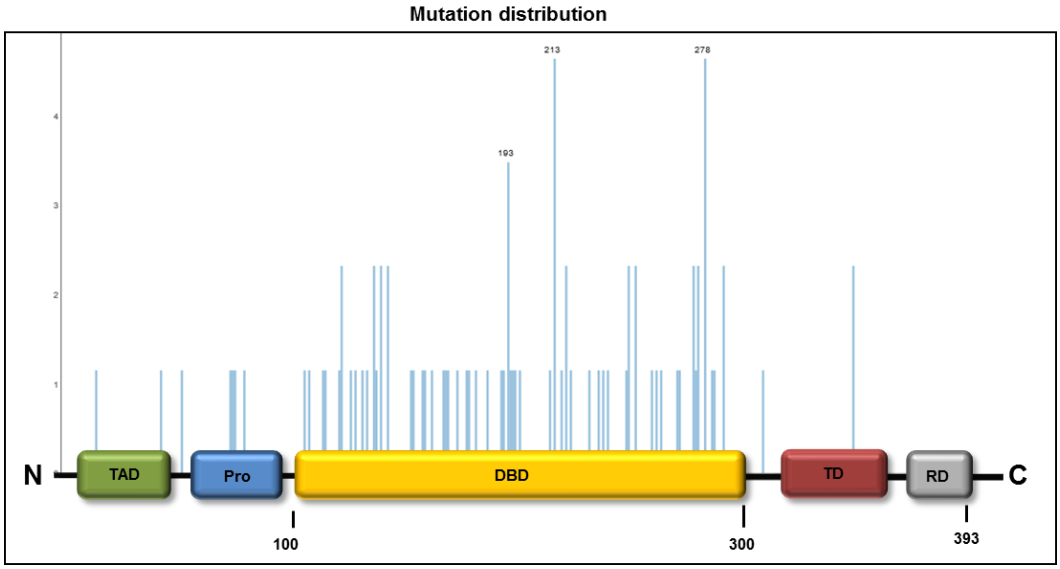

Figure 42: *TP53* mutation distribution. Distribution of all missense and loss of function mutations identified in our cohorts of patients. Mutations mainly affect the DNA-binding domain, falling in recurrent "hotspot" regions, for example at codons 193, 213 and 278.

Our research also allowed the identification of somatic mutations in the gene encoding the hepatocyte nuclear factor HNF1a.

The *HNF1A* gene is located on chromosome 12. Firstly identified in the liver, this transcription factor is also expressed in the pancreas, the kidney, and the intestine, playing important roles in regulating the development and functions of these tissues [221]–[223]. HNF1a regulates targets such as glucose transporter 2, pyruvate kinase, and collectrin [224]. Germline mutations in *HNF1A* are associated with maturity onset diabetes of the young 3 (MODY3), a rare autosomal dominantly inherited form of diabetes [225] whereas biallelic somatic alterations were observed in 60% of hepatocellular adenomas [226], [227]. *HNF1A* mutations were also reported in colorectal cancer with microsatellite instability [228], in endometrial cancer [229] and in pancreatic ductal adenocarcinoma, where it was demonstrated that *HNF1A* knockdown activated the Akt/mTOR signaling pathway [196]. Moreover, in pancreatic ductal adenocarcinoma HNF1A inhibition induces the resistance of pancreatic cancer cells to gemcitabine by targeting ABCB1 [230].

However, mutations in *HNF1A* have never been previously reported in association with esophageal adenocarcinoma.

We firstly identified one missense variant, mapping in the DNA binding region, and one frameshift variant in the transactivation domain. We detected 8 additional *HNF1A* mutations in 7 samples of the cohort of 169 cases (one of them carrying 2 mutations in the gene). Five different missense changes and 2 frameshifts were identified, with 2 patients carrying the same variant (p.Ala161Thr).

Therefore, our study identified a new gene mutated in EAC. Mutations in this gene were mainly found in conjunction with mutations in other genes;

supporting the idea that *HNF1A* mutations might contribute to tumor severity and progression. Further studies will be required to understand the role this gene can have in EAC evolution.

Other genes, found less frequently mutated in EAC tumor samples, resulted however to have a prognostic effect, especially on the event of recurrence. In particular, variants in the *MSH6* gene seem to be related to recurrence in all EACs (P=0.0439), and mutations in the *APC* gene seem to have an effect on recurrence in the Low grade group of patients (P=0.0183).

The *MSH6* gene is located on chromosome 2 and encodes for a protein involved in DNA repair during DNA replication [231]. Mutations in this gene have been associated with constitutional mismatch repair deficiency (CMMRD) syndrome and Lynch syndrome, conditions that increase the risk of developing many types of cancer, particularly colorectal cancer [232], [233].

The *APC* gene is located on chromosome 5 and encodes for a tumor suppressor protein, which a critical role in several processes such as cell migration and adhesion, transcriptional activation, and apoptosis [234]. The APC protein negatively regulates beta-catenin and E-cadherin, which are involved in cell adhesion. Mutations in *APC* alter β-catenin regulation, leading to abnormal cell migration and chromosome instability [235]. Germinal mutations in *APC* are identified in familial adenomatous polyposis (FAP) patients, with predisposition to colorectal cancer [236]. Somatic mutations in the *APC* gene may be involved in the development of gastric cancers [237].

In conclusion, our study showed that combining high throughput sorting technology and massive parallel sequencing allowed a better definition of inter- and intra-tumor heterogeneity and of EAC mutational status compared to whole-tumor samples analysis. Further studies will improve

the accurate understanding of the different tumor alterations and how they can lead to diverse outcomes and histopathological features, and will allow to evaluate the predictive role of biomarkers.

In the attempt to better characterize EAC also from an epigenetic point of view, in the second part of this project we focused on the analysis of miRNA483-3p and miRNA221, found to be aberrantly expressed in EAC in a preliminary study. miRNAs expression was evaluated in a larger cohort of EAC cases, confirming their up-regulation compared to healthy controls (P<0.0001).

Possible correlations between miR221 and miR483-3p expression and clinical-pathological features in EAC were evaluated.
Higher expression of both miR483-3p and miR221 was found to be associated with poorer cancer specific survival (P=0.0293 and P=0.0059 respectively), especially in the Lauren intestinal subtype (P=0.0059; P=0.0024) and, for miR221, also in the EACSGE Low grade subtype (P=0.0110).
Mann-Whitney test revealed a correlation with miR483-3p expression levels and recurrence in the Lauren subtype (P=0.0459) while miR221 up-regulation correlated with recurrence in all EAC cohort, (P=0.0002), in the Lauren intestinal subtype (P=0.0003) and in the EACSGE Low grade subgroup (P=0.0079).
Moreover, median expression levels of miRNAs 483-3p and 221 were higher in patients with advanced tumor stages (miR483-3p P=0.0532 (stages 1-2); P=0.0174 (stages 1-3); miR221 P=0.0257 (stages 1-3), P=0.0134 (stages 1-4)).

The *hsa-mir-221* is located in an intergenic region in chromosome Xp11.3 and it's encoded tandemly with *hsa-mir-222*. miR221 and miR222 are

highly homologous miRNAs sharing the same “seed sequence.” (Figure 43) [238].

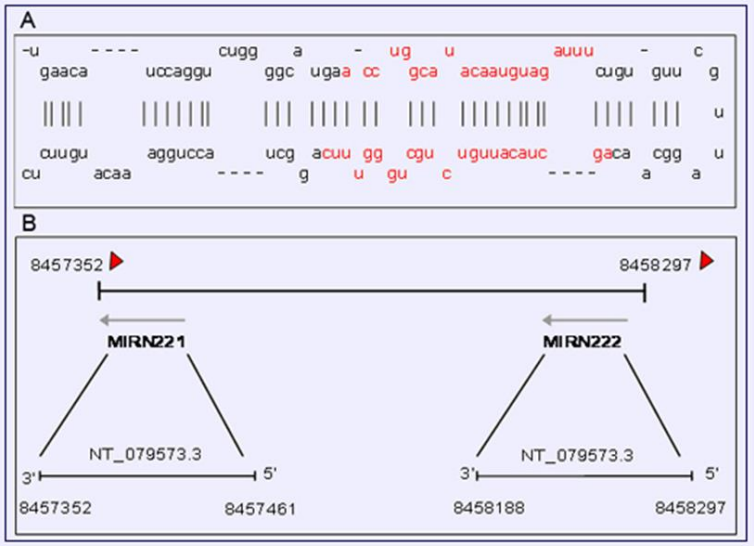

Figure 43: miR221. A: Stem-loop structure of miR221**. B:** Genomic localization of miR221 (MIRN221) and miR222(MIRN222) on chromosomal band Xp11.3. Image from Tabasi et al., 2009 [238].

miR221 was reported to be up-regulated in a variety of human neoplasms including, bladder [239], pancreatic [240], gastric [241] thyroid [242] and hepatocellular carcinoma [243]. miR221 over-expression correlates with tumor aggressive features, such as the presence of metastasis and multifocal lesions in hepatocellular carcinoma [244]. In few cases, non-oncogenic functions of miR221 were reported [245], suggesting that miR221 effects could also depend on cellular context. In vitro [243], [244] and in vivo [246] experiments demonstrated that miR221 caused an increase in cell proliferation rate and invasion capability.

A study by Matsuzaki and colleagues reported increased levels of miR221/222 in esophageal adenocarcinoma compared to the surrounding Barrett's esophagus: the overexpression of miR221/222 seems to be linked to increased levels of bile acids, and it reduces the levels of p27Kip1 and CDX2 [247]. Overexpression of miR221 has important consequences on many important pathways related to cell cycle regulation and apoptosis [248]. Among the target genes of miR221 already identified we can find: the cyclin-dependent kinase inhibitors *CDKN1B*/p27 and *CDKN1C*/p57 [243] the pro-apoptotic factors *BMF* [244], *BBC3/PUMA* [249], *PTEN* and *TIMP* [250].

In EAC, miR221 mediates 5-FU chemoresistance by direct targeting of *DKK2*, leading to alteration of the Wnt/β-catenin pathway. Moreover, miR221 knockdown reduction resulted in alteration of EMT-associated genes such as E-cadherin and vimentin and in slower xenograft tumor growth in nude mice [251].

hsa-mir-483 is located within intron 2 of the *IGF2* locus at the 11p15.5 chromosome region and encodes for two mature miRNAs: miR483-3p and miR483-5p [252] (Figure 44).

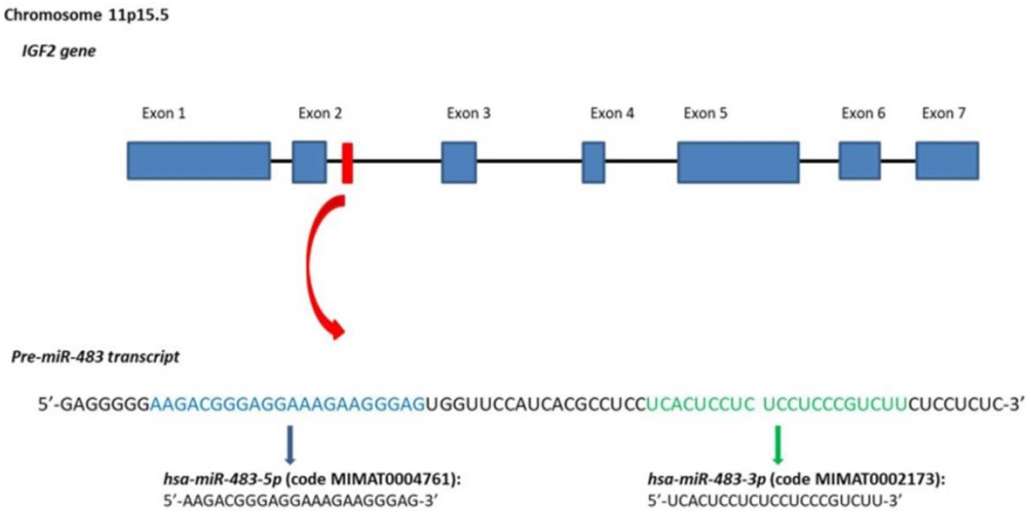

Figure 44: miR483. Genomic localization of miR483 on chromosomal band 11p15.5. miR483 encodes for two mature miRNAs: miR483-3p and miR483-5p [253]

IGF2 is an imprinted gene, expressed by the paternal allele that encodes a fetal insulin growth factor. Defects in the imprinting at the *IGF2* locus are observed in the Beckwith-Wiedemann syndrome, and increase the incidence of pediatric malignancies such as nephroblastoma (Wilms' tumor), hepatoblastoma, and rhabdomyosarcoma [254]. miR483-3p is over-expressed in 100% of Wilms' tumor [253], but studies observed that high levels of miR483-3p are also present in adult tumors such as colon, breast, and hepatocellular carcinoma [255]–[257].

A co-regulation with *IGF2* mRNA was detected, although some tumors exhibited high expression of miR483-3p without a concomitant increase of *IGF2*, suggesting that miR483-3p could cooperate with *IGF2* or act as an autonomous oncogene [253]. miR483-3p can be regulated by CTNNB11, which itself is a target of miR483-3p, triggering a negative regulatory loop [253], [258]. Moreover, studies have shown that miR483-3p expression is affected by the extracellular glucose concentration [259]. Functional studies have explained the oncogenic role of miR483-3p through its direct targeting of the apoptotic effector BBC3/PUMA, one of the principal effectors of TP53 apoptotic pathway [257], [260], and it was shown that

overexpressed miR483-3p can protect tumor cells from apoptosis [257]. In adrenocortical cancer miR483-3p is found over-expressed, leading to a significantly reduced *PUMA* expression [260]. In pancreatic cancer miR483-3p was identified as a negative regulator of SMAD4, a central mediator of TGFβ transduction that acts as a tumor suppressor gene inhibiting cell proliferation [197].
However, observations in literature are discordant, showing that miR483-3p can have both oncogenic and tumor suppressive roles. It has been reported that mature miR483-3p is down-regulated in gastric, nasopharyngeal, and some cases of hepatocellular carcinomas [261]–[264].

Little is known about miR483-3p involvement in EAC, thus we conducted preliminary studies in EAC cell lines. We used a miRNA mimic, in order to evaluate the effects of miR483-3p up-regulation and we evaluated the expression levels of *SMAD4*, *PUMA* and *CTNNB1,* identified, from a review of the literature, as three of the major genes modulated by miR483-3p. While no significant differences were observed in the levels of *PUMA* or *CTNNB1,* expression of *SMAD4* significantly decreased after the transfection with miR483-3p mimic in vitro (P=0.0343).
However, in EAC tissues we could not detect any correlation between SMAD4 loss and miR483-3p up-regulation, suggesting that different regulatory mechanisms might be involved, i.e. promoter hypermethylation [111].

In conclusion, the analysis of miR221 and miR483-3p revealed that they are up-regulated in EAC and that they correlate with poorer clinical outcomes, especially in the Lauren intestinal and EACSGE Low grade subtypes. Thus, miRNA profiling seems a promising strategy to stratify patients at higher risk of developing more aggressive tumors. Further studies will be required to interpret the role of these miRNAs in cancer

pathways and identifying their target genes in esophageal adenocarcinoma.

Combining the genetic and epigenetic characteristics with clinical variables can help for stratifying cancer subtypes, in order to improve the conventional histopathological classification and select subtype-specific therapeutic options.

6. CONCLUSIONS

In conclusion:

- Combining selective sorting technology and next generation sequencing allowed to better define EAC inter- and intra-tumor heterogeneity, compared to whole tumor samples analysis. We were able to reveal genetic alterations that would have been otherwise missed, and multiple subclones in the same tumor were identified. Further studies are needed to investigate whether these subclones are responsible for treatment response and disease recurrence.

- We identified mutations in *HNF1A* gene, which encodes for a transcription factor that acts as a tumor suppressor in other cancers. This is the first time that mutations in this gene are reported in EAC. This finding suggests that *HNF1A* mutations might contribute to tumor severity and progression in EAC too. Future studies will reveal the role this gene can have in EAC evolution.

- miR221 and miR483-3p were found up-regulated in EAC and they correlated with recurrence, tumor stage and poorer cancer specific survival, particularly in the Lauren intestinal and EACSGE Low grade subtypes. These miRNAs seem promising markers to stratify patients at higher risk for more aggressive tumors. However, further studies will be required to understand their role and their target genes in EAC.

7. TABLES

Table 1: Clinical and epidemiological information for EAC cases included in the genetic study. SEX: F=Female M= Male. CSS (Cancer Specific Survival): 1=Death. Recurrence 1=Yes. Lauren Classification: INT= Intestinal; DIF= Diffuse; MIX= Mixed. EACSGE classification: L= Low Grade; H= High Grade. Cases from EAC1 to EAC38 underwent cell sorting with DEPArray and Oncoseek analysis; Cases from EAC115 to EAC283 belong to the secondo cohort who was subjected to NGS target panel. Cases from EAC1 to EAC114 (excluding EAC2 and EAC5) underwent miRNA analysis.

ID	SEX	AGE	CSS	Follow-up (months)	Recurrence	Stage (7ed)	Lauren classification	EACSGE classification
EAC1	F	53	0	72	1	2	INT	L
EAC2	M	43	0	60	0	2	DIF	
EAC3	F	76	0	1	0	3	DIF	H
EAC4	M	66	1	36	1	2	INT	L
EAC5	M	71	*1*	*11*	1	3	INT	
EAC6	F	82	*0*	84	0	3	INT	L
EAC7	M	83	0	27	0	3	INT	L
EAC8	M	86	1	13	1	3	INT	H
EAC9	M	62	1	3	1	3	INT	H
EAC10	M	72	1	58	1	1	DIF	
EAC11	M	76	0	12	0	3	INT	H
EAC12	M	58	0	53	0	3	INT	L
EAC13	F	28	1	22	1	4	INT	L
EAC14	F	83	0	0	0	3	INT	L
EAC15	F	60	0	84	0	2	INT	L
EAC16	M	78	1	36	1	2	INT	H
EAC17	M	59	0	24	1	2	INT	L

EAC18	M	75	1	8	1	3	INT	H
EAC19	F	44	1	35	1	3	DIF	H
EAC20	M	79	0	0	0	4	DIF	H
EAC21	M	63	0	56	0	2	INT	L
EAC22	M	84	0	84	0	2	INT	L
EAC23	F	77	0	4	n.a.	3	INT	L
EAC24	F	78	1	10	1	3	INT	L
EAC25	M	80	0	71	0	1	DIF	H
EAC26	M	74	0	19	0	3	INT	H
EAC27	M	68	0	0	0	3	INT	L
EAC28	M	72	0	6	0	3	INT	H
EAC29	M	67	0	14	0	2	INT	L
EAC30	M	82	0	14	1	3	INT	L
EAC31	M	66	*1*	*33*	1	3	INT	L
EAC32	M	54	1	15	0	3	INT	H
EAC33	M	87	*0*	*0*	0	2	INT	L
EAC34	M	61	1	12	1	3	INT	H
EAC35	M	82	1	6	1	4	INT	L
EAC36	M	65	*1*	29	1	3	INT	L
EAC37	M	62	1	5	1	2	INT	L
EAC38	F	54	0	6	0	2	DIF	L
EAC39	F	75	1	45	1	4	INT	L
EAC40	M	77	1	60	1	4	INT	H
EAC41	M	75	0	16	0	1	INT	H
EAC42	M	69	0	24	0	3	INT	H
EAC43	F	70	1	48	1	3	DIF	H
EAC44	M	66	1	15	1	3	INT	H
EAC45	F	54	1	12	1	4	INT	H
EAC46	M	73	1	24	1	1	INT	H
EAC47	M	70	0	6	0	3	INT	L
EAC48	M	71	1	4	1	3	INT	H
EAC49	M	77	1	22	1	3	INT	H

EAC50	M	69	*1*	*2*	1	3	INT	H
EAC51	M	68	0	0	0	3	INT	H
EAC52	M	70	0	7	0	1	INT	L
EAC53	M	57	1	6	1	4	INT	L
EAC54	M	72	0	7	0	3	INT	H
EAC55	M	80	0	4	0	3	INT	H
EAC56	M	76	1	n.a.	1	2	INT	L
EAC57	M	69	0	7	0	4	INT	H
EAC58	M	65	0	11	1	4	INT	L
EAC59	F	80	0	0	n.a.	3	DIF	H
EAC60	M	75	0	35	0	3	INT	L
EAC61	M	82	1	20	1	3	INT	L
EAC62	F	58	0	15	0	2	INT	L
EAC63	M	72	0	53	0	3	INT	L
EAC64	M	72	0	29	0	3	INT	L
EAC65	M	63	0	36	0	1	INT	
EAC66	M	83	0	18	0	1	INT	
EAC67	F	67	0	29	0	1	INT	
EAC68	M	66	0	31	0	1	INT	
EAC69	M	63	0	38	0	1	INT	
EAC70	M	62	0	58	0	1	INT	
EAC71	M	52	0	57	0	1	INT	
EAC72	F	60	0	41	0	1	INT	
EAC73	M	66	0	84	0	1	INT	
EAC74	F	83	0	3	0	1	INT	
EAC75	M	72	1	0	n.a.	3	DIF	H
EAC76	F	80	0	67	0	1	MIX	H
EAC77	F	74	1	3	0	2	DIF	H
EAC78	M	71	1	31	1	3	INT	
EAC79	M	57	1	29	1	3	INT	
EAC80	M	78	1	11	n.a.	4	MIX	
EAC81	M	70	0	29	0	3	INT	

EAC82	M	55	0	30	1	3	INT	
EAC83	M	67	0	57	1	3	INT	
EAC84	M	68	0	10	0	3	INT	
EAC85	M	82	0	24	1	2	INT	
EAC86	M	46	0	25	0	2	INT	
EAC87	M	47	0	28	0	3	INT	
EAC88	M	60	0	49	0	2	DIF	
EAC89	M	73	0	62	0	4	INT	
EAC90	M	79	0	48	0	2	INT	
EAC91	M	41	1	33	1	3	INT	
EAC92	F	51	1	62	1	2	INT	
EAC93	F	48	0	98	0	3	n.a.	
EAC94	F	62	1	46	1	2	INT	
EAC95	F	45	1	16	1	3	INT	
EAC96	M	61	1	22	1	2	INT	
EAC97	M	77	0	102	0	2	INT	
EAC98	M	13	0	84	0	3	MIX	
EAC99	M	78	1	38	1	3	INT	
EAC100	M	67	1	24	1	2	DIF	
EAC101	M	77	0	56	0	2	INT	
EAC102	M	62	1	33	1	4	INT	
EAC103	M	61	1	24	1	4	INT	
EAC104	F	49	1	27	1	3	n.a.	
EAC105	F	62	1	34	1	3	INT	
EAC106	M	73	0	18	1	2	INT	
EAC107	M	51	1	0,46	1	3	INT	
EAC108	M	70	1	66	1	3	MIX	
EAC109	M	62	1	29	1	2	INT	
EAC110	F	69	0	29	1	3	INT	
EAC111	M	44	0	133	0	3	INT	
EAC112	F	68	1	40	1	3	INT	
EAC113	F	76	0	31	0	2	INT	

EAC114	M	77	0	16	0	2	INT	
EAC115	M	67	0	133	0	2	INT	H
EAC116	F	78	1	13	1	3	INT	H
EAC117	F	73	1	42	1	3	INT	H
EAC118	M	60	0	101	0	2	INT	0
EAC119	M	62	0	9	0	2	INT	H
EAC120	M	82	0	46	0	2	INT	H
EAC121	M	23	0	82	1	3	INT	L
EAC122	F	81	0	30	0	1	INT	H
EAC123	F	78	0	1	0	3	INT	H
EAC124	M	85	0	1	0	3	INT	L
EAC125	M	76	1	42	1	1	INT	L
EAC126	M	46	1	12	1	3	DIFF	H
EAC127	M	46	1	44	1	3	DIFF	H
EAC128	M	66	0	5	0	2	INT	L
EAC129	M	71	0	85	0	3	INT	H
EAC130	M	78	0	5	0	3	MIX	H
EAC131	M	48	0	11	0	4	INT	H
EAC132	M	76	0	17	0	4	INT	L
EAC133	M	54	0	3	0	3	DIFF	H
EAC134	M	79	1	25	1	3	DIFF	H
EAC135	M	76	0	16	0	3	INT	H
EAC136	M	80	1	28	1	3	INT	H
EAC137	M	66	1	83	1	3	INT	H
EAC138	M	63	1	24	1	2	INT	L
EAC139	M	78	0	8	0	3	INT	H
EAC140	M	69	1	26	1	3	INT	H
EAC141	M	39	1	55	1	3	INT	H
EAC142	M	62	1	15	1	2	INT	H
EAC143	M	58	0	7	0	3	INT	H
EAC144	M	84	1	9	1	2	INT	H
EAC145	M	43	0	154	0	3	INT	L

EAC146	M	73	1	30	1	2	INT	H
EAC147	F	81	0	8	0	1	INT	L
EAC148	M	65	1	66	1	3	INT	L
EAC149	F	76	1	10	1	3	INT	H
EAC150	M	73	1	17	1	3	INT	L
EAC151	M	81	1	20	1	4	DIFF	H
EAC152	M	75	0	13	0	2	INT	H
EAC153	M	67	1	11	1	3	INT	H
EAC154	M	67	1	5	1	2	MIX	H
EAC155	F	85	1	10	1	4	INT	L
EAC156	M	55	0	137	0	2	MIX	H
EAC157	M	72	1	19	1	4	MIX	L
EAC158	M	70	0	7	0	2	INT	L
EAC159	M	48	1	11	1	3	INT	L
EAC160	F	84	0	7	0	2	INT	L
EAC161	M	57	0	113	1	3	INT	L
EAC162	M	73	1	22	1	3	INT	L
EAC163	M	67	1	12	1	1	INT	L
EAC164	M	56	0	63	0	3	DIFF	L
EAC165	M	61	1	19	1	3	INT	H
EAC166	M	48	0	102	0	3	INT	H
EAC167	M	83	0	3	0	2	INT	L
EAC168	F	71	1	14	1	3	INT	H
EAC169	M	75	1	6	1	3	INT	H
EAC170	M	74	0	41	0	3	INT	L
EAC171	M	75	1	4	1	4	MIX	H
EAC172	M	52	1	25	1	3	INT	H
EAC173	F	85	0	2	0	2	INT	H
EAC174	M	71	0	56	0	4	DIFF	H
EAC175	M	47	0	62	1	3	INT	H
EAC176	M	85	1	12	1	4	DIFF	L
EAC177	M	58	0	100	1	2	INT	L

EAC178	M	76	0	62	0	3	INT	H
EAC179	M	81	1	12	1	4	INT	H
EAC180	M	61	1	39	1	3	INT	L
EAC181	M	58	0	42	0	3	INT	H
EAC182	M	69	0	1	0	4	INT	H
EAC183	M	36	1	32	1	3	INT	L
EAC184	F	83	0	5	1	3	INT	H
EAC185	M	38	1	45	1	2	INT	H
EAC186	M	62	0	81	0	3	MIX	H
EAC187	M	70	0	12	0	2	INT	L
EAC188	M	77	1	36	1	4	INT	L
EAC189	M	76	1	4	1	4	INT	L
EAC190	M	83	1	12	1	3	DIFF	H
EAC191	F	80	0	1	0	3	MIX	H
EAC192	F	73	0	64	0	2	INT	L
EAC193	M	60	0	1	0	4	INT	H
EAC194	M	64	1	7	1	4	INT	H
EAC195	M	78	1	6	1	3	INT	L
EAC196	M	80	0	2	0	2	INT	L
EAC197	F	59	1	16	1	3	MIX	H
EAC198	F	55	1	44	1	3	INT	H
EAC199	F	44	0	114	0	3	INT	H
EAC200	M	47	0	62	0	3	INT	H
EAC201	M	45	0	141	0	2	INT	H
EAC202	M	78	0	40	0	2	INT	L
EAC203	M	66	0	3	0	3	INT	L
EAC204	M	78	1	5	1	4	INT	H
EAC205	M	79	0	16	0	4	INT	L
EAC206	M	65	1	19	1	3	INT	H
EAC207	M	66	0	180	0	3	INT	H
EAC208	F	72	1	8	1	4	INT	H
EAC209	M	88	1	34	1	3	INT	H

EAC210	M	82	0	32	0	3	INT	L
EAC211	M	73	1	10	1	3	INT	H
EAC212	M	68	1	32	1	3	INT	H
EAC213	M	75	1	21	1	2	INT	H
EAC214	M	77	0	30	0	2	INT	L
EAC215	M	58	1	7	1	3	MIX	H
EAC216	M	76	1	11	1	3	INT	H
EAC217	M	64	0	118	1	2	INT	L
EAC218	M	64	0	1	0	4	DIFF	H
EAC219	F	82	1	28	1	4	INT	H
EAC220	M	70	0	24	0	3	INT	H
EAC221	M	84	0	132	0	2	INT	L
EAC222	M	68	0	27	0	3	DIFF	H
EAC223	M	50	0	18	0	4	INT	L
EAC224	F	43	0	29	0	2	DIFF	H
EAC225	M	83	0	2	0	3	INT	H
EAC226	M	75	1	6	1	4	DIFF	H
EAC227	M	71	1	3	1	3	INT	H
EAC228	M	76	1	19	1	3	DIFF	H
EAC229	F	64	0	39	0	2	INT	L
EAC230	M	42	0	70	0	2	INT	H
EAC231	M	50	1	5	1	3	DIFF	H
EAC232	M	74	0	12	0	3	INT	H
EAC233	M	83	1	22	1	3	INT	H
EAC234	M	60	1	9	1	4	MIX	H
EAC235	M	59	0	4	0	3	MIX	H
EAC236	F	85	0	31	1	4	DIFF	H
EAC237	M	81	0	1	0	3	INT	L
EAC238	F	77	1	21	1	3	INT	H
EAC239	M	72	1	35	1	3	INT	H
EAC240	M	64	0	42	1	3	INT	L
EAC241	M	79	0	2	0	4	MIX	H

EAC242	M	66	0	7	0	2	INT	0
EAC243	M	65	0	10	0	3	INT	H
EAC244	M	56	0	33	0	3	INT	L
EAC245	M	77	1	12	1	4	INT	H
EAC246	M	82	0	6	0	4	INT	H
EAC247	F	76	0	2	0	4	MIX	H
EAC248	M	44	1	17	1	4	MIX	H
EAC249	M	79	0	61	0	3	INT	H
EAC250	M	72	0	5	0	3	INT	L
EAC251	M	70	0	11	0	2	INT	L
EAC252	M	64	0	7	0	4	DIFF	H
EAC253	M	84	0	4	0	3	INT	H
EAC254	M	80	0	9	0	3	INT	L
EAC255	F	76	0	29	0	4	INT	H
EAC256	M	81	0	6	1	4	DIFF	H
EAC257	M	84	0	2	0	2	INT	L
EAC258	M	76	0	2	0	4	DIFF	H
EAC259	F	80	0	28	1	3	INT	L
EAC260	M	81	0	1	0	3	INT	H
EAC261	M	81	0	6	0	4	INT	H
EAC262	M	82	0	6	0	3	INT	L
EAC263	F	77	0	31	0	3	DIFF	L
EAC264	M	65	0	1	0	3	INT	H
EAC265	M	61	0	2	0	3	INT	H
EAC266	M	81	0	10	1	4	INT	L
EAC267	M	72	0	18	0	2	INT	L
EAC268	M	67	0	1	0	2	INT	H
EAC269	M	65	0	1	0	2	INT	L
EAC270	M	83	0	2	0	3	INT	H
EAC271	F	75	0	2	0	3	MIX	H
EAC272	M	57	0	16	0	3	INT	L
EAC273	M	77	0	12	0	3	INT	L

EAC274	F	86	0	1	0	3	INT	L
EAC275	M	85	0	8	0	4	INT	H
EAC276	M	85	0	1	0	3	INT	L
EAC277	F	87	0	2	0	3	INT	H
EAC278	M	78	0	2	0	2	INT	H
EAC279	F	88	0	2	0	4	INT	H
EAC280	M	75	0	2	0	3	INT	L
EAC281	F	81	0	1	0	3	INT	L
EAC282	M	85	0	2	0	4	INT	H
EAC283	M	85	0	1	0	3	INT	L

Table 2: Genes present in the target panel DEPArray™ OncoSeek Panel.

ABL1	5	*CDK4*	10	*ERBB4*	8	*GNA11*	2	*KDR*	9	*MYCN*	9	*RET*	6
AKT1	2	*CDK6*	10	*EZH2*	1	*GNAQ*	2	*KIT*	24	*NOTCH1*	3	*SMAD4*	10
ALK	12	*CDKN2A*	2	*FBXW7*	6	*GNAS*	2	*KRAS*	11	*NPM1*	1	*SMARCB1*	4
APC	9	*CSF1R*	2	*FGFR1*	12	*HNF1A*	4	*MAP2K1*	5	*NRAS*	3	*SMO*	5
AR	10	*CTNNB1*	1	*FGFR2*	13	*HRAS*	2	*MET*	16	*PDGFRA*	13	*SRC*	1
ATM	19	*DDR2*	1	*FGFR3*	14	*IDH1*	1	*MLH1*	1	*PIK3CA*	19	*STK11*	5
BRAF	12	*DNMT3A*	1	*FGFR4*	9	*IDH2*	2	*MPL*	1	*PTEN*	14	*TP53*	21
CCND1	8	*EGFR*	19	*FLT3*	4	*JAK2*	2	*MSH6*	4	*PTPN11*	2	*TSC1*	1
CDH1	3	*ERBB2*	14	*FOXL2*	1	*JAK3*	3	*MYC*	9	*RB1*	12	*VHL*	3

Genes with contiguous, overlapping coverage

Genes with comprehensive coding exon coverage

Genes with amplicons for CNA calling and SNV calling

Genes with only amplicons for CNA calling

Table 3: Sequence of the primers used in the study.

	Primers	Sequence
Whole Genome LOW PASS PCR	**Amplicon PCR Forward**	5′-AATGATACGGCGACCACCGAGATC-3′
	Amplicon PCR Reverse	5′-CAAGCAGAAGACGGCATACGA-3′
Sanger Validation	**HNF1A.x4.F**	5′-GTGGCTATTTCTGCAGGGC-3′
	HNF1A.x4.R	5′-CCCCACATACCACTTACCGT-3′
qPCR	**h ACT IIF**	5′-CCTGGCACCCAGCACAAT-3′
	h ACT IIR	5′-GGGCCGGACTCGTCATACT-3′
	SMAD4 F	5′-CATCCACCAAGTAATCGTGCAT-3′
	SMAD4 R	5′-CCAACTTTCCCAACATTCCTGT-3′
	PUMA.F	5′-GACCTCAACGCACAGTACGAG-3′
	PUMA.R	5′-ACAATCTCATCATGGGACTCCT-3′
	CTNNB1.F	5′-GCAGAGTGCTGAAGGTGCTA-3′
	CTNNB1.R	5′-TCTGTCAGGTGAAGTCCTAAAGC-3′

Table 4: Genes represented in the custom EAC panel IDT (Integrated DNA Technology).

Gene Name	Gene Name
ALK	KRAS
APC	MAP2K1
ARID2	MET
ATM	MSH6
CDK6	NRAS
CDKN2A	PIK3CA
CHEK2	PTEN
CTNNB1	RET
EGFR	SMAD4
ERBB2	SMARCA4
FLT3	SRC
HNF1A	STK11
IDH2	TP53
JAK3	TSSC1

Table 5: Growth medium and storage conditions for EAC cell lines.

	OE19	OE33	FLO1
Growth medium	RPMI1640 (EuroClone, Milan, Italy) 10% (v/v) FBS, 100 U/mL penicillin, 100 µg/mL streptomycin and 2mM L-glutamine (supplements from Sigma-Aldrich, St. Louis, Missouri, USA)		DMEM (EuroClone, Milan, Italy) 10% (v/v) FBS, 100 U/mL penicillin, 100 µg/mL streptomycin and 2mM L-glutamine (supplements from Sigma-Aldrich, St. Louis, Missouri, USA).
Storage conditions	Frozen with 70% medium, 20% FBS, 10% DMSO at about 2.5 x 10^6 cells/ampoule		Frozen with 90% FBS 10% DMSO at about 2.5 x 10^6 cells/ampoule

Table 6: Somatic mutations and CNAs identified in sorted tumor populations with the OncoSeek panel analysis. Only cases with variants identified are shown. In red: hyperdiploid tumor populations; gray: pseudodiploid tumor populations. The values reported represent the alternative allele frequency of the detected variants; yellow: missense mutations; green: loss of function mutations (indel and nonsense); violet: CNAs.

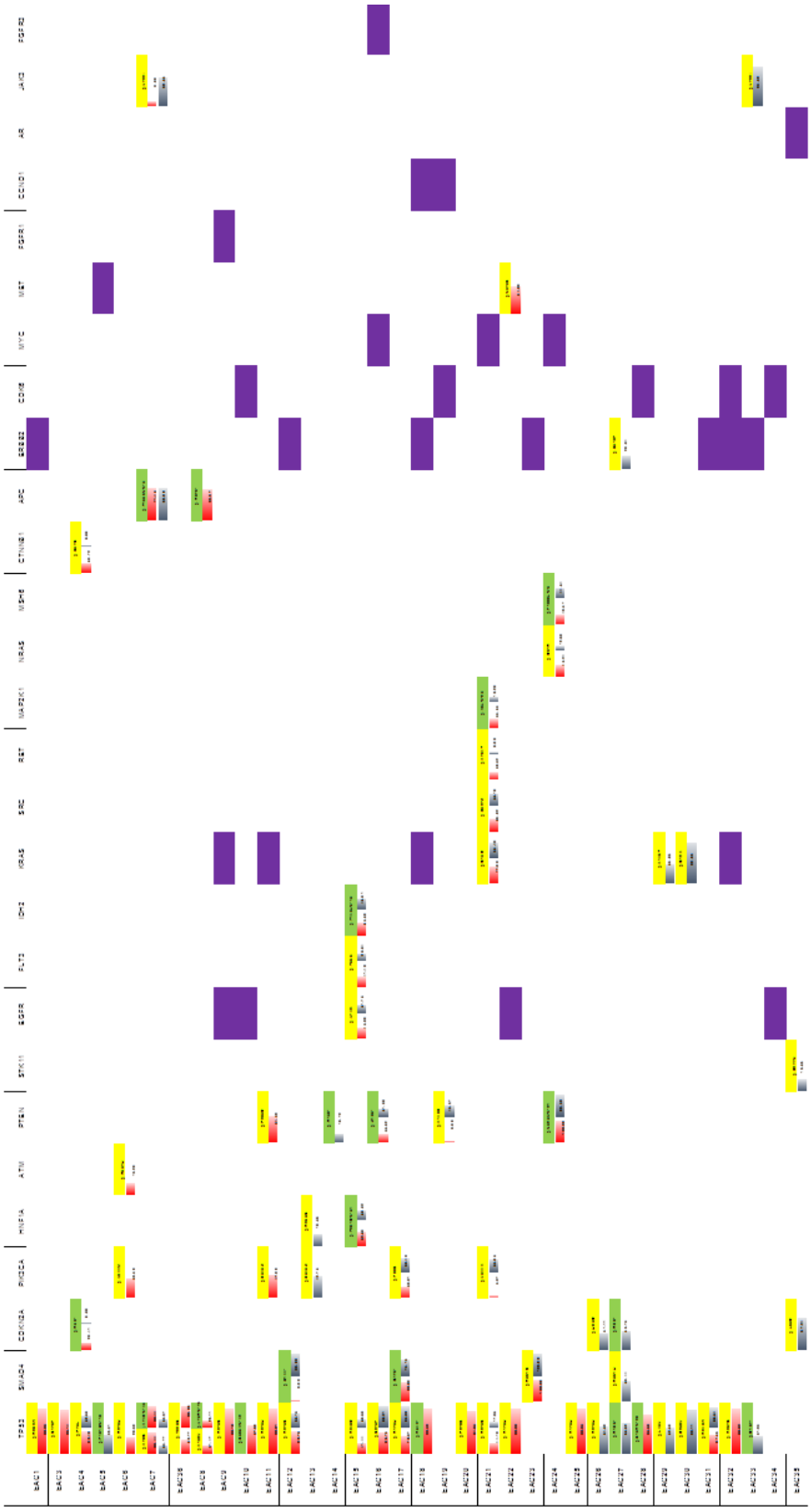

Table 7: Somatic mutations identified in 169 cases EAC cohort with custom target panel analysis. Only genes found mutated are reported. Missense mutations are shown in yellow, loss of function mutations (frameshift and nonsense) are in green, splicing and inframe mutations are in light blue.

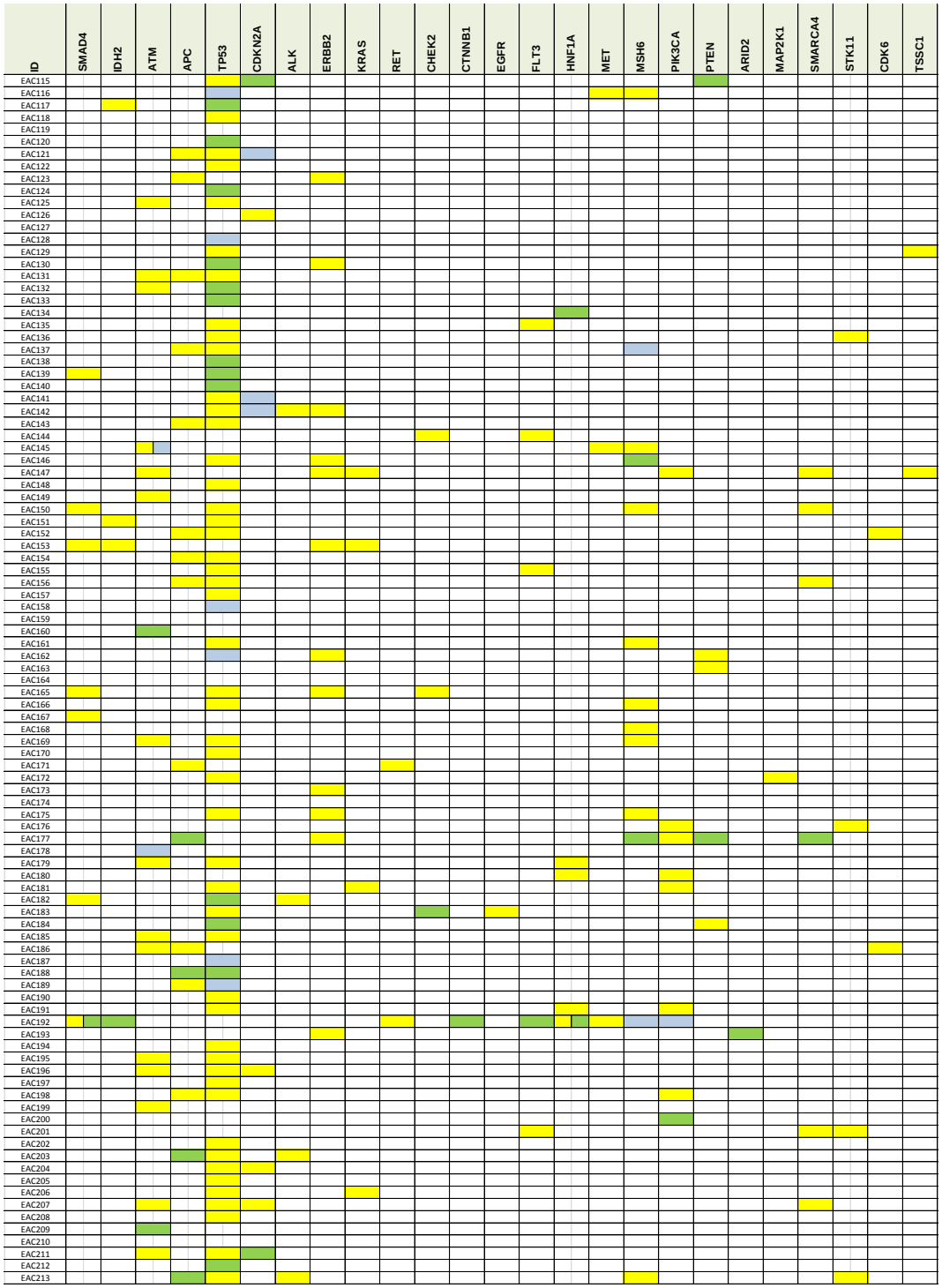

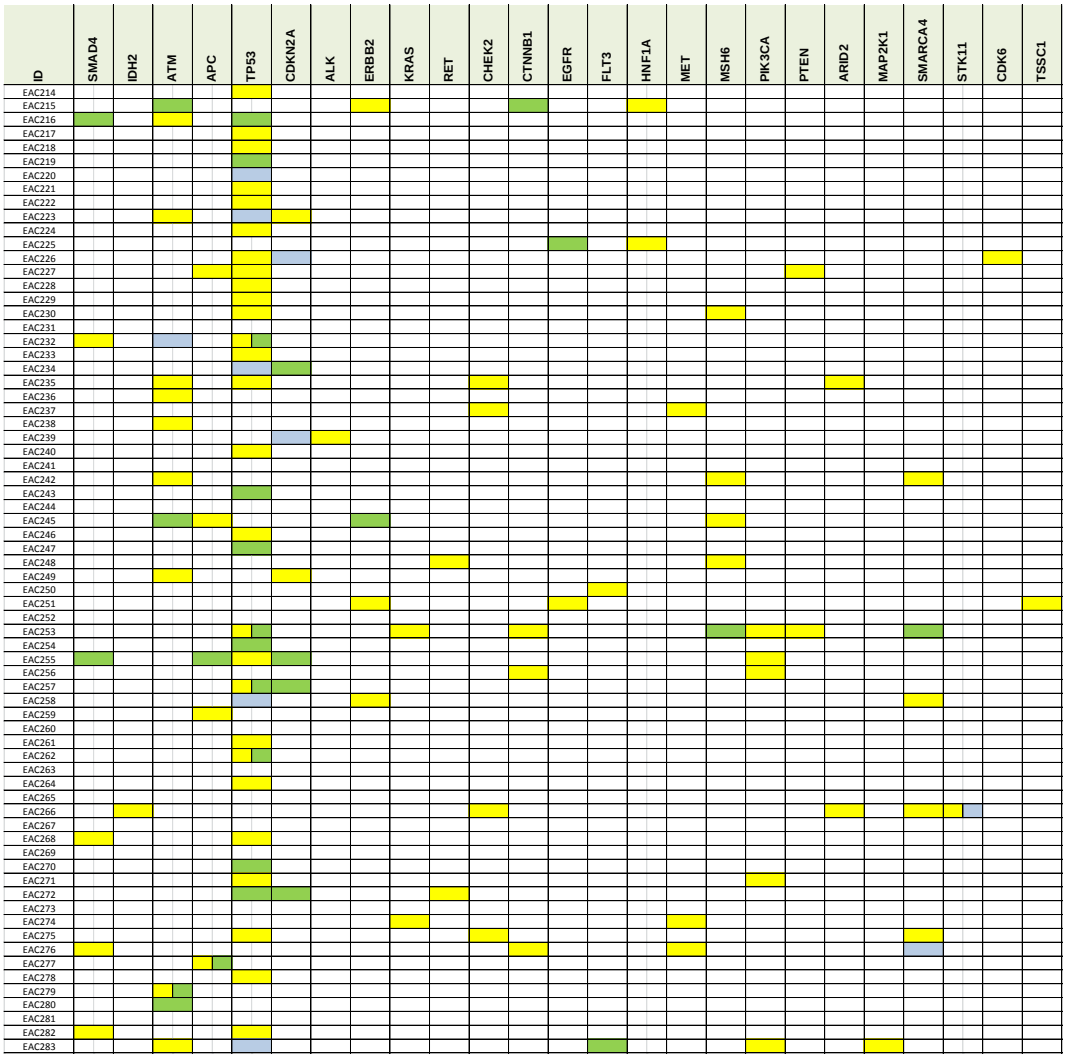
ID
SMAD4
IDH2
ATM
APC
TP53
CDKN2A
ALK
ERBB2
KRAS
RET
CHEK2
CTNNB1
EGFR
FLT3
HNF1A
MET
MSH6
PIK3CA
PTEN
ARID2
MAP2K1
SMARCA4
STK11
CDK6
TSSC1
EAC214
EAC215
EAC216
EAC217
EAC218
EAC219
EAC220
EAC221
EAC222
EAC223
EAC224
EAC225
EAC226
EAC227
EAC228
EAC229
EAC230
EAC231
EAC232
EAC233
EAC234
EAC235
EAC236
EAC237
EAC238
EAC239
EAC240
EAC241
EAC242
EAC243
EAC244
EAC245
EAC246
EAC247
EAC248
EAC249
EAC250
EAC251
EAC252
EAC253
EAC254
EAC255
EAC256
EAC257
EAC258
EAC259
EAC260
EAC261
EAC262
EAC263
EAC264
EAC265
EAC266
EAC267
EAC268
EAC269
EAC270
EAC271
EAC272
EAC273
EAC274
EAC275
EAC276
EAC277
EAC278
EAC279
EAC280
EAC281
EAC282
EAC283

Table 8: SMAD4 immunoreactivity and miR483-3p expression levels. In red: Up-regulated miRNA , considering a cut-off value of 3.15 and SMAD4 protein loss, considering a cut-off value 30%; In green: down-regulated miRNA and high SMAD4 expression (<30% loss). n.a.= not available

ID	% of SMAD4 LOSS	miR483-3p fold-change
EAC7	0	2,5
EAC6	0	2,99
EAC15	0	1,51
EAC46	0	2,48
EAC42	0	53,53
EAC41	0	18,22
EAC26	0	6,54
EAC18	0	3,31
EAC47	0	18,23
EAC14	0	3,85
EAC5	0	n.a.
EAC20	0	0,72
EAC11	0	0,77
EAC33	0	3,45
EAC64	0	15,56
EAC29	0	3,74
EAC34	10	2,18
EAC43	10	6,89
EAC13	10	1,59
EAC60	10	24,7
EAC61	10	5.03
EAC59	10	7,33
EAC76	10	19,61
EAC3	15	6,69
EAC40	20	5,1
EAC2	20	n.a.
EAC25	20	2,79
EAC31	30	2,19

EAC45	40	18,05
EAC9	40	0,87
EAC24	40	37,49
EAC39	45	3,43
EAC32	50	14
EAC30	50	0,33
EAC23	50	5,61
EAC10	50	16,12
EAC4	60	0,12
EAC63	60	3,14
EAC77	60	42,25
EAC19	80	1,48
EAC75	80	15,69
EAC21	80	11,53
EAC44	90	3,55
EAC38	90	10,76
EAC12	90	1,91
EAC36	90	11,95
EAC62	90	11,78
EAC22	90	1,66
EAC48	95	12,28
EAC50	95	6,2
EAC1	99	16,45
EAC16	100	1,02
EAC17	100	1,4
EAC49	100	27,36
EAC35	100	11,75

8. REFERENCES

[1] F. Bray, J. Ferlay, I. Soerjomataram *et al.,* "Global cancer statistics 2018: GLOBOCAN estimates of incidence and mortality worldwide for 36 cancers in 185 countries," *CA. Cancer J. Clin.*, 2018; 68: 394–424.

[2] J. R. Siewert and K. Ott, "Are Squamous and Adenocarcinomas of the Esophagus the Same Disease?," *Semin. Radiat. Oncol.*, 2007; 17: 38–44.

[3] M. Arnold, I. Soerjomataram, J. Ferlay *et al.,* "Global incidence of oesophageal cancer by histological subtype in 2012," *Gut*, 2015; 64: 381–387.

[4] G. Edgren, H. O. Adami, E. W. Vainio *et al.,* "A global assessment of the oesophageal adenocarcinoma epidemic," *Gut*, 2013, 62: 1406–1414.

[5] J. Lagergren and P. Lagergren, "Recent developments in esophageal adenocarcinoma," *CA. Cancer J. Clin.*, 2013; 63: 232–248.

[6] L. M. Brown, S. S. Devesa and W. H. Chow, "Incidence of adenocarcinoma of the esophagus among white Americans by sex, stage, and age," *J. Natl. Cancer Inst.*, 2008; 100: 1184–1187.

[7] S. H. Xie and J. Lagergren, "The Male Predominance in Esophageal Adenocarcinoma," *Clin. Gastroenterol. Hepatol.*, 2016; 14: 338-347.

[8] N. Zaidi and R. J. Kelly, "The management of localized esophageal squamous cell carcinoma: Western approach," *Chin. Clin. Oncol.*, 2017; 6: 46.

[9] T. W. Rice, E. H. Blackstone and V. W. Rusch, "Editorial: 7th edition of the AJCC cancer staging manual: Esophagus and esophagogastric

junction," *Ann. Surg. Oncol.*, 2010; 17: 1721–1724.

[10] K. Wang, A. Johnson, S. M. Ali *et al.*, "Comprehensive Genomic Profiling of Advanced Esophageal Squamous Cell Carcinomas and Esophageal Adenocarcinomas Reveals Similarities and Differences," *Oncologist*, 2015; 20: 1132–1139.

[11] Cancer Genome Atlas Research Network, "Integrated genomic characterization of oesophageal carcinoma," *Nature*, 2017; 541: 169–174.

[12] J. Lagergren, R. Bergström, A. Lindgren *et al.,* "Symptomatic Gastroesophageal Reflux as a Risk Factor for Esophageal Adenocarcinoma," *N. Engl. J. Med.*, 1999; 340: 825–831.

[13] V. Bhardwaj, A. Horvat, O. Korolkova *et al.*, "Prevention of DNA damage in Barrett's esophageal cells exposed to acidic bile salts," *Carcinogenesis*, 2016; 37: 1161–1169.

[14] S. J. Spechler, R. C. Fitzgerald, G. A. Prasad *et al.,* "History, Molecular Mechanisms, and Endoscopic Treatment of Barrett's Esophagus," *Gastroenterology*, 2010; 138: 854–869.

[15] M. M. Abdel-Latif, S. Duggan, J. V. Reynolds *et al.,* "Inflammation and esophageal carcinogenesis," *Curr. Opin. Pharmacol.*, 2009; 9: 396–404.

[16] K. R. McQuaid, L. Laine, M. B. Fennerty *et al.*, "Systematic review: The role of bile acids in the pathogenesis of gastro-oesophageal reflux disease and related neoplasia," *Aliment. Pharmacol. Ther.*, 2011; 34: 146–165.

[17] M. B. Cook, D. A. Corley, L. J. Murray *et al.*, "Gastroesophageal reflux in relation to adenocarcinomas of the esophagus: A pooled analysis from the Barrett's and Esophageal Adenocarcinoma Consortium (BEACON)," *PLoS One*, 2014, 9: e103508.

[18] S. J. Spechler and R. F. Souza, "Barrett's Esophagus," *N. Engl. J. Med.*, 2014; 371:836–845.

[19] N. J. Shaheen and J. E. Richter, "Barrett's oesophagus," *Lancet*,

2009; 373: 850–861.

[20] R. Anaparthy and P. Sharma, "Progression of Barrett oesophagus: Role of endoscopic and histological predictors," *Nature Reviews Gastroenterology and Hepatology*, 2014; 11: 525–534.

[21] F. Hvid-Jensen, L. Pedersen, A. M. Drewes *et al.,* "Incidence of Adenocarcinoma among Patients with Barrett's Esophagus," *N. Engl. J. Med.*, 2011; 365: 1375–1383.

[22] S. Bhat, H. G. Coleman, F. Yousef *et al.*, "Risk of malignant progression in Barrett's Esophagus patients: Results from a large population-based study," *J. Natl. Cancer Inst.*, 2011; 103: 1049–1057.

[23] M. Solaymani-Dodaran, R. F. A. Logan, J. West *et al.,* "Risk of oesophageal cancer in Barrett's oesophagus and gastro-oesophageal reflux," *Gut*, 2004; 53: 1070–1074.

[24] T. L. Vaughan and R. C. Fitzgerald, "Precision prevention of oesophageal adenocarcinoma," *Nat. Rev. Gastroenterol. Hepatol.*, 2015; 12: 243–248.

[25] J. T. Chang and D. A. Katzka, "Gastroesophageal reflux disease, barrett esophagus, and esophageal adenocarcinoma," *Arch. Intern. Med.*, 2004; 164: 1482–1488.

[26] G. S. Dulai, J. Gornbein, K. L. Kahn *et al.,* "Preoperative prevalence of Barrett's esophagus in esophageal adenocarcinoma: A systematic review," *Gastroenterology*, 2002; 122: 26–33.

[27] C. A. J. Ong, P. Lao-Sirieix and R. C. Fitzgerald, "Biomarkers in Barrett's esophagus and esophageal adenocarcinoma: Predictors of progression and prognosis," *World J. Gastroenterol.*, 2010; 16: 5669–5681.

[28] C. Y. Kong, K. J. Nattinger, T. J. Hayeck *et al.*, "The impact of obesity on the rise in esophageal adenocarcinoma incidence: Estimates from a disease simulation model," *Cancer Epidemiol. Biomarkers Prev.*, 2011; 20: 2450–2456.

[29] J. A. Abrams, R. Z. Sharaiha, L. Gonsalves *et al.*, "Dating the rise of esophageal adenocarcinoma: Analysis of connecticut tumor registry data, 1940-2007," *Cancer Epidemiol. Biomarkers Prev.*, 2011; 20: 183–185.

[30] C. Hoyo, M. B. Cook, F. Kamangar *et al.*, "Body mass index in relation to oesophageal and oesophagogastric junction adenocarcinomas: A pooled analysis from the international BEACON consortium," *Int. J. Epidemiol.*, 2012; 41: 1706–1718.

[31] A. Kubo and D. A. Corley, "Body mass index and adenocarcinomas of the esophagus or gastric cardia: A systematic review and meta-analysis," *Cancer Epidemiol. Biomarkers Prev.*, 2006; 15: 872–878.

[32] H. Hampel, N. S. Abraham and H. B. El-Serag, "Meta-analysis: Obesity and the risk for gastroesophageal reflux disease and its complications," *Ann. Intern. Med.*, 2005; 143: 199–211.

[33] S. Singh, A. N. Sharma, M. H. Murad *et al.*, "Central adiposity is associated with increased risk of esophageal inflammation, metaplasia, and adenocarcinoma: A systematic review and meta-analysis," *Clin. Gastroenterol. Hepatol.*, 2013; 11: 1399-1412.

[34] H. B. El-Serag, "Role of obesity in GORD-related disorders," *Gut*, 2008; 57: 281–284.

[35] A. K. Chandar and P. G. Iyer, "Role of Obesity in the Pathogenesis and Progression of Barrett's Esophagus," *Gastroenterol. Clin. North Am.*, 2015; 44: 249–264.

[36] J. Lagergren, "Influence of obesity on the risk of esophageal disorders," *Nat. Rev. Gastroenterol. Hepatol.*, 2011; 8: 340–347.

[37] A. K. Chandar, S. Devanna, C. Lu *et al.*, "Association of Serum Levels of Adipokines and Insulin With Risk of Barrett's Esophagus: A Systematic Review and Meta-Analysis," *Clin. Gastroenterol. Hepatol.*, 2015; 13: 2241-2255.

[38] Q. He, J. D. Li, W. Huang *et al.*, "Metabolic syndrome is associated with increased risk of Barrett esophagus: A meta-analysis," *Medicine*

(Baltimore), 2016; 95: e4338.

[39] K. Lagergren, F. Mattsson and J. Lagergren, "Abdominal fat and male excess of esophageal adenocarcinoma," *Epidemiology*, 2013; 24: 465–466.

[40] H. B. El-Serag, A. Hashmi, J. Garcia *et al.*, "Visceral abdominal obesity measured by CT scan is associated with an increased risk of Barrett's oesophagus: A case-control study," *Gut*, 2014; 63: 220–229.

[41] F. J. Xie, Y. P. Zhang, Q. Q. Zheng *et al.*, "Helicobacter pylori infection and esophageal cancer risk: An updated meta-analysis," *World J. Gastroenterol.*, 2013; 19: 6098–6107.

[42] S. Nie, T. Chen, X. Yang *et al.*, "Association of Helicobacter pylori infection with esophageal adenocarcinoma and squamous cell carcinoma: A meta-analysis," *Dis. Esophagus*, 2014; 27: 645–653.

[43] E. J. Snider, D. E. Freedberg and J. A. Abrams, "Potential Role of the Microbiome in Barrett's Esophagus and Esophageal Adenocarcinoma," *Dig. Dis. Sci.*, 2016; 61: 2217–2225.

[44] J. C. Atherton and M. J. Blaser, "Coadaptation of Helicobacter pylori and humans: Ancient history, modern implications," *J. Clin. Invest.*, 2009; 119: 2475–2487.

[45] A. Raghunath, A. P. S. Hungin, D. Wooff *et al.*, "Prevalence of Helicobacter pylori in patients with gastro-oesophageal reflux disease: Systematic review," *BMJ*, 2003; 326: 737.

[46] J. Lv, L. Guo, J. J. Liu *et al.*, "Alteration of the esophageal microbiota in Barrett's esophagus and esophageal adenocarcinoma," *World J. Gastroenterol.*, 2019; 25: 2149–2161.

[47] H. G. Coleman, S. H. Xie and J. Lagergren, "The Epidemiology of Esophageal Adenocarcinoma," *Gastroenterology*, 2018; 154: 390–405.

[48] M. B. Cook, F. Kamangar, D. C. Whiteman *et al.*, "Cigarette smoking and adenocarcinomas of the esophagus and esophagogastric

junction: A pooled analysis from the International BEACON Consortium," *J. Natl. Cancer Inst.*, 2010; 102: 1344–1353.

[49] D. C. Whiteman and L. F. Wilson, "The fractions of cancer attributable to modifiable factors: A global review," *Cancer Epidemiol.*, 2016; 44: 203–221.

[50] N. D. Freedman, L. J. Murray, F. Kamangar *et al.*, "Alcohol intake and risk of oesophageal adenocarcinoma: A pooled analysis from the BEACON Consortium," *Gut*, 2011; 60: 1029–1037.

[51] Z. Lou, H. Xing and D. Li, "Alcohol consumption and the neoplastic progression in Barrett's esophagus: A systematic review and meta-analysis," *PLoS One*, 2014; 9: e105612.

[52] A. Kubo, G. Block, C. P. Quesenberry *et al.*, "Effects of dietary fiber, fats, and meat intakes on the risk of barrett's esophagus," *Nutr. Cancer*, 2009; 61: 607–616.

[53] H. G. Coleman, L. J. Murray, B. Hicks *et al.*, "Dietary fiber and the risk of precancerous lesions and cancer of the esophagus: A systematic review and meta-analysis," *Nutr. Rev.*, 2013; 71: 474–482.

[54] K. Lagergren, J. Lagergren and N. Brusselaers, "Hormone replacement therapy and oral contraceptives and risk of oesophageal adenocarcinoma: A systematic review and meta-analysis," *Int. J. Cancer*, 2014; 135: 2183–2190.

[55] R. E. Verbeek, L. F. Spittuler, A. Peute *et al.*, "Familial Clustering of Barrett's Esophagus and Esophageal Adenocarcinoma in a European Cohort," *Clin. Gastroenterol. Hepatol.*, 2014; 12: 1656-1663.

[56] H. To, N. J. Clemons, C. P. Duong *et al.*, "The Genetics of Barrett's Esophagus: A Familial and Population-Based Perspective," *Dig. Dis. Sci.*, 2016; 61: 1826–1834.

[57] R. E. Fecteau, J. Kong, A. Kresak *et al.*, "Association Between Germline Mutation in VSIG10L and Familial Barrett Neoplasia," *JAMA Oncol.*, 2016; 2: 1333–1339.

[58] Z. Su, L. J. Gay, A. Strange *et al.*, "Common variants at the MHC locus and at chromosome 16q24.1 predispose to Barrett's esophagus," *Nat. Genet.*, 2012; 44: 1131–1136.

[59] D. M. Levine, W. E. Ek, R. Zhang *et al.*, "A genome-wide association study identifies new susceptibility loci for esophageal adenocarcinoma and Barrett's esophagus," *Nat. Genet.*, 2013; 45: 1487–1493.

[60] C. Palles, L. Chegwidden, X. Li *et al.*, "Polymorphisms near TBX5 and GDF7 are associated with increased risk for Barrett's esophagus," *Gastroenterology*, 2015; 148: 367–378.

[61] J. Becker, A. May, C. Gerges *et al.*, "The Barrett-associated variants at GDF7 and TBX5 also increase esophageal adenocarcinoma risk," *Cancer Med.*, 2016; 5: 888–891.

[62] A. M. J. Van Nistelrooij, H. A. van der Korput, L. Broer *et al.*, "Single nucleotide polymorphisms in CRTC1 and BARX1 are associated with esophageal adenocarcinoma," *J. Carcinog.*, 2015; 14: 5.

[63] P. Gharahkhani, R. C. Fitzgerald, T. L. Vaughan *et al.*, "Genome-wide association studies in oesophageal adenocarcinoma and Barrett's oesophagus: a large-scale meta-analysis," *Lancet Oncol.*, 2016; 17: 1363–1373.

[64] J. Becker, A. May, C. Gerges *et al.*, "Supportive evidence for FOXP1, BARX1, and FOXF1 as genetic risk loci for the development of esophageal adenocarcinoma," *Cancer Med.*, 2015; 4: 1700–1704.

[65] M. F. Buas, Q. He, L. G. Johnson *et al.*, "Germline variation in inflammation-related pathways and risk of Barrett's oesophagus and oesophageal adenocarcinoma," *Gut*, 2017; 66: 1739–1747.

[66] W. E. Ek, K. Lagergren, M. Cook *et al.*, "Polymorphisms in genes in the androgen pathway and risk of Barrett's esophagus and esophageal adenocarcinoma," *Int. J. Cancer*, 2016; 138: 1146–1152.

[67] M. F. Buas, D. M. Levine, K. W. Makar *et al.*, "Integrative post-genome-wide association analysis of CDKN2A and TP53 SNPs and

risk of esophageal adenocarcinoma," *Carcinogenesis*, 2014; 35: 2740–2747.

[68] W. M. Westra, A. M. Rygiel, N. Mostafavi *et al.*, "The Y-chromosome F haplogroup contributes to the development of Barrett s esophagus-Associated esophageal adenocarcinoma in a white male population," *Dis. Esophagus*, 2020; 33: doaa011.

[69] W. E. Ek, D. M. Levine, M. D'Amato *et al.*, "Germline genetic contributions to risk for esophageal adenocarcinoma, barrett's esophagus, and gastroesophageal reflux," *J. Natl. Cancer Inst.*, 2013; 105: 1711–1718.

[70] J. R. Siewert and H. J. Stein, "Carcinoma of the cardia: Carcinoma of the gastroesophageal junction - Classification, pathology and extent of resection," *Dis. Esophagus*, 1996; 9: 173–182.

[71] J. R. Siewert, M. Feith, M. Werner *et al.*, "Adenocarcinoma of the esophagogastric junction: Results of surgical therapy based on anatomical/topographic classification in 1,002 consecutive patients," *Ann. Surg.*, 2000; 232: 353–361.

[72] J. R. Siewert and H. J. Stein, "Classification of adenocarcinoma of the oesophagogastric junction," *Br. J. Surg.*, 1998; 85: 1457–1459.

[73] M. Chevallay, E. Bollschweiler, S. M. Chandramohan *et al.*, "Cancer of the gastroesophageal junction: a diagnosis, classification, and management review," *Ann. N. Y. Acad. Sci.*, 2018; 1434: 132-138.

[74] M. Feith, H. J. Stein and J. R. Siewert, "Adenocarcinoma of the Esophagogastric Junction: Surgical Therapy Based on 1602 Consecutive Resected Patients," *Surg. Oncol. Clin. North Am.*, 2006; 15: 751–764.

[75] S. Mattioli, A. Ruffato, M. P. Di Simone *et al.*, "Immunopathological Patterns of the Stomach in Adenocarcinoma of the Esophagus, Cardia, and Gastric Antrum: Gastric Profiles in Siewert Type I and II Tumors," *Ann. Thorac. Surg.*, 2007; 83: 1814–1819.

[76] T. W. Rice, D. T. Patil and E. H. Blackstone, "8th edition AJCC/UICC

staging of cancers of the esophagus and esophagogastric junction: Application to clinical practice," *Ann. Cardiothorac. Surg.*, 2017; 6: 119–130.

[77] T. W. Rice, H. Ishwaran, M. K. Ferguson *et al.*, "Cancer of the Esophagus and Esophagogastric Junction: An Eighth Edition Staging Primer," *J. Thorac. Oncol.*, 2017; 12: 36–42.

[78] IARC, *WHO classification of tumors 5th ed.*, 5th ed. Lyon, 2019.

[79] A. K. Lam, "Updates on World Health Organization Classification and Staging of oesophageal tumours: Implications for future clinical practice," *Hum. Pathol.*, 2020; S0046-8177(20)30221-5.

[80] Y. S. Suh, D. S. Han, S. H. Kong *et al.*, "Should adenocarcinoma of the esophagogastric junction be classified as esophageal cancer? A comparative analysis according to the seventh AJCC TNM classification," *Ann. Surg.*, 2012; 255: 908–915.

[81] J. M. Leers, S. R. DeMeester, N. Chan *et al.*, "Clinical characteristics, biologic behavior, and survival after esophagectomy are similar for adenocarcinoma of the gastroesophageal junction and the distal esophagus," *J. Thorac. Cardiovasc. Surg.*, 2009; 138: 594–602.

[82] A. Ruffato, S. Mattioli, O. Perrone *et al.*, "Esophagogastric metaplasia relates to nodal metastases in adenocarcinoma of esophagus and cardia," *Ann. Thorac. Surg.*, 2013; 95: 1147–1153.

[83] P. Lauren, "The two histological main types of gastric carcinoma: diffuse and so-called intestinal type carcinoma. An attempt at a histo-clinical classification," *Acta Pathol. Microbiol. Scand.*, 1965; 64: 31–49.

[84] F. Berlth, E. Bollschweiler, U. Drebber *et al.*, "Pathohistological classification systems in gastric cancer: Diagnostic relevance and prognostic value," *World J. Gastroenterol.*, 2014; 20: 5679–5684.

[85] R. T. van der Kaaij, P. Snaebjornsson, F. E. Voncken *et al.*, "The prognostic and potentially predictive value of the Laurén classification in oesophageal adenocarcinoma," *Eur. J. Cancer*, 2017;

76: 27–35.

[86] W. Polkowski, J. W. van Sandick, G. J. Offerhaus *et al.*, "Prognostic value of Lauren classification and c-erbB-2 oncogene overexpression in adenocarcinoma of the esophagus and gastroesophageal junction," *Ann. Surg. Oncol.*, 1999; 6: 290–297.

[87] S. E. Al-Batran, R. D. Hofheinz, C. Pauligk *et al.*, "Histopathological regression after neoadjuvant docetaxel, oxaliplatin, fluorouracil, and leucovorin versus epirubicin, cisplatin, and fluorouracil or capecitabine in patients with resectable gastric or gastro-oesophageal junction adenocarcinoma (FLOT4-AIO): results from the phase 2 part of a multicentre, open-label, randomised phase 2/3 trial," *Lancet Oncol.*, 2016; 17: 1697–1708.

[88] A. M. Frankell, S. Jammula, X. Li *et al.*, "The landscape of selection in 551 esophageal adenocarcinomas defines genomic biomarkers for the clinic," *Nat. Genet.*, 2019; 51: 506–516.

[89] C. Lengauer, K. W. Kinzler and B. Vogelstein, "Genetic instabilities in human cancers," *Nature*, 1998; 396: 643–649.

[90] M. S. Lawrence, P. Stojanov, P. Polak *et al.*, "Mutational heterogeneity in cancer and the search for new cancer-associated genes," *Nature*, 2013; 499: 214–218.

[91] R. Beroukhim, C. H. Mermel, D. Porter *et al.*, "The landscape of somatic copy-number alteration across human cancers," *Nature*, 2010; 463: 899–905.

[92] A. M. Dulak, P. Stojanov, S. Peng *et al.*, "Exome and whole-genome sequencing of esophageal adenocarcinoma identifies recurrent driver events and mutational complexity," *Nat. Genet.*, 2013; 45: 478–486.

[93] K. Nones, N. Waddell, N. Wayte *et al.*, "Genomic catastrophes frequently arise in esophageal adenocarcinoma and drive tumorigenesis," *Nat. Commun.*, 2014; 5: 5224.

[94] M. Secrier, X. Li, N. de Silva *et al.*, "Mutational signatures in

esophageal adenocarcinoma define etiologically distinct subgroups with therapeutic relevance," *Nat. Genet.*, 2016; 48: 1131–1141.

[95] M. Malumbres and A. Carnero, "Cell cycle deregulation: a common motif in cancer.," *Prog.cell cycle res.*, 2003; 5: 5–18.

[96] C. S. Ross-Innes, J. Becq, A. Warren *et al.*, "Whole-genome sequencing provides new insights into the clonal architecture of Barrett's esophagus and esophageal adenocarcinoma," *Nat. Genet.*, 2015; 47: 1038–1046.

[97] A. Weiss and L. Attisano, "The TGFbeta superfamily signaling pathway," *Wiley Interdiscip. Rev. Dev. Biol.*, 2013; 2: 47–63.

[98] H. L. Moses and R. Serra, "Regulation of differentiation by TGF-β," *Curr. Opin. Genet. Dev.*, 1996; 6: 581–586.

[99] J. R. E. Rees, B. A. Onwuegbusi, V. E. Save *et al.*, "In vivo and in vitro evidence for transforming growth factor-β1- mediated epithelial to mesenchymal transition in esophageal adenocarcinoma," *Cancer Res.*, 2006; 66: 9583–9590.

[100] H. Davis, E. Raja, K. Miyazono *et al.*, "Mechanisms of action of bone morphogenetic proteins in cancer," *Cytokine Growth Factor Rev.*, 2016; 27: 81–92.

[101] B. Bragdon, O. Moseychuk, S. Saldanha *et al.*, "Bone Morphogenetic Proteins: A critical review," *Cell. Signal.*, 2011; 23: 609–620.

[102] J. Que, M. Choi, J. W. Ziel *et al.*, "Morphogenesis of the trachea and esophagus: Current players and new roles for noggin and Bmps," *Differentiation*, 2006; 4: 422–437.

[103] J. W. Van Baal, F. Milano, A. M. Rygiel *et al.*, "A comparative analysis by SAGE of gene expression profiles of Barrett's esophagus, normal squamous esophagus, and gastric cardia," *Gastroenterology*, 2005; 129: 1274–1281.

[104] F. Milano, J. W. van Baal, N. S. Buttar *et al.*, "Bone Morphogenetic Protein 4 Expressed in Esophagitis Induces a Columnar Phenotype in Esophageal Squamous Cells," *Gastroenterology*, 2007; 132:

2412–2421.

[105] L. Mari, F. Milano, K. Parikh *et al.*, "A pSMAD/CDX2 complex is essential for the intestinalization of epithelial metaplasia," *Cell Rep.*, 2014; 7: 1197–1210.

[106] R. J. Badreddine and K. K. Wang, "Barrett esophagus: An update," *Nat. Rev. Gastroenterol. Hepatol.*, 2010; 7: 369–378.

[107] D. W. Perng, K. T. Chang, K. C. Su *et al.*, "Exposure of airway epithelium to bile acids associated with gastroesophageal reflux symptoms: A relation to transforming growth factor-β1 production and fibroblast proliferation," *Chest*, 2007; 132: 1548–1556.

[108] B. H. A. Von Rahden, H. J. Stein, M. Feith *et al.*, "Overexpression of TGF-β1 in esophageal (Barrett's) adenocarcinoma is associated with advanced stage of disease and poor prognosis," *Mol. Carcinog.*, 2006; 45: 786–794.

[109] F. Liu, C. Pouponnot and J. Massagué, "Dual role of the Smad4/DPC4 tumor suppressor in TGFβ-inducible transcriptional complexes," *Genes Dev.*, 1997; 11: 3157–3167.

[110] A. D. Singhi, T. J. Foxwell, K. Nason *et al.*, "Smad4 loss in esophageal adenocarcinoma is associated with an increased propensity for disease recurrence and poor survival," *Am. J. Surg. Pathol.*, 2015; 39: 487–495.

[111] B. A. Onwuegbusi, A. Aitchison, S. F. Chin *et al.*, "Impaired transforming growth factor β signalling in Barrett's carcinogenesis due to frequent SMAD4 inactivation," *Gut*, 2006; 55: 764–774.

[112] M. D. Stachler, A. Taylor-Weiner, S. Peng *et al.*, "Paired exome analysis of Barrett's esophagus and adenocarcinoma," *Nat. Genet.*, 2015; 47: 1047–1055.

[113] N. Agrawal, Y. Jiao, C. Bettegowda *et al.*, "Comparative genomic analysis of esophageal adenocarcinoma and squamous cell carcinoma," *Cancer Discov.*, 2012; 2: 899–905.

[114] G. Contino, T. L. Vaughan, D. Whiteman *et al.*, "The Evolving

Genomic Landscape of Barrett's Esophagus and Esophageal Adenocarcinoma," *Gastroenterology*, 2017; 153: 657-673.

[115] H. Alvarez, J. Opalinska, L. Zhou *et al.*, "Correction: Widespread Hypomethylation Occurs Early and Synergizes with Gene Amplification during Esophageal Carcinogenesis," *PLoS Genet.*, 2011; 7: e1001356.

[116] E. Xu, J. Gu, E. T. Hawk *et al.*, "Genome-wide methylation analysis shows similar patterns in Barrett's esophagus and esophageal adenocarcinoma," *Carcinogenesis*, 2013; 34: 2750–2756.

[117] M. Di Trapani, N. Manaresi and G. Medoro, "DEPArray™ system: An automatic image-based sorter for isolation of pure circulating tumor cells," *Cytometry Part A*, 2018; 93: 1260–1266.

[118] F. Isidori, D. Malvi, S. Fittipaldi *et al.*, "Genomic profiles of primary and metastatic esophageal adenocarcinoma identified via digital sorting of pure cell populations: Results from a case report," *BMC Cancer*, 2018; 18: 889.

[119] D. P. Bartel, "MicroRNAs: Genomics, Biogenesis, Mechanism, and Function," *Cell*, 2004; 116: 281–297.

[120] E. Huntzinger and E. Izaurralde, "Gene silencing by microRNAs: Contributions of translational repression and mRNA decay," *Nat. Rev. Genet.*, 2011; 12: 99–110.

[121] R. C. Friedman, K. K. H. Farh, C. B. Burge *et al.*, "Most mammalian mRNAs are conserved targets of microRNAs," *Genome Res.*, 2009; 19: 92–105.

[122] S. K. Singh, M. Pal Bhadra, H. J. Girschick *et al.*, "MicroRNAs - Micro in size but macro in function," *FEBS Journal*, 2008; 275: 4929–4944.

[123] N. Ludwig, P. Leidinger, K. Becker *et al.*, "Distribution of miRNA expression across human tissues," *Nucleic Acids Res.*, 2016; 44: 3865–3877.

[124] D. De Rie, I. Abugessaisa, T. Alam *et al.*, "An integrated expression

atlas of miRNAs and their promoters in human and mouse," *Nat. Biotechnol.*, 2017; 35: 872–878.

[125] A. Rodriguez, S. Griffiths-Jones, J. L. Ashurst *et al.*, "Identification of mammalian microRNA host genes and transcription units," *Genome Res.*, 2004; 14: 1902–1910.

[126] V. N. Kim and J. W. Nam, "Genomics of microRNA," *Trends Genet.*, 2006; 22: 165–173.

[127] Y. Lee, M. Kim, J. Han *et al.*, "MicroRNA genes are transcribed by RNA polymerase II," *EMBO J.*, 2004; 23: 4051–4060.

[128] J. Han, Y. Lee, K. H. Yeom *et al.*, "The Drosha-DGCR8 complex in primary microRNA processing," *Genes Dev.*, 2004; 18: 3016–3027.

[129] G. Michlewski, S. Guil, C. A. Semple, *et al.*, "Posttranscriptional Regulation of miRNAs Harboring Conserved Terminal Loops," *Mol. Cell*, 2008; 32: 383–393.

[130] V. N. Kim, "MicroRNA precursors in motion: Exportin-5 mediates their nuclear export," *Trends Cell Biol.*, 2004; 14: 156–159.

[131] E. Bernstein, A. A. Caudy, S. M. Hammond *et al.*, "Role for a bidentate ribonuclease in the initiation step of RNA interference," *Nature*, 2001; 409: 363–366.

[132] T. P. Chendrimada, R. I. Gregory, E. Kumaraswamy *et al.*, "TRBP recruits the Dicer complex to Ago2 for microRNA processing and gene silencing," *Nature*, 2005; 436: 740–744.

[133] S. M. Hammond, E. Bernstein, D. Beach *et al.*, "An RNA-directed nuclease mediates post-transcriptional gene silencing in Drosophila cells," *Nature*, 2000; 404: 293–296.

[134] S. Djuranovic, A. Nahvi and R. Green, "A parsimonious model for gene regulation by miRNAs," *Science*, 2011; 331: 550–553.

[135] M. Acunzo, G. Romano, D. Wernicke *et al.*, "MicroRNA and cancer - A brief overview," *Adv. Biol. Regul.*, 2015; 57: 1–9.

[136] G. A. Calin, C. D. Dumitru, M. Shimizu *et al.*, "Frequent deletions and down-regulation of micro-RNA genes miR15 and miR16 at

13q14 in chronic lymphocytic leukemia," *Proc. Natl. Acad. Sci. U. S. A.*, 2002; 99: 15524–15529.

[137] L. A. MacFarlane and P. R. Murphy, "MicroRNA: Biogenesis, Function and Role in Cancer," *Curr. Genomics*, 2010; 11: 537–561.

[138] G. Di Leva and C. M. Croce, "Roles of small RNAs in tumor formation," *Trends Mol. Med.*, 2010; 16: 257–267.

[139] A. Feber, L. Xi, J. D. Luketich *et al.*, "MicroRNA expression profiles of esophageal cancer," *J. Thorac. Cardiovasc. Surg.*, 2008; 135: 255–260.

[140] C. M. Smith, D. I. Watson, M. Z. Michael *et al.*, "MicroRNAs, development of Barrett's esophagus, and progression to esophageal adenocarcinoma," *World J. Gastroenterol.*, 2010; 16: 531–537.

[141] K. S. Garman, K. Owzar, E. R. Hauser *et al.*, "MicroRNA expression differentiates squamous epithelium from barrett's esophagus and esophageal cancer," *Dig. Dis. Sci.*, 2013; 58: 3178–3188.

[142] B. Revilla-Nuin, P. Parrilla, J. J. Lozano *et al.*, "Predictive value of microRNAs in the progression of Barrett esophagus to adenocarcinoma in a long-term follow-up study," *Ann. Surg.*, 2013; 257: 886–893.

[143] J. Gu, Y. Wang and X. Wu, "MicroRNA in the Pathogenesis and Prognosis of Esophageal Cancer," *Curr. Pharm. Des.*, vol. 19, no. 7, pp. 1292–1300, Jan. 2013.

[144] J. Lv, H. P. Zhao, K. Dai *et al.*, "Circulating exosomal miRNAs as potential biomarkers for Barrett's esophagus and esophageal adenocarcinoma," *World J. Gastroenterol.*, 2020; 26: 2889–2901.

[145] A. Bansal, X. Hong, I. H. Lee *et al.*, "MicroRNA expression can be a promising strategy for the detection of barrett's esophagus: A pilot study," *Clin. Transl. Gastroenterol.*, 2014; 5: e65.

[146] S. Gao, Z. Y. Zhao, Z. Y. Zhang *et al.*, "Prognostic Value of MicroRNAs in Esophageal Carcinoma: A Meta-Analysis," *Clin. Transl. Gastroenterol.*, 2018; 9: 203.

[147] R. J. Clark, M. P. Craig, S. Agrawal *et al.*, "microRNA involvement in the onset and progression of Barrett's esophagus: A systematic review," *Oncotarget*, 2018; 9: 8179–8196.

[148] A. A. Svoronos, D. M. Engelman and F. J. Slack, "OncomiR or tumor suppressor? The duplicity of MicroRNAs in cancer," *Cancer Res.*, 2016; 76: 3666–3670.

[149] S. Wang, N. Liu, Q. Tang *et al.*, "MicroRNA-24 in Cancer: A Double Side Medal With Opposite Properties," *Front. Oncol.*, 2020; 10:553714.

[150] B. Njei, T. R. Mccarty and J. W. Birk, "Trends in esophageal cancer survival in United States adults from 1973 to 2009: A SEER database analysis," *J. Gastroenterol. Hepatol.*, 2016; 31: 1141–1146.

[151] M. Rutegård, K. Charonis, Y. Lu *et al.*, "Population-based esophageal cancer survival after resection without neoadjuvant therapy: An update," *Surgery*, 2012; 152: 903–910.

[152] K. S. Grant, S. R. DeMeester, V. Kreger *et al.*, "Effect of Barrett's esophagus surveillance on esophageal preservation, tumor stage, and survival with esophageal adenocarcinoma," *J. Thorac. Cardiovasc. Surg.*, 2013; 146: 31–37.

[153] A. Dubecz, I. Gall, N. Solymosi *et al.*, "Temporal trends in long-term survival and cure rates in esophageal cancer: A SEER database analysis," *J. Thorac. Oncol.*, 2012; 7: 443–447.

[154] J. Lagergren, E. Smyth, D. Cunningham *et al.*, "Oesophageal cancer," *Lancet*, 2017; 390: 2383–2396.

[155] A. K. Rustgi and H. B. El-Serag, "Esophageal Carcinoma," *N. Engl. J. Med.*, 2014; 371: 2499–2509.

[156] R. C. Fitzgerald, M. di Pietro, K. Ragunath *et al.*, "British Society of Gastroenterology guidelines on the diagnosis and management of Barrett's oesophagus," *Gut*, 2014; 63: 7–42.

[157] J. A. Ajani, T. A. D'Amico, D. J. Bentrem *et al.*, "Esophageal and esophagogastric junction cancers, Version 2.2019," *J. Natl. Compr.*

Cancer Netw., 2019; 17: 855–883.

[158] O. Pech, A. Behrens, A. May *et al.*, "Long-term results and risk factor analysis for recurrence after curative endoscopic therapy in 349 patients with high-grade intraepithelial neoplasia and mucosal adenocarcinoma in Barrett's oesophagus," *Gut*, 2008; 57: 1200–1206.

[159] M. A. Morgan, W. G. Lewis, A. Casbard *et al.*, "Stage-for-stage comparison of definitive chemoradiotherapy, surgery alone and neoadjuvant chemotherapy for oesophageal carcinoma," *Br. J. Surg.*, 2009; 96: 1300–1307.

[160] P. van Hagen, M. C. Hulshof, J. J. van Lanschot *et al.*, "Preoperative Chemoradiotherapy for Esophageal or Junctional Cancer," *N. Engl. J. Med.*, 2012; 366: 2074–2084.

[161] S. E. Al-Batran, N. Homann, C. Pauligk *et al.*, "Effect of neoadjuvant chemotherapy followed by surgical resection on survival in patients with limited metastatic gastric or gastroesophageal junction cancer: The AIO-FLOT3 trial," *JAMA Oncol.*, 2017; 3: 1237–1244.

[162] D. Cunningham, W. H. Allum, S. P. Stenning *et al.*, "Perioperative Chemotherapy versus Surgery Alone for Resectable Gastroesophageal Cancer," *N. Engl. J. Med.*, 2006; 355: 11–20.

[163] M. Ychou, V. Boige, J. P. Pignon *et al.*, "Perioperative chemotherapy compared with surgery alone for resectable gastroesophageal adenocarcinoma: An FNCLCC and FFCD multicenter phase III trial," *J. Clin. Oncol.*, 2011; 29: 1715–1721.

[164] Medical Research Council Oesophageal Cancer Working Group, "Surgical resection with or without preoperative chemotherapy in oesophageal cancer: A randomised controlled trial," *Lancet*, 2002; 359: 1727–1733.

[165] S. E. Al-Batran, N. Homann, C. Pauligk *et al.*, "Perioperative chemotherapy with fluorouracil plus leucovorin, oxaliplatin, and docetaxel versus fluorouracil or capecitabine plus cisplatin and

epirubicin for locally advanced, resectable gastric or gastro-oesophageal junction adenocarcinoma (FLOT4): a randomised, phase 2/3 trial," *Lancet*, 2019; 393: 1948–1957.

[166] J. Shapiro, J. J. B. van Lanschot, M. C. C. M. Hulshof *et al.*, "Neoadjuvant chemoradiotherapy plus surgery versus surgery alone for oesophageal or junctional cancer (CROSS): Long-term results of a randomised controlled trial," *Lancet Oncol.*, 2015; 16: 1090–1098.

[167] V. E. Wang, J. R. Grandis and A. H. Ko, "New strategies in esophageal carcinoma: Translational insights from signaling pathways and immune checkpoints," *Clin. Cancer Res.*, 2016; 22: 4283–4290.

[168] A. C. Pinto, F. Ades, E. de Azambuja *et al.*, "Trastuzumab for patients with HER2 positive breast cancer: Delivery, duration and combination therapies," *Breast*, 2013; 22: S152-155.

[169] T. Akiyama, C. Sudo, H. Ogawara *et al.*, "The product of the human c-erbB-2 gene: A 185-kilodalton glycoprotein with tyrosine kinase activity," *Science*, 1986; 232: 1644–1646.

[170] C. Gravalos and A. Jimeno, "HER2 in gastric cancer: A new prognostic factor and a novel therapeutic target," *Ann. Oncol.*, 2008; 19: 1523–1529.

[171] Y. Y. Janjigian, D. Werner, C. Pauligk *et al.*, "Prognosis of metastatic gastric and gastroesophageal junction cancer by HER2 status: A European and USA International collaborative analysis," *Ann. Oncol.*, 2012; 23: 2656–2662.

[172] Y. J. Bang, E. Van Cutsem, A. Feyereislova *et al.*, "Trastuzumab in combination with chemotherapy versus chemotherapy alone for treatment of HER2-positive advanced gastric or gastro-oesophageal junction cancer (ToGA): A phase 3, open-label, randomised controlled trial," *Lancet*, 2010; 376: 687–697.

[173] E. Van Cutsem, Y. J. Bang, F. Feng-Yi *et al.*, "HER2 screening data from ToGA: targeting HER2 in gastric and gastroesophageal

junction cancer," *Gastric Cancer*, 2015; 18: 476–484.

[174] F. Sanchez-Vega, J. F. Hechtman, P. Castel *et al.*, "EGFR and MET amplifications determine response to HER2 inhibition in ERBB2-amplified esophagogastric cancer," *Cancer Discov.*, 2019; 9: 199–209.

[175] B. Mawalla, X. Yuan, X. Luo *et al.*, "Treatment outcome of anti-angiogenesis through VEGF-pathway in the management of gastric cancer: A systematic review of phase II and III clinical trials," *BMC Res. Notes*, 2018; 11: 21.

[176] J. K. Lennerz, E. L. Kwak, A. Ackerman *et al.*, "MET amplification identifies a small and aggressive subgroup of esophagogastric adenocarcinoma with evidence of responsiveness to crizotinib," *J. Clin. Oncol.*, 2011; 29: 4803–4810.

[177] E. Van Cutsem, B. Karaszewska, Y. K. Kang *et al.*, "A multicenter phase II study of AMG 337 in patients with MET-amplified gastric/gastroesophageal junction/esophageal adenocarcinoma and other MET-amplified solid tumors," *Clin. Cancer Res.*, 2019; 25: 2414–2423.

[178] E. L. Kwak , P. LoRusso, O. Hamid *et al.*, "Clinical activity of AMG 337, an oral MET kinase inhibitor, in adult patients (pts) with MET-amplified gastroesophageal junction (GEJ), gastric (G), or esophageal (E) cancer," *J. Clin. Oncol.*, 2015; 33:1.

[179] A. Parrales and T. Iwakuma, "Targeting oncogenic mutant p53 for cancer therapy," *Front. Oncol.*, 2015; 5: 288.

[180] V. J. N. Bykov, N. Issaeva, A. Shilov *et al.*, "Restoration of the tumor suppressor function to mutant p53 by a low-molecular-weight compound," *Nat. Med.*, 2002; 8: 282–288.

[181] J. M. R. Lambert, A. Moshfegh, P. Hainaut *et al.*, "Mutant p53 reactivation by PRIMA-1 MET induces multiple signaling pathways converging on apoptosis," *Oncogene*, 2010; 29: 1329–1338.

[182] D. S. Liu, M. Read, C. Cullinane *et al.*, "APR-246 potently inhibits

tumour growth and overcomes chemoresistance in preclinical models of oesophageal adenocarcinoma," *Gut*, 2015; 64: 1506–1516.

[183] D. S. Liu, C. P. Duong, S. Haupt *et al.*, "Inhibiting the system xC-/glutathione axis selectively targets cancers with mutant-p53 accumulation," *Nat. Commun.*, 2017; 8: 14844.

[184] V. J. N. Bykov and K. G. Wiman, "Mutant p53 reactivation by small molecules makes its way to the clinic," *FEBS Letters*, 2014; 588: 2622–2627.

[185] R. Caspa Gokulan, M. T. Garcia-Buitrago and A. I. Zaika, "From genetics to signaling pathways: molecular pathogenesis of esophageal adenocarcinoma," *Biochim. Biophys. Acta Rev. Cancer*, 2019; 1872: 37–48.

[186] J. D. Wolchok and T. A. Chan, "Cancer: Antitumour immunity gets a boost," *Nature*, 2015; 515: 496–498.

[187] D. T. Le, J. N. Durham, K. N. Smith *et al.*, "Mismatch repair deficiency predicts response of solid tumors to PD-1 blockade," *Science*, 2017; 357: 409–413.

[188] T. Doi, S. A. Piha-Paul, S. I. Jalal *et al.*, "Updated results for the advanced esophageal carcinoma cohort of the phase 1b KEYNOTE-028 study of pembrolizumab," *J. Clin. Oncol.*, 2016; 34:4046.

[189] N. Murugaesu, G. A. Wilson, N. J. Birkbak *et al.*, "Tracking the genomic evolution of esophageal adenocarcinoma through neoadjuvant chemotherapy," *Cancer Discov.*, 2015; 5: 821–832.

[190] C. Graziano, A. Wischmeijer, T. Pippucci *et al.*, "Syndromic intellectual disability: A new phenotype caused by an aromatic amino acid decarboxylase gene (DDC) variant," *Gene*, 2015; 559: 144–148.

[191] J. T. Robinson *et al.*, "Integrative genomics viewer," *Nat. Biotechnol.*, 2011; 29: 24–26.

[192] J. C. Rockett, K. Larkin, S. J. Darnton *et al.*, "Five newly established oesophageal carcinoma cell lines: Phenotypic and immunological

characterization," *Br. J. Cancer*, 1997; 75: 258–263.

[193] J. J. Boonstra, R. van Marion, D. G. Beer *et al.*, "Verification and unmasking of widely used human esophageal adenocarcinoma cell lines," *J. Natl. Cancer Inst.*, 2010; 102: 271–274.

[194] S. J. Hughes, Y. Nambu, O. S. Soldes *et al.*, "Fas/APO-1 (CD95) Is Not Translocated to the Cell Membrane in Esophageal Adenocarcinoma," *Cancer Res.*, 1997; 57: 5571-5578.

[195] C. Bolognesi, C. Forcato, G. Buson *et al.*, "Digital Sorting of Pure Cell Populations Enables Unambiguous Genetic Analysis of Heterogeneous Formalin-Fixed Paraffin-Embedded Tumors by Next Generation Sequencing," *Sci. Rep.*, 2016; 6: 20944.

[196] Z. Luo, Y. Li, H. Wang *et al.*, "Hepatocyte Nuclear Factor 1A (HNF1A) as a possible tumor suppressor in pancreatic cancer," *PLoS One*, 2015; 10: e0121082.

[197] J. Hao, S. Zhang, Y. Zhou *et al.*, "MicroRNA 483-3p suppresses the expression of DPC4/Smad4 in pancreatic cancer," *FEBS Lett.*, 2011; 585: 207–213.

[198] F. T. Bosman, P. Yan, S. Tejpar *et al.*, "Tissue biomarker development in a multicentre trial context: A feasibility study on the PETACC3 stage II and III colon cancer adjuvant treatment trial," *Clin. Cancer Res.*, 2009; 15: 5528–5533.

[199] P. Yan, D. Klingbiel, Z. Saridaki *et al.*, "Reduced expression of SMAD4 is associated with poor survival in colon cancer," *Clin. Cancer Res.*, 2016; 22: 3037–3047.

[200] T. S. Gerashchenko, E. V. Denisov, N. V. Litviakov *et al.*, "Intratumor heterogeneity: Nature and biological significance," *Biochemistry (Mosc)*, 2013; 78: 1201–1215.

[201] N. Navin, A. Krasnitz, L. Rodgers *et al.*, "Inferring tumor progression from genomic heterogeneity," *Genome Res.*, 2010; 20: 68–80.

[202] J. E. Visvader, "Cells of origin in cancer," *Nature*, 2011; 469: 314–

322.

[203] R. Fisher, L. Pusztai and C. Swanton, “Cancer heterogeneity: Implications for targeted therapeutics,” *Br. J.Cancer*, 2013; 108: 479–485.

[204] O. W. McBride, D. Merry and D. Givol, “The gene for human p53 cellular tumor antigen is located on chromosome 17 short arm (17p13),” *Proc. Natl. Acad. Sci. U. S. A.*, 1986; 83: 130–134.

[205] D. P. Lane, “p53, guardian of the genome,” *Nature*, 1992; 358: 15–16.

[206] V. A. Belyi, P. Ak, E. Markert *et al.*, “The origins and evolution of the p53 family of genes,” *Cold Spring Harb. perspect. biol.*, 2010; 2: a001198.

[207] M. H. G. Kubbutat, S. N. Jones and K. H. Vousden, “Regulation of p53 stability by Mdm2,” *Nature*, 1997; 387: 299–303.

[208] K. H. Vousden and D. P. Lane, “p53 in health and disease,” *Nat. Rev. Mol. Cell Biol.*, 2007; 8: 275–283.

[209] Y. Aylon and M. Oren, “New plays in the p53 theater,” *Curr. Opin. Genet. Dev.*, 2011; 21: 86–92.

[210] A. I. Robles and C. C. Harris, “Clinical outcomes and correlates of TP53 mutations and cancer,” *Cold Spring Harb. perspect. biol.*, 2010; 2: a001016.

[211] Y. Cho, S. Gorina, P. D. Jeffrey *et al.*, “Crystal structure of a p53 tumor suppressor-DNA complex: Understanding tumorigenic mutations,” *Science*, 1994; 265: 346–355.

[212] M. Fischer, “Census and evaluation of p53 target genes,” *Oncogene*, 2017; 36: 3943–3956.

[213] A. Sigal and V. Rotter, “Oncogenic mutations of the p53 tumor suppressor: The demons of the guardian of the genome,” *Cancer Res.*, 2000; 60: 6788–6793.

[214] J. Milner, E. A. Medcalf and A. C. Cook, “Tumor suppressor p53: analysis of wild-type and mutant p53 complexes,” *Mol. Cell. Biol.*,

1991; 11: 12–19.

[215] M. Oren and V. Rotter, “Mutant p53 gain-of-function in cancer,” *Cold Spring Harb. perspect. biol.*, 2010; 2: a001107.

[216] W. Eicheler, D. Zips, A. Dörfler *et al.*, “Splicing mutations in TP53 in human squamous cell carcinoma lines influence immunohistochemical detection,” *J. Histochem. Cytochem.*, 2002; 50: 197–204.

[217] D. M. Tolbert, A. E. Noffsinger, M. A. Miller *et al.*, “p53 immunoreactivity and single-strand conformational polymorphism analysis often fail to predict p53 mutational status,” *Mod Pathol.*, 1999; 12: 54–60.

[218] L. T. Vassilev, B. T. Vu, B. Graves *et al.*, “In Vivo Activation of the p53 Pathway by Small-Molecule Antagonists of MDM2,” *Science*, 2004; 303: 844–848.

[219] J. Huang, “Current developments of targeting the p53 signaling pathway for cancer treatment,” *Pharmacol. Ther.* 2020; 107720.

[220] S. Trino, I. Iacobucci, D. Erriquez *et al.*, “Targeting the p53-MDM2 interaction by the small-molecule MDM2 antagonist Nutlin-3a: A new challenged target therapy in adult Philadelphia positive acute lymphoblastic leukemia patients,” *Oncotarget*, 2016; 7: 12951–12961.

[221] L. Bjørkhaug, A. Bratland, P. R. Njølstad *et al.*, “Functional dissection of the HNF-1alpha transcription factor: A study on nuclear localization and transcriptional activation,” *DNA Cell Biol.*, 2005; 24: 661–669.

[222] D. T. Odom, N. Zizlsperger, D. B. Gordon *et al.*, “Control of Pancreas and Liver Gene Expression by HNF Transcription Factors,” *Science*, 2004; 303: 1378–1381.

[223] F. Tronche and M. Yaniv, “HNF1, a homeoprotein member of the hepatic transcription regulatory network,” *BioEssays*, 1992; 14: 579–587.

[224] M. Pontoglio, J. Barra, M. Hadchouel *et al.*, "Hepatocyte nuclear factor 1 inactivation results in hepatic dysfunction, phenylketonuria, and renal Fanconi syndrome," *Cell*, 1996; 84: 575–585.

[225] C. Bellanné-Chantelot, C. Carette, J. P. Riveline *et al.*, "The type and the position of HNF1A mutation modulate age at diagnosis of diabetes in patients with maturity-onset diabetes of the young (MODY)-3," *Diabetes*, 2008; 57: 503–508.

[226] E. Jeannot, L. Mellottee, P. Bioulac-Sage *et al.*, "Spectrum of HNF1A somatic mutations in hepatocellular adenoma differs from that in patients with MODY3 and suggests genotoxic damage," *Diabetes*, 2010; 59: 1836–1844.

[227] O. Bluteau, E. Jeannot, P. Bioulac-Sage *et al.*, "Bi-allelic inactivation of TCF1 in hepatic adenomas," *Nat. Genet.*, 2002; 32: 312–315.

[228] I. Lemm, A. Lingott, E. Pogge v Strandmann *et al.*, "Loss of HNF1alpha function in human renal cell carcinoma: frequent mutations in the VHL gene but not the HNF1alpha gene," *Mol Carcinog.*, 1999; 24: 305–314.

[229] S. Rebouissou, C. Rosty, F. Lecuru *et al.*, "Mutation of TCF1 encoding hepatocyte nuclear factor 1α in gynecological cancer," *Oncogene*, 2004; 23: 7588–7592.

[230] Y. Lu, D. Xu, J. Peng *et al.*, "HNF1A inhibition induces the resistance of pancreatic cancer cells to gemcitabine by targeting ABCB1," *EBioMedicine*, 2019; 44: 403–418.

[231] M. A. Edelbrock, S. Kaliyaperumal and K. J. Williams, "Structural, molecular and cellular functions of MSH2 and MSH6 during DNA mismatch repair, damage signaling and other noncanonical activities," *Mutat. Res.*, 2013; 743: 53–66.

[232] R. H. Sijmons and R. M. W. Hofstra, "Review: Clinical aspects of hereditary DNA Mismatch repair gene mutations," *DNA Repair*, 2016; 38: 155–162.

[233] K. Tamura, M. Kaneda, M. Futagawa *et al.*, "Genetic and genomic

basis of the mismatch repair system involved in Lynch syndrome," *Int. J. Clin. Oncol.,* 2019; 24: 999–1011.

[234] T. Senda, A. Shimomura and A. Iizuka-Kogo, "Adenomatous polyposis coli (Apc) tumor suppressor gene as a multifunctional gene," *Anat. Sci. Int.*, 2005; 80: 121–131.

[235] J. M. Bugter, N. Fenderico and M. M. Maurice, "Mutations and mechanisms of WNT pathway tumour suppressors in cancer," *Nat. Rev. Cancer*, 2021; 21: 5-21.

[236] H. J. Järvinen and P. Peltomäki, "The complex genotype-phenotype relationship in familial adenomatous polyposis," *Eur. J. Gastroenterol. Hepatol.*, 2004; 16: 5–8.

[237] J. C. Rubinstein, S. A. Khan, E. R. Christison-Lagay *et al.*, "APC mutational patterns in gastric adenocarcinoma are enriched for missense variants with associated decreased survival," *Genes Chromosom. Cancer*, 2020; 59: 64–68.

[238] S. A. Tabasi and A. E. Erson, "Gene Section Atlas of Genetics and Cytogenetics in Oncology and Haematology MIR221 (microRNA 221)," *Atlas Genet Cytogenet Oncol Haematol*, 2009; 13: 566-569.

[239] F. Gottardo, C. G. Liu, M. Ferracin *et al.*, "Micro-RNA profiling in kidney and bladder cancers," *Urol. Oncol. Semin. Orig. Investig.*, 2007; 25: 387–392.

[240] J. L. Eun, Y. Gusev, J. Jiang *et al.*, "Expression profiling identifies microRNA signature in pancreatic cancer," *Int. J. Cancer*, 2007; 120:1046–1054.

[241] K. Liu, G. Li, C. Fan *et al.*, "Increased expression of microRNA-221 in gastric cancer and its clinical significance," *J. Int. Med. Res.*, 2012; 40: 467–474.

[242] R. Visone, L. Russo, P. Pallante *et al.*, "MicroRNAs (miR)-221 and miR-222, both overexpressed in human thyroid papillary carcinomas, regulate p27Kip1 protein levels and cell cycle," *Endocr. Relat. Cancer*, 2007; 14: 791–798.

[243] F. Fornari, L. Gramantieri, M. Ferracin *et al.*, "MiR-221 controls CDKN1C/p57 and CDKN1B/p27 expression in human hepatocellular carcinoma," *Oncogene*, 2008; 27: 5651–5661.

[244] L. Gramantieri, F. Fornari, M. Ferracin *et al.*, "MicroRNA-221 targets Bmf in hepatocellular carcinoma and correlates with tumor multifocality," *Clin. Cancer Res.*, 2009; 15: 5073–5081.

[245] N. Felli, L. Fontana, E. Pelosi *et al.*, "MicroRNAs 221 and 222 inhibit normal erythropoiesis and erythroleukemic cell growth via kit receptor down-modulation," *Proc. Natl. Acad. Sci. U. S. A.*, 2005; 102: 18081–18086.

[246] E. Callegari, B. K. Elamin, F. Giannone *et al.*, "Liver tumorigenicity promoted by microRNA-221 in a mouse transgenic model," *Hepatology*, 2012; 56: 1025–1033.

[247] J. Matsuzaki, H. Suzuki, H. Tsugawa *et al.*, "Bile acids increase levels of microRNAs 221 and 222, leading to degradation of CDX2 during esophageal carcinogenesis," *Gastroenterology*, 2013; 145: 1300–1311.

[248] M. Garofalo, C. Quintavalle, G. Romano *et al.*, "miR221/222 in Cancer: Their Role in Tumor Progression and Response to Therapy," *Curr. Mol. Med.*, 2011; 12: 27–33.

[249] C. Z. Zhang, J. X. Zhang, A. L. Zhang *et al.*, "MiR-221 and miR-222 target PUMA to induce cell survival in glioblastoma," *Mol. Cancer*, 2010; 9: 229.

[250] M. Garofalo, G. Di Leva, G. Romano *et al.*, "miR-221&222 Regulate TRAIL Resistance and Enhance Tumorigenicity through PTEN and TIMP3 Downregulation," *Cancer Cell*, 2009; 16: 498–509.

[251] Y. Wang, Y. Zhao, A. Herbst *et al.*, "MiR-221 mediates chemoresistance of esophageal adenocarcinoma by direct targeting of DKK2 expression," *Ann. Surg.*, 2016; 264: 804–814.

[252] H. Fu, Y. Tie, C. Xu *et al.*, "Identification of human fetal liver miRNAs by a novel method," *FEBS Lett.*, 2005; 579: 3849–3854.

[253] F. Pepe, R. Visone and A. Veronese, “The glucose-regulated MiR-483-3p influences key signaling pathways in cancer,” *Cancers*, 2018; 10: 181.

[254] P. Lapunzina and M. M. Cohen, “Risk of tumorigenesis in overgrowth syndromes: A comprehensive review,” *Am. J. Med. Genet. Semin. Med. Genet.*, 2005; 137: 53–71.

[255] C. Livingstone, “IGF2 and cancer,” *Endoc. Relat. Cancer*, 2013; 20: 321-339.

[256] S. Rainier, L. A. Johnson, C. J. Dobry *et al.*, “Relaxation of imprinted genes in human cancer,” *Nature*, 1993; 362: 747–749.

[257] A. Veronese, L. Lupini, J. Consiglio *et al.*, “Oncogenic role of miR-483-3p at the IGF2/483 locus,” *Cancer Res.*, 2010; 70: 3140–3149.

[258] A. Veronese, R. Visone, J. Consiglio *et al.*, “Mutated β-catenin evades a microRNA-dependent regulatory loop,” *Proc. Natl. Acad. Sci. U. S. A.*, 2011; 108: 4840–4845.

[259] F. Pepe, S. Pagotto, S. Soliman *et al.*, “Regulation of miR-483-3p by the O-linked N-acetylglucosamine transferase links chemosensitivity to glucose metabolism in liver cancer cells,” *Oncogenesis*, 2017; 6: e328.

[260] D. M. Özata, S. Caramuta, D. Velázquez-Fernández *et al.*, “The role of microRNA deregulation in the pathogenesis of adrenocortical carcinoma,” *Endocr. Relat. Cancer*, 2011; 18: 643–655.

[261] D. Kong, Y. S. Piao, S. Yamashita *et al.*, “Inflammation-induced repression of tumor suppressor miR-7 in gastric tumor cells,” *Oncogene*, 2012; 31: 3949–3960.

[262] W. Wang, L. J. Zhao, Y. X. Tan *et al.*, “MiR-138 induces cell cycle arrest by targeting cyclin D3 in hepatocellular carcinoma,” *Carcinogenesis*, 2012; 33: 1113–1120.

[263] W. Wang, L. J. Zhao, Y. X. Tan, *et al.*, “Identification of deregulated miRNAs and their targets in hepatitis B virus-associated hepatocellular carcinoma,” *World J. Gastroenterol.*, 2012; 18: 5442–

5453.
[264] C. Yi, Q. Wang, L. Wang *et al.*, “MiR-663, a microRNA targeting p21 WAF1/CIP1, promotes the proliferation and tumorigenesis of nasopharyngeal carcinoma,” *Oncogene*, 2012; 31: 4421–4433.